Chapter 1

Pair transfer in a nutshell

1.1 Simultaneous versus successive Cooper pair transfer in nuclei

Cooper pair transfer is commonly thought to be tantamount to simultaneous transfer. In this process a nucleon goes over through the NN–interaction v, the second one does it making use of the correlations with its partner (cf. Figs. 1.1.1 and **??** (I)). Consequently, in the independent particle limit, simultaneous transfer should not be possible (see Sect. **??**). Nonetheless, it remains operative. This is because, in this limit, the particle transferred through v does it together with a second one which profits from the non–orthogonality of the wavefunctions describing the single–particle motion in target and projectile (Figs. 1.1.2 and **??** (II)). This is the reason why this (non–orthogonality) transfer amplitude has to be treated on equal footing with the previous one representing, within the overcomplete basis employed, a natural contribution to simultaneous transfer (cf. also the discussion carried out in Ch.**??** in connection with the overlap Ω_n Eq. (**??**)). In other words, $T^{(1)}$ gives the wrong cross section, even at the level of simultaneous transfer, as it violates two–nucleon transfer sum rules[1]. In fact $(T^{(1)} - T^{(1)}_{NO})$ is the correct, sum rule conserving two–nucleon transfer amplitude to lowest order (first) in v (Fig. 1.1.2). The resulting cancellation is quite conspicuous in actual nuclei, in keeping with the fact that Cooper pairs are weakly correlated systems (see e.g. Figs. 1.4.2 (b) and 1.4.3, see also Fig. 1.4.4). This is the reason why the successive transfer process in which v acts twice, is the dominant mechanism in pair transfer reactions (within this context see Sect. 1.3). While this mechanism seems antithetical to the transfer of correlated fermions pairs (bosons), it probes, in the nuclear case, the same pairing correlations as simultaneous transfer does (Sect. 1.4). This is because nuclear Cooper pairs (quasi–bosons) are quite extended objects, the two nucleons being (virtually) correlated over distances much larger than typical nuclear dimensions (cf. Fig. 1.1.3; cf. also Sect. **??**). In a two–nucleon transfer process this

[1] Broglia, R. A. et al. (1972), Bayman, B. F. and Clement (1972); cf. also Chapter **??**

virtual property becomes real, the difference between the character of simultaneity and of succession becoming strongly blurred.

Within this context, let us refer to the Josephson effect, associated with the Cooper pair tunneling across a thin barrier separating two metallic superconductors. Because the probability of one–electron–tunneling is of the order of 10^{-10}, (conventional) simultaneous tunneling associated with a probability of $(10^{-10})^2$ would hardly be observed (cf. Sect 1.3). Nonetheless, Josephson currents are standard measures in low temperature laboratories[2].

The same arguments related to the large value of the correlation length is operative in explaining the fact that Coulomb repulsion is rather weak between partners of Cooper pairs which are, in average, at a distance $\xi(\approx 10^4$ Å) much larger than the Wigner–Seitz radius r_s typical of metallic elements ($\approx 1-2$ Å). Consequently, it can be overwhelmed by the long range electron phonon pairing. Similarly, in widely extended light halo nuclei, the short range bare pairing interaction plays little role, becoming subcritical (cf. Sect. **??**). The fact that such systems are nonetheless bound, although weakly, testifies to the dominant role the exchange of collective vibrations between halo nucleons have in binding the associated halo Cooper pair (e.g. ^{11}Li(gs), and, arguably, also[3] of ^{12}Be (0^{+*}; 2.251 MeV) to the core (^{9}Li(gs) and ^{10}Be respectively) (cf. Section **??** and Fig. **??**).

The above arguments are at the basis of the fact that second order DWBA theory which add both successive and non–orthogonality contributions to the simultaneous transfer amplitudes, provides a quantitative account of the experimental findings (see e.g. Fig. **??** and Chapter **??**).

1.2 Two–nucleon transfer probabilities, enhancement factor

As discussed in Chapter **??** the enhancement factor in a two–nucleon transfer reaction can be defined in terms of two–particle units[4], similar to what is done in the case of electromagnetic decay (Weisskopf units)[5]. Let us, for simplicity, write such a relation as

$$\left.\frac{d\sigma}{d\Omega}\right)_{2n} = \left|\langle f|P^\dagger|i\rangle\right|^2 \left(\frac{d\sigma}{d\Omega}\right)^{(0)}_{2n}, \tag{1.2.1}$$

where $\left(\frac{d\sigma}{d\Omega}\right)^{(0)}_{2n}$ is the absolute differential cross section associated with a typical pure single–pair configuration $|j^2(0)\rangle$ (or the average value over pairs based on the valence orbitals). In the case of a superfluid nucleus like e.g. ^{120}Sn and for i =gs(A)

[2] cf. e.g. Rogalla and Kes (2012) and references therein.

[3] See e.g. Johansen et al. (2013).

[4] cf. e.g. Broglia, R. A. et al. (1972); Broglia, R.A. et al. (1973) and references therein.

[5] See e.g. Bohr and Mottelson (1969).

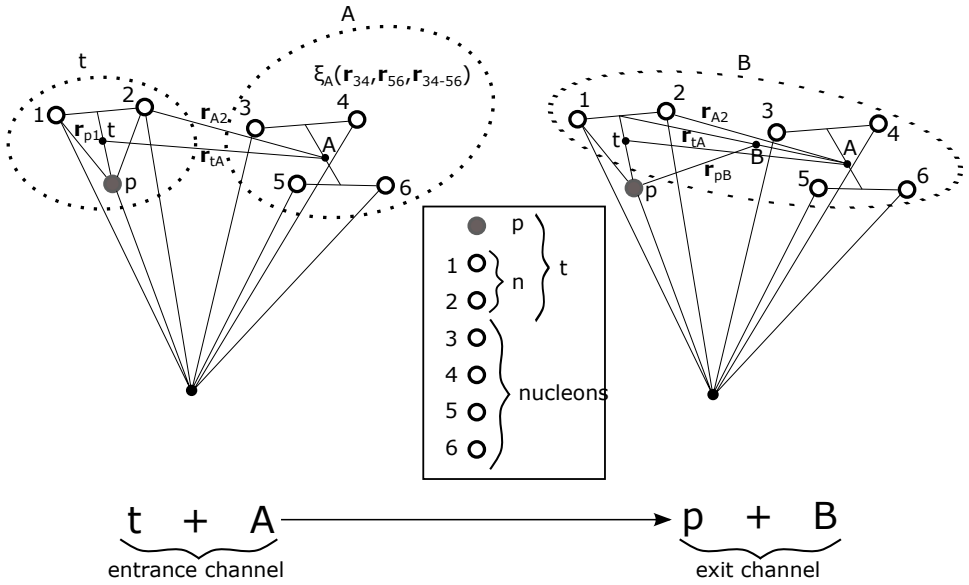

$$\frac{d\sigma}{d\Omega} = \frac{\mu_i \mu_f}{(2\pi\hbar^2)^2}\frac{k_f}{k_i}\left|T^{(1)} + T^{(2)}_{succ} - T^{(1)}_{NO}\right|^2$$

$$\phi_t(\mathbf{r}_{p1},\sigma_1,\mathbf{r}_{p2},\sigma_2)\chi^{1/2}_{m_s}(\sigma_p)\psi_A(\xi_A)\chi^{(+)}_{tA}(\mathbf{r}_{tA}) \qquad \chi^{1/2}_{m_s}(\sigma_p)\psi_B(\xi_B)\chi^{(-)}_{pB}(\mathbf{r}_{pB})$$

$$\left(\phi_d(\mathbf{r}_{p1},\sigma_1)\phi_d(\mathbf{r}_{p2},\sigma_2)\chi^{(+)}_{tA}(\mathbf{r}_{tA})\right)$$

$$\Psi_{A+2}(\xi_A,\mathbf{r}_{A1},\sigma_1,\mathbf{r}_{A2},\sigma_2) = \psi_A(\xi_A)\sum_{l_i,j_i}[\phi^{A+2}_{l_i,j_i}(\mathbf{r}_{A1},\sigma_1,\mathbf{r}_{A2},\sigma_2)]^0_0$$

$$= \psi_A(\xi_A)\sum_{nm} a_{nm}\left[\varphi^{A+2}_{n,l_i,j_i}(\mathbf{r}_{A1},\sigma_1)\varphi^{A+2}_{m,l_i,j_i}(\mathbf{r}_{A2},\sigma_2)\right]^0_0$$

$$T^{(1)} = 2\sum_{\sigma_1,\sigma_2,\sigma_p}\int d\xi_A d\mathbf{r}_{tA} d\mathbf{r}_{p1} d\mathbf{r}_{A2}\psi_A(\xi_A)\sum_{l_i,j_i}[\phi^{A+2}_{l_i,j_i}(\mathbf{r}_{A1},\sigma_1,\mathbf{r}_{A2},\sigma_2)]^{0*}_0$$
$$\times\chi^{(-)*}_{pB}(\mathbf{r}_{pB})\chi^{1/2*}_{m_s}(\sigma_p)v(r_{p1})\phi_t(\mathbf{r}_{p1},\sigma_1,\mathbf{r}_{p2},\sigma_2)\chi^{1/2}_{m_s}(\sigma_p)\psi_A(\xi_A)\chi^{(+)}_{tA}(\mathbf{r}_{tA})$$
$$= 2\sum_{\sigma_1,\sigma_2,\sigma_p}\int d\mathbf{r}_{tA} d\mathbf{r}_{p1} d\mathbf{r}_{A2}\sum_{l_i,j_i}[\phi^{A+2}_{l_i,j_i}(\mathbf{r}_{A1},\sigma_1,\mathbf{r}_{A2},\sigma_2)]^{0*}_0$$
$$\times\chi^{(-)*}_{pB}(\mathbf{r}_{pB})\chi^{1/2*}_{m_s}(\sigma_p)v(r_{p1})\phi_t(\mathbf{r}_{p1},\sigma_1,\mathbf{r}_{p2},\sigma_2)\chi^{1/2}_{m_s}(\sigma_p)\chi^{(+)}_{tA}(\mathbf{r}_{tA})$$

Figure 1.1.1: Contribution of simultaneous transfer, in first order DWBA, to the reaction $A(t,p)B(\equiv A+2)$. The nucleus A is schematically assumed to contain four nucleons, the triton being composed of two neutrons and one proton. The set of coordinates used to describe the entrance and exit channels are shown in the upper part, while in the lower part the simultaneous two–nucleon transfer amplitude is written in detail (cf. Potel, G. et al. (2013b)). Of notice that the expression of $T^{(1)}$ violates, in the independent particle basis used, the two–nucleon transfer sum rule by exactly $T^{(1)}_{NO}$, amplitude operative also in lowest order of v (Fig. 1.1.2; see also text). It is of notice that of all the relative motion coordinates, only those describing the relative motion of (t,A) and of (p,B) have asymptotic values.

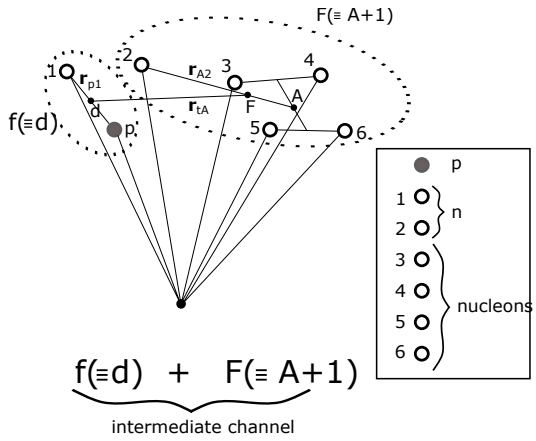

$$\chi^{1/2}_{m_s}(\sigma_p)\phi_d(\mathbf{r}_{p1},\sigma_1)\psi_A(\xi_A)\varphi^{A+1}_{l_f,j_f,m_f}(\mathbf{r}_{A2},\sigma_2)$$

$$G(\mathbf{r}_{dF},\mathbf{r}'_{dF}) = i\sum_l \sqrt{2l+1}\frac{f_l(k_{dF},r_<)g_l(k_{dF},r_>)}{k_{dF}r_{dF}r'_{dF}}\left[Y^l(\hat{r}_{dF})Y^l(\hat{r}'_{dF})\right]^0_0$$

$$T^{(2)}_{succ} = 2\sum_{l_i,j_i}\sum_{l_f,j_f,m_f}\sum_{\substack{\sigma_1\sigma_2\\ \sigma'_1\sigma'_2}}\int d\xi_A d\mathbf{r}_{dF}d\mathbf{r}_{p1}d\mathbf{r}_{A2}\chi^{(-)*}_{pB}(\mathbf{r}_{pB})\chi^*_B(\xi_B)v(\mathbf{r}_{p1})\phi_d(\mathbf{r}_{p1})\varphi^{A+1}_{l_f,j_f,m_f}(\mathbf{r}_{A2},\sigma_2)$$

$$\times\chi^{1/2}_{m_s}(\sigma_p)\Psi_A(\xi_A)\frac{2\mu_{dF}}{\hbar^2}\int d\xi'_A d\mathbf{r}'_{dF}d\mathbf{r}'_{p1}d\mathbf{r}'_{A2}G(\mathbf{r}_{dF},\mathbf{r}'_{dF})$$

$$\times\chi^{(+)}_{tA}(\mathbf{r}_{tA})\psi^*_A(\xi'_A)v(\mathbf{r}'_{p2})\phi_d(\mathbf{r}'_{p1})\varphi^{A+1}_{l_f,j_f,m_f}(\mathbf{r}'_{A2},\sigma'_2)$$

$$= 2\sum_{l_i,j_i}\sum_{l_f,j_f,m_f}\sum_{\substack{\sigma_1\sigma_2\\ \sigma'_1\sigma'_2}}\int d\mathbf{r}_{dF}d\mathbf{r}_{p1}d\mathbf{r}_{A2}\chi^{(-)*}_{pB}(\mathbf{r}_{pB})v(\mathbf{r}_{p1})\phi_d(\mathbf{r}_{p1})\left[\varphi^{A+2}_{l_f,j_f,m_f}(\mathbf{r}_{A1},\sigma_1,\mathbf{r}_{A2},\sigma_2)\right]^0_0$$

$$\times\frac{2\mu_{dF}}{\hbar^2}\int d\mathbf{r}'_{dF}d\mathbf{r}'_{p1}d\mathbf{r}'_{A2}G(\mathbf{r}_{dF},\mathbf{r}'_{dF})\chi^{(+)}_{tA}(\mathbf{r}'_{tA})v(\mathbf{r}'_{p2})\phi_d(\mathbf{r}'_{p1},\sigma'_1)\phi_d(\mathbf{r}'_{p2},\sigma'_2)\varphi^{A+1}_{l_f,j_f,m_f}(\mathbf{r}'_{A2},\sigma'_2)$$

$$T^{(1)}_{NO} = 2\sum_{l_i,j_i}\sum_{l_f,j_f,m_f}\sum_{\substack{\sigma_1\sigma_2\\ \sigma'_1\sigma'_2}}\int d\xi_A d\mathbf{r}_{dF}d\mathbf{r}_{p1}d\mathbf{r}_{A2}\chi^{(-)*}_{pB}(\mathbf{r}_{pB})\chi^*_B(\xi_B)v(\mathbf{r}_{p1})\phi_d(\mathbf{r}_{p1})\varphi^{A+1}_{l_f,j_f,m_f}(\mathbf{r}_{A2},\sigma_2)$$

$$\times\chi^{1/2}_{m_s}(\sigma_p)\Psi_A(\xi_A)\frac{2\mu_{dF}}{\hbar^2}\int d\xi'_A d\mathbf{r}'_{dF}d\mathbf{r}'_{p1}d\mathbf{r}'_{A2}$$

$$\times\chi^{(+)}_{tA}(\mathbf{r}_{tA})\psi^*_A(\xi'_A)\phi_d(\mathbf{r}'_{p1})\mathbb{I}\varphi^{A+1}_{l_f,j_f,m_f}(\mathbf{r}'_{A2},\sigma'_2)$$

$$= 2\sum_{l_i,j_i}\sum_{l_f,j_f,m_f}\sum_{\substack{\sigma_1\sigma_2\\ \sigma'_1\sigma'_2}}\int d\mathbf{r}_{dF}d\mathbf{r}_{p1}d\mathbf{r}_{A2}\chi^{(-)*}_{pB}(\mathbf{r}_{pB})v(\mathbf{r}_{p1})\phi_d(\mathbf{r}_{p1})\left[\varphi^{A+2}_{l_f,j_f,m_f}(\mathbf{r}_{A1},\sigma_1,\mathbf{r}_{A2},\sigma_2)\right]^0_0$$

$$\times\frac{2\mu_{dF}}{\hbar^2}\int d\mathbf{r}'_{dF}d\mathbf{r}'_{p1}d\mathbf{r}'_{A2}\chi^{(+)}_{tA}(\mathbf{r}'_{tA})\phi_d(\mathbf{r}'_{p1},\sigma'_1)\phi_d(\mathbf{r}'_{p2},\sigma'_2)\varphi^{A+1}_{l_f,j_f,m_f}(\mathbf{r}'_{A2},\sigma'_2)$$

Figure 1.1.2: Successive and non–orthogonality contributions to the amplitude describing two–nucleon transfer in second order DWBA, entering in the expression of the absolute differential cross section $d\sigma/d\Omega = \frac{\mu_i\mu_f}{(4\pi\hbar^2)^2}\frac{k_f}{k_i}\left|T^{(1)}+T^{(2)}_{succ}-T^{(2)}_{NO}\right|^2$. Concerning $T^{(1)}$ we refer to Fig. 1.1.1. In the upper part of the figure the coordinates used to describe the intermediate channel $d + F(\equiv A+1)$ are given, while in the lower part the corresponding expressions are displayed (Potel, G. et al., 2013b) in the case of a (t, p) process. Schematically, the three contributions $T^{(1)}$, $T^{(2)}_{succ}$ and $T^{(2)}_{NO}$ to the transfer amplitude can be written as $\langle pB|v|tA\rangle$, $\sum\langle pB|v|dF\rangle\langle dF|v|tA\rangle$ and $\sum\langle pB|v|dF\rangle\langle dF|\mathbf{1}|tA\rangle$ respectively, where v is the proton–neutron interaction and $\mathbf{1}$ the unit oprerator. Within this context, while $T^{(2)}_{NO}$ receives contributions from the intermediate (virtual) closed $(d + F)$ channel as $T^{(2)}_{succ}$ does, it is first order in v as $T^{(1)}$.

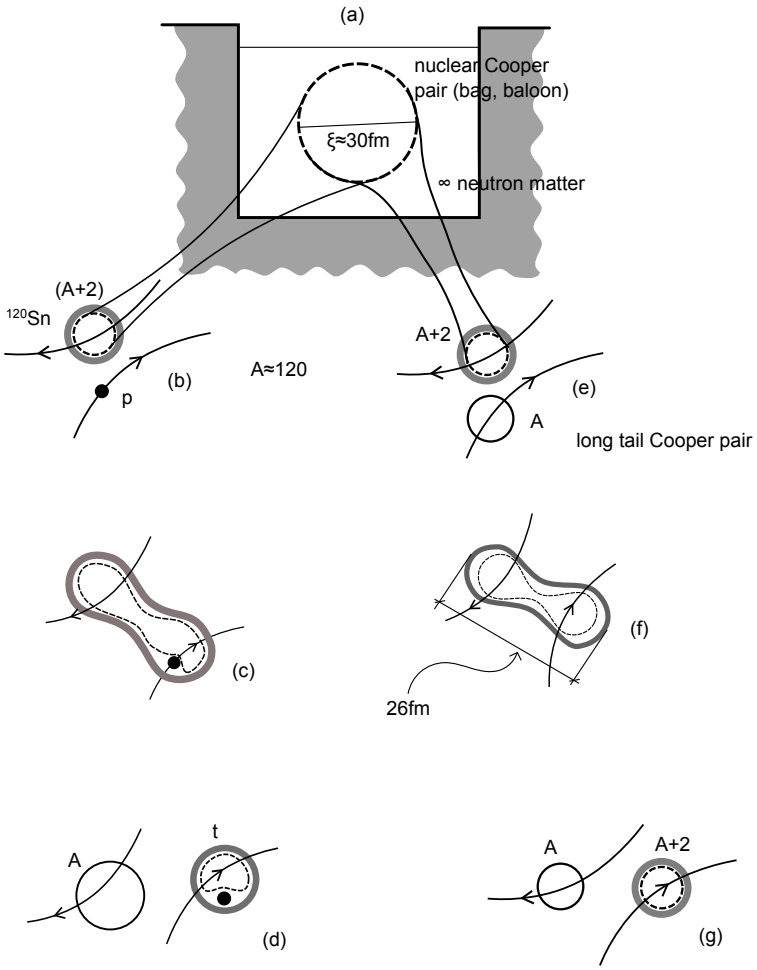

Figure 1.1.3: The correlation length associated with a nuclear Cooper pair is of the order of $\xi \approx \hbar v_F/\Delta \approx 30$ fm (see App. 1.4).(**a**) in neutron matter at typical densities of the order of 0.5–0.8 saturation density, the NN–$^1S_0$ short range force, eventually renormalized by medium polarization effects, makes pairs of nucleons moving in time reversal states to correlate over distances of the order of 5–6 times typical nuclear radii. How can one get evidence for such an extended object? Certainly not when the Cooper bag (balloon) is introduced in (**b**) the mean field of a superfluid nucleus which, acting as an external field, constrains the Cooper pair to be within the nuclear radius with some spill out (long tail of Cooper pair, grey, shaded area extending outside the nuclear surface defined by $R_0 = 1.2A^{1/3}$ fm). But yes in (**c**), (**d**) that is in the case of two–nucleon transfer process (e.g. (p,t) reaction) in which the absolute cross section can change by orders of magnitude in going from pure two–particle (uncorrelated configurations) to long tail Cooper pair spill outs. This effect is expected to become stronger by allowing , pair transfer between similar superfluid nuclei, in which case one profits of the same type of correlations (superfluidity) as resulting from very similar pair mean fields (**e**), (**f**), (**g**) (cf. e.g. von Oertzen, W. (2013) and references therein; see also Eqs. (**??**) and (**??**). For the case under discussion $\Omega_n = 1$). Within this context, it is apparent that pairs of nucleons will feel equally well pairing correlations whether they are transferred simultaneously or one after the other (cf. (**c**) and (**f**)).

and f =gs(A+2) as well as $f = 2qp$(A+2) one can write

$$\left|\langle f|P^{\dagger}|i\rangle\right|^2 = \begin{cases} \alpha_0'^2 = (\sum_{\nu>0} U'_\nu V'_\nu)^2 = \left(\frac{\Delta}{G}\right)^2 = \left(\frac{12A}{\sqrt{A}25}\right)^2 \approx \frac{A}{4} \approx 30 \ (f = gs), \\ U_\nu^4 \approx 1 \ (f = 2qp). \end{cases} \tag{1.2.2}$$

Thus, the expected enhancement factor[6] is given by the ratio,

$$R = \frac{\frac{d\sigma}{d\Omega}(gs \to gs)\Big)_{2n}}{\frac{d\sigma}{d\Omega}(gs \to 2qp)\Big)_{2n}} \approx 30. \tag{1.2.3}$$

In other words, in superfluid nuclei one expects the 0^+ pairing vibrational states to carry a (summed) cross section of the order of 3% that of the $gs \to gs$ transition (cf. Fig. **??**). Now, in defining the quantity R used was made of (1.2.1). Because both numerator and denominator are linear in $\left(\frac{d\sigma}{d\Omega}\right)^{(0)}_{2n}$, one could as well posit that one has used (1.2.2) in defining R.

The situation is quite different when one intends to define the probability associated with a transfer process. One could be tempted again to use (1.2.1) for the case of $2n$–transfer and eventually

$$\left(\frac{d\sigma}{d\Omega}\right)_{1n} = S\left(\frac{d\sigma}{d\Omega}\right)^{(0)}_{1n}, \tag{1.2.4}$$

in the case of $1n$–transfer, S being known in the literature as the spectroscopic factor, and used here for illustration purposes only. However, in trying to define an enhancement factor in terms of P_{2n}/P_{1n}^2, the approximate relations (1.2.1) and (1.2.4) will now condition the physics one is trying to extract from the experimental (empirical) information. In fact, in this case the actual values of $\left(\frac{d\sigma}{d\Omega}\right)^{(0)}_{1n}$ and of $\left(\frac{d\sigma}{d\Omega}\right)^{(0)}_{2n}$ will play an important role, and this could hardly be correct. In fact, the proper definition of the transfer probabilities is to be made in terms of the total reaction cross section.

For this purpose let us remind some useful relations. In particular that of the differential reaction cross section

$$\frac{d\sigma}{d\Omega} = |f(\theta)|^2, \tag{1.2.5}$$

where

$$f(\theta) = \frac{1}{k}\sum_l (2l+1)e^{i\delta_l}\sin\delta_l P_l(\cos\theta), \tag{1.2.6}$$

δ_l being the partial wave l phase shift. Let us now use for simplicity the results associated with hard sphere scattering[7] in the low and high energy limit. Making

[6] See e.g. Brink, D. and Broglia (2005) p. 324

[7] cf. e.g. Sakurai (1994)

use of the fact that in the case under discussion the phase shifts δ_l are related to the regular and irregular spherical Bessel functions,

$$\tan\delta_l = \frac{j_l(kR)}{n_l(kR)}, \tag{1.2.7}$$

and that $\sin^2\delta_l = \tan^2\delta_l/(1+\tan^2\delta_l)$, one can write in the case in which $kR \ll 1$, i.e. in the low–energy, long wavelength, regime

$$\tan\delta_l \approx \frac{-(kR)^{2l+1}}{(2l+1)[(2l-1)!!]^2}, \tag{1.2.8}$$

implying that one can ignore all δ_l with $l \neq 0$. Because $\delta_0 = -kR$ (cf. (1.2.7)) regardless the value of k, one obtains,

$$\frac{d\sigma}{d\Omega} = \frac{\sin^2\delta_0}{k^2} = R^2, \tag{1.2.9}$$

and thus

$$\sigma_{tot} = \int \frac{d\sigma}{d\Omega} d\Omega = 4\pi R^2 \quad (kR \ll 1), \tag{1.2.10}$$

a cross section which is four times the geometric cross section πR^2, namely the area of the disc of radius R that blocks the propagation of the incoming (plane) wave, and has the same value as that of a hard sphere. Because $kR \ll 1$ implies long wavelength scattering, it is not surprising that quantal effects are important, so as to overwhelm the classical picture. Let us now consider the high energy limit $kR \gg 1$. The total cross section is in this case, given by

$$\begin{aligned}\sigma_{tot} = \int |f_l(\theta)|^2 d\Omega = \frac{1}{k^2}\int_0^{2\pi} d\phi \int_{-1}^{1} d(\cos\theta) \sum_{l=1}^{kR}\sum_{l'=1}^{kR}(2l+1)(2l'+1) \\ \times e^{i\delta_l}\sin\delta_l e^{-i\delta_{l'}}\sin\delta_{l'} P_l P_{l'} = \frac{4\pi}{k^2}\sum_{l=1}^{kR}(2l+1)\sin^2\delta_l = \frac{4\pi}{k^2}\sum_{l=1}^{kR}(2l+1)\,p_l.\end{aligned} \tag{1.2.11}$$

Making use of the relation

$$\sin^2\delta_l = \frac{\tan^2\delta_l}{1+\tan^2\delta_l} = \frac{[j_l(kR)]^2}{[j_l(kR)]^2+[n_l(kR)]^2} \approx \sin^2\left(kR - \frac{\pi l}{2}\right), \tag{1.2.12}$$

and the fact that so many l–values contribute to (1.2.11), one can replace $\sin^2\delta_l$ by its average value 1/2. Because the number of terms of the sum is roughly kR, the same being true for the average value of $(2l+1)$. Thus one can write

$$\sigma_{tot} = \frac{4\pi}{k^2}(kR)^2\frac{1}{2} = 2\pi R^2, \quad (kR \gg 1) \tag{1.2.13}$$

which, in this short wavelength limit, is not the geometric cross section either. In fact, (1.2.13) can be split into two contributions each of value πR^2. One due to reflection in which it can be shown that there is no interference amongst contributions from different l–values. A second one (coherent contribution in the forward direction) called shadow because for hard–sphere scattering at high energies, waves with impact parameter less than R must be deflected. Consequently, behind the scatterer there must be zero probability for finding the scattered particle and a shadow must be generated.

In terms of wave mechanics, this shadow is due to the destructive interference between the original wave (which would be there even if the scatterer was absent), and the newly scattered wave. Thus, one needs scattering in order to create a shadow. This contribution is intimately related to the optical theorem[8]

$$\sigma_{tot} = \frac{4\pi}{k}\Im[f(\theta = 0, k)] = \frac{4\pi}{k}[f_{shad}(\theta = 0, k)] = \frac{4\pi}{k^2}\sum_l (2l + 1)\sin^2\delta_l, \quad (1.2.14)$$

to which it provides its physical interpretation. In fact, there are two independent ways of measuring σ_{tot}, namely: i) by integrating the differential cross section $d\sigma/d\Omega = |f(\theta)|^2$ moving around the detector, ii) measuring the attenuation of the incoming beam. Both procedures should give the same result. One then identifies $(4\pi/k)f(\theta = 0, k)$ with the attenuation arising from the interference of the elastic wave with the incoming wave. Of notice that in (1.2.11) the factor $(\pi/k^2)(2l + 1) = \pi\lambda\!\!\!^{-}(2l + 1)$ is the area of a ring with radius $b = (l + 1/2)\lambda\!\!\!^{-}$ and width $\lambda\!\!\!^{-}$ due to quantal uncertainties. Thus

$$\sigma_{tot} = 2\pi(R + \lambda\!\!\!^{-}/2)^2 \quad (kR \gg 1). \quad (1.2.15)$$

The quantity

$$\lambda\!\!\!^{-} = \frac{\lambda}{2\pi} = \frac{h}{2\pi p} = \frac{\hbar}{p} = \frac{1}{k} = \frac{\hbar}{\sqrt{2mE}}, \quad (1.2.16)$$

is the reduced de Broglie wavelength for a massive particle ($E = p^2/2m$). For a proton of energy $E_p \approx 20$ MeV, typical of beams used in ^{120}Sn$(p, t)^{118}$Sn(gs) and ^{120}Sn$(p, d)^{119}$Sn(j) reactions (cf. Figs. **??**, **??** and **??**)[9] $\lambda\!\!\!^{-} \approx 1$ fm, to be compared with the value $R \approx 6$ fm of the radius of ^{120}Sn. Consequently, we are in a situation of type (1.2.15), that is,

$$\sigma_{tot} = 2\pi(6 + 0.5)^2 \text{ fm}^2 \approx 2.7 \text{ b}. \quad (1.2.17)$$

Because typical values of the absolute one–particle cross section associated with the (p, d) reaction mentioned above are few mb (cf. Fig. **??** right panel) one can use, for order of estimate purposes,

$$P_1 \approx \frac{5.35 \text{ mb}}{2.7 \text{ b}} \approx 10^{-3}, \quad (1.2.18)$$

[8] Sakurai (1994) pp. 420–421

[9] Of notice that the reduced wavelength of a photon ($p = E/c$) of the same energy ($E = 20$ MeV) is $\lambda\!\!\!^{-}(= \lambda/2\pi = \hbar/p = \hbar c/E) \approx 10$ fm (cf. Table 2.1 p. 22 Satchler (1980)).

as the typical probability for such processes. Consequently, one may argue that the probability for a pair of nucleons to simultaneously tunnel in e.g. the (p, t) process mentioned above is $(P_1)^2 \approx 10^{-6}$, as near impossible as no matter. Within this context we note that the integrated gs $\rightarrow$ gs absolute cross section $\sigma(^{120}\mathrm{Sn}(p, t)^{118}\mathrm{Sn(gs)}) \approx$ 2.5±0.2 mb (cf. Figs. **??** and **??**). This fact implies that the empirical two–nucleon transfer probability is of the order of $P_2 \approx 10^{-3}$. Consequently, $P_2/(P_1)^2 \approx 10^3$, a ratio which can hardly be explained in terms of a physical enhancement factor.

The above contradictions[10] are, to a large extent, connected with the fact that one is addressing the subject of pairing correlations in nuclei as probed by two–nucleon transfer reactions, treating separately the associated questions of structure and reactions, while they are but complementary aspects of the same physics. Let us elaborate on this point.

When one turns on, in an open shell atomic nucleus like e.g. $^{120}_{50}\mathrm{Sn}_{70}$, a pairing interaction of strength larger than critical, the system moves into an independent pair regime[11] (cf. e.g. Sects. **??** and **??** as well as Fig. **??**; see Fig. 1.2.1). This fact has essentially no consequence concerning the one–particle transfer mechanism, exception made regarding the size of the mismatch between the relative motion–incoming (p+^{120}Sn(gs)) and –outgoing (d+^{119}Sn(gs)) trajectories (Q–value and recoil effect), in keeping with the fact that one has to break a Cooper pair to populate a single quasiparticle state. From a structure point of view the depletion of the occupation probability measured in a (p, d) process is correlated with the corresponding increase in occupation observed in (d, p) (U^2, V^2 factors). Aside from the quantitative values, this is also observed in dressed single–particle states, the single–particle sum rule implying both the (A-1) and (A+1) system (see App. **??**). Concerning the phase coherence of the pair correlated wavefunction it has no consequence for one–particle transfer process, in keeping with the fact that $|e^{i\phi}\sqrt{P_1}|^2 = P_1$.

The situation is very different concerning (Cooper) pair transfer. From a reaction point of view, and in keeping with the non–orthogonality existing between the wavefunctions in target and projectile, the associated contributions to the transfer process have to be eliminated. This is in keeping with the fact that simultaneous two–nucleon transfer can take place also in first order in the proton–neutron interaction v_{np}. When this is a consequence of the correlation between the partners of the Cooper pair (cf. Fig. **??** (I)) it constitutes a *bona fide* contribution. Not when it is a consequence of non–orthogonality (see Fig. **??** (II)). Continuing within the realm of reaction theory, second order processes in v_{np} are to be

[10] Within this context it is of notice that similar questions were rised by Bardeen (1962, 1961); Pippard (2012); Cohen et al. (1962); McDonald (2001) in connection with the prediction of Josephson (Josephson (1962)) that there should be a contribution to the current through an insulating barrier between two superconductors which would behave like direct tunneling of condensed pairs. This is in keeping with the fact that a single electron has a probability of $\approx 10^{-10}$ of getting through, the "classical" estimate of simultaneous pair tunneling being $\approx 10^{-20}$, an impossible observation as stated above (cf. App. 1.8).

[11] Regime which is conditioned by the "external" mean field. In other words, regime which express itself provided there is nucleon density available (see Sect. 1.2).

included (Fig. **??**) and as a rule neglect higher orders in keeping with the small value of P_2 ($\approx 10^{-3}$, cf. also Table **??**). Let us now bring structure into the discussion. The fact that the wave function of the nucleons in the pair are phase–coherent ($\left(U_\nu + V_\nu e^{-2i\phi} a^\dagger_\nu a^\dagger_{\bar{\nu}}\right)|0\rangle$) implies that one has to add the amplitudes before one takes modulus squared (cf. also Sect. 1.6 and Sect. 1.7), that is,

$$P_2 = \lim_{\epsilon\to 0}\left|\frac{1}{\sqrt{2}}\left(e^{i\phi'}\sqrt{P_1} + e^{i\phi}\sqrt{P_1}\right)\right|^2$$
$$= P_1 \lim_{\epsilon\to 0}(1+\cos\epsilon) = 2P_1 \quad (\epsilon = \phi - \phi'), \tag{1.2.19}$$

again, an unexpected quantum mechanical result as e.g. (1.2.13). Because the range of v_{np} ($a \approx 1$ fm) is much smaller than the correlation length ($\xi \approx 20$–30 fm), in the successive process (1.2.19), the Cooper pair tunnels between target and projectile equally formed and "unharmed" as in the simultaneous process. Think again that in the nuclear pairing correlated system only Cooper pairs exist (in which the partners nucleons are correlated over 20–30 fm from each other) and not single nucleons (normal system) at ≈ 4 fm (2 fm being the radius of the Wigner–Seitz nucleus cell) from each other (cf. Fig. 1.2.1). To the extent that the mean field acting as an "external" field allows particle density to be present, the properties of independent Cooper pair motion will explicit themselves. And thus is a physical condition which is assumed fulfilled each time one will make use of Fig. 1.2.1 (b). In other words, inside ^{120}Sn all Cooper pairs will be found within a volume of radius $R_0 \approx 6$ fm, in the same way in which a Cooper pair will be distributed over two similar volumes during the contact time in e.g. a Sn+Sn heavy ion reaction[12] (see also Sect. 1.2). This explains the importance of long–range induced pairing interaction (exchange of phonons) in general, let alone in very extended light halo nuclei like ^{11}Li.

Within this context we note that the (approximate) form of the (local) pair wavefunction can be written as (cf. Leggett (2006) p. 185; for the non local nuclear version cf. e.g. Broglia and Winther (1983))

$$F(r) \approx \Delta N(0)\frac{\sin k_F r}{k_F}\exp\left(\frac{\sqrt{2}r}{\xi}\right), \tag{1.2.20}$$

where $N(0)$ is the density of levels at the Fermi energy for one spin orientation. For $r \leq \xi$ the pair wavefunction is approximately proportional to that of two particles at the Fermi energy moving freely in a relative s–wave state. In a typi-

[12]The interest of picture 1.2.1 (b) can also be exemplified by referring to a single stable nucleus lying along the stability valley, with the fact that the moment of inertia of heavy deformed nuclei is considerably smaller than the rigid moment of inertia, but still larger than the irrotational one ($5\mathcal{J}_{irrot} \lesssim \mathcal{J} \lesssim \mathcal{J}_r/2$). Even confined within the mean field of the nucleus, the small but finite number of pairs of correlated nucleons having the "intrinsic", infinite–matter–like tendency displayed if Fig. 1.2.1 (b), will average out the different orientations of the rotating system and react to it in terms of an effective deformation smaller than the one related to the B($E2$) collective (rotational) values. However, constrained as they are they cannot fully profit of pairing superfluidity.

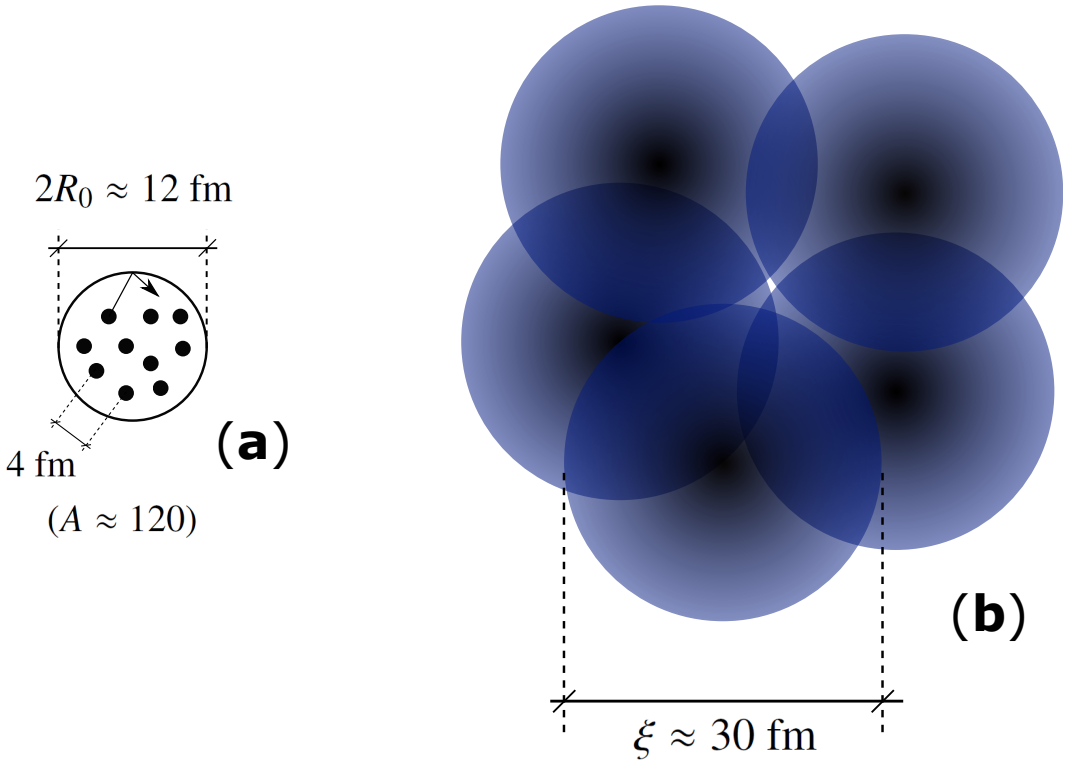

Figure 1.2.1: (**a**) Schematic representation of independent–particle motion and (**b**) independent–pair motion. In the first case nucleons (fermions) move independently of each other reflecting elastically from the wall of the mean field created by all the other nucleons, each of which is associated with a Wigner–Seitz cell of radius $d = \left((4\pi/3)R_0^3/A\right)^{1/3}$ implying a relative distance of $2d$ (the actual numbers correspond to e.g. ^{120}Sn). Switching on the pairing interaction (bare plus induced) leads to Cooper pair formation in which the correlation length is ξ. Thus, pair of nucleons moving in time reversal states close to the Fermi energy will tend to recede from each other lowering their relative momentum ($2d \rightarrow \xi$) thus boosting the stability of the system, provided that the external mean field allows it. Or better, to the extent that there is nucleon density available to do so, something controlled by the single–particle potential. From this point on, and at least for the levels lying close to the Fermi surface, one cannot talk about particles but about Cooper pairs (unless one does not intervene the system with an external field, e.g. (p, d) and provides the energy, angular and linear momentum needed to break a pair). Of course that the system to the right under the influence of an external field (like e.g. the HF of ^{120}Sn) Cooper pairs will be constrained within its boundaries. But this will be true with two nuclei of ^{120}Sn at a relative (CM) distance much larger than $2R_0$ (≈ 12 fm). The pair field associated with a Cooper pair will extend from one to the other partner of the heavy ion reaction through the weakly overlapping interaction region, allowing two nucleons to correlate over ξ and, eventually, in a reaction like e.g. Sn+Sn$\rightarrow$ Sn(gs)+Sn(gs) allow for the transfer of two nucleons correlated over tens of fm.

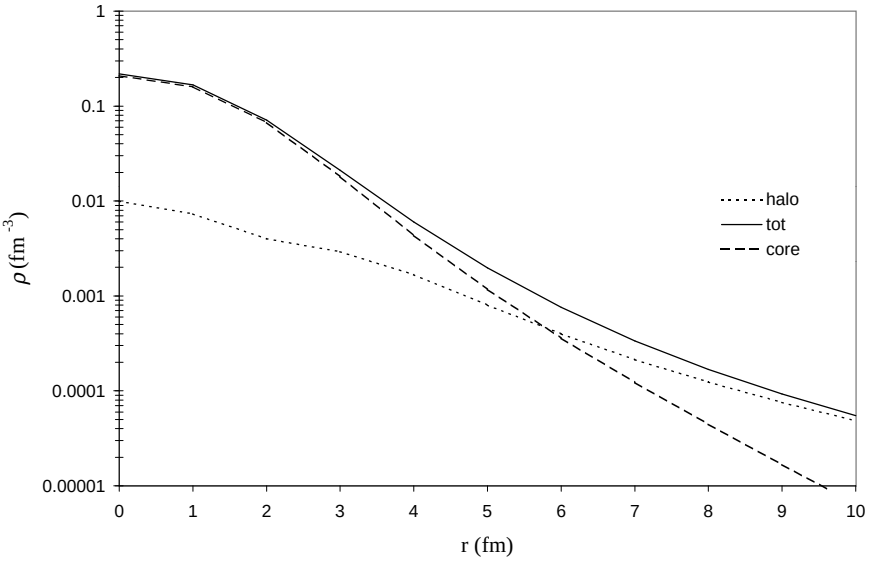

Figure 1.2.2: The nuclear density associated with ^{11}Li, as resulting from the microscopic NFT calculations which are at the basis of the results displayed in Figs. **??** and **??** (Barranco, F. et al. (2001)). The contribution arising from the core (^{9}Li) is displayed with a dashed curve, while that associated with the two halo neutrons (cf. Eqs. (**??**)–(**??**)) is shown in term of a dotted curve. The sum of these two contributions labeled tot (total) is drawn with a continuous curve.

cal metallic superconductor ξ is of the order of 10^4 Å, much larger than the inter electron spacing ($\approx$ 1 Å). Note that relative to the Fermi energy, the correlation energy ($E_{corr} = (-1/2)N(0)\Delta^2$) associated with Cooper pairing is very small, $\approx 10^{-7} - 10^{-8}$. Arguably, the most important consequence of this fact, is the exponentially large radius and thus very small value of the relative momentum associated with Cooper pairs. In other words, the typical scenario for a very small value of the localization kinetic energy and thus of the quantality parameter (cf. App. **??**), implying that the two partners, are rigidly anchored to each other (Cooper pair). This phenomenon is at the basis of the emergence of new elementary modes of excitation (pairing vibrations for single Cooper pairs, pairing rotations for few ones, supercurrents and Josephson currents for macroscopic amounts of them).

The situation sounds, in principle, very different from atomic nuclei, in keeping with the fact that nuclear Cooper pairs are, as a rule, subject to an overwhelming external (mean) fields ($|E_{corr}| \approx 1$ MeV $\ll |U(r \approx R_0)| \approx |V_0/2| \approx 25$ MeV). But even in this case, one can posit that the transition from independent particle to independent pair motion implies that Cooper pair partners recede from each other. Let us clarify this point for the case of a single pair, e.g. ^{208}Pb(gs). It is true that allowing the pair of neutrons to correlate in the valence orbitals leads to a pair wavefunction which is angle correlated ($\Omega_{12} \approx 0$), as compared to the pure $j^2(0)(j = g_{9/2})$ configuration[13]. On the other hand, the correlated pair addition mode (Tab. **??** and **??**) will display a sizeable spill out as compared to the pure two particle state, and thus a lower density and larger related average distance between Cooper pair partners. This is also the reason why close to $\approx 40\%$ of the pairing matrix elements is contributed by the induced pairing interaction resulting from the exchange of long wavelength, low–lying, collective modes, the other $\approx 60\%$ resulting from the bare nucleon–nucleon $^1S_0$ pairing interaction (cf. Fig. **??**). In carrying out the above arguments the values of $(E_{corr}/\epsilon_F)^2 \approx \left(\frac{1\,\text{MeV}}{37\,\text{MeV}}\right)^2 \approx 10^{-3}$ and $\xi = \frac{\hbar v_F}{2E_{corr}} \approx 30$ fm ($(\frac{v_F}{c}) \approx 0.3$), valid for nuclei along the stability valley, were used.

The situation described above becomes clearer, even if extreme, in the case of ^{11}Li. In this case, the Fermi momentum is $k_F \approx 0.8\,\text{fm}^{-1}$, the radius $R \approx 4.58$fm, much larger than $R_0 = 2.7$ fm expected from systematics. Furthermore essentially all of the correlation energy ($E_{corr} \approx 0.5$ MeV, $(E_{corr}/\epsilon_F)^2 \approx (0.5/14)^2 \approx 10^{-3}, \xi \approx 20$ fm ($v_F/c \approx 0.1$)) is associated with the exchange of the dipole pigmy resonance between the halo neutrons. It is of notice that in this case, renormalization effects due to the clothing of single–particle states by vibrations, in particular the lowest lying quadrupole vibration of the core ^{9}Li, are as strong as mean field effects, as testified by parity inversion and the appearance of a new magic number, namely $N = 6$ (cf. Fig. **??** (I)). Again in this case $s^2_{1/2}(0)$ and $p^2_{1/2}(0)$ are not correlated in Ω_{12}, while the Cooper state probability density displays a clear angular correlation (see Figs. **??** (II) and **??**). Nonetheless, the average distance between the partners of the neutron halo Cooper pair, is considerably larger than that associated with the

[13] Bertsch, G. F. et al. (1967), Ferreira, L. et al. (1984); Matsuo, M. (2013).

^{9}Li core nucleons, as testified by the following figures (cf. also Fig. 1.2.2):

$$\text{a)} \quad R(^{11}\text{Li}) = 4.58 \pm 0.13\,\text{fm} \quad (V = (4\pi/3)\,R^3 = 402.4\,\text{fm}^3) \tag{1.2.21}$$

$$\text{b)} \quad R_0(^{11}\text{Li}) = 2.7\,\text{fm} \quad (V = 82.4\,\text{fm}^3) \tag{1.2.22}$$

$$\text{c)} \quad R_0(^{9}\text{Li}) = 2.5\,\text{fm} \quad (V = 65.4\,\text{fm}^3), \tag{1.2.23}$$

and associated mean distance between nucleons,

$$\text{a)} \quad \left(\frac{402.4\,\text{fm}^3}{2}\right)^{1/3} \approx 5.9\,\text{fm}, \tag{1.2.24}$$

$$\text{b)} \quad \left(\frac{82.4\,\text{fm}^3}{11}\right)^{1/3} \approx 1.96\,\text{fm}, \tag{1.2.25}$$

$$\text{c)} \quad \left(\frac{65.4\,\text{fm}^3}{9}\right)^{1/3} \approx 1.94\,\text{fm}. \tag{1.2.26}$$

The above quantities are to be compared with the standard definition,

$$d = \left(\frac{\frac{4\pi}{3}R^3}{A}\right)^{1/3} = \left(\frac{4\pi}{3}\right)^{1/3} r_0 \approx 1.93\,\text{fm}, \tag{1.2.27}$$

consistent with the standard parametrization $R_0 = r_0 A^{1/3}$ of the nuclear radius written in terms of the Wigner–Seitz–like radius r_0 (=1.2 fm) of the sphere associated with each nucleon, derived from systematics of stable nuclei lying along the stability valley.

1.2.1 Interplay between mean field and correlation length

In Fig. 1.2.1 one displays a schematic representation of two *gedanken experiments*: (**a**) (*independent particle motion*) non–interacting nucleons confined in a mean field potential, e.g. a Saxon–Woods potential with standard parametrization (Bohr and Mottelson (1969)); (**b**) *independent pair motion*, nucleons interacting through an effective pairing interaction, sum of a short (v_p^{bare}) and long range (v_p^{ind}) NN–pairing potential, confined by a mean field whose parameters are freely adjusted so as to profit at best the pair coupling scheme.

In other words, one moves from a situation in which one assumes: (a)$H = T + v \approx T + U$ (ansatz $\langle v - U \rangle \approx 0$) to another in which (b) $H = T + v \approx T + U' + v_p^{eff}$ (ansatz $\langle v - U' - v_p^{eff} \rangle \approx 0$ and $|U'| < |U|$, $|v_p^{eff}| \ll |U'|$). Moving from the first to the second situation pairs of nucleons moving in time reversal states will tend

to recede from each other. Now, to the extent that one is interested in describing real nuclei lying along the stability valley like e.g. ^{120}Sn, one will rightly posit that the ansatz (a) is more realistic than (b), in keeping with the fact that $(U' + v_p^{eff})$ represent a much smaller fraction of v than U does. Consequently, the right view seems to be that of (a) plus pairing, in which case Cooper pair partners approach each other, if nothing else, because of angular correlation[14]. The "correctness" of picture (b) reemerges, as already stated, in connection with heavy ion collisions between superfluid nuclei in keeping with the fact that one– and two–particle transfer reactions absolute cross sections have the same order of magnitude. And it is likely that picture (b) becomes quite useful already in discussing the structure of light halo nuclei. Within this context we note that the fact that ${}^{9}_{3}\mathrm{Li}_6$ is well bound ($N = 6$ isotone parity–inverted closed shell), ${}^{10}_{3}\mathrm{Li}_7$ is not while ${}^{11}_{3}\mathrm{Li}_8$ is again bound, indicates that we are confronted with a pairing phenomenon. Allowing the two neutrons moving outside $N = 6$ closed shell to correlate in the configurations $j^2(0)(s^2_{1/2}, p^2_{1/2}, d^2_{5/2} \dots)$ through a short range bare pairing interaction, e.g. the v_{14} Argonne NN–potential, does not lead to a bound state. The system lowers the relative momentum of the pair exchanging at the same time the low–lying dipole vibration of the associated diffuse system becoming, eventually, bound, ever so weakly ($S_{2n} = 380$ MeV). The radius of the resulting system ($R(^{11}\mathrm{Li})$=4.58 ± 0.13 fm) corresponds, in the parametrization $R_0 = 1.2A^{1/3}$ fm, to an effective mass $A \approx 60$. So undoubtedly the system has swelled. Although the correlation length of the neutron Cooper is restricted to $2 \times R(^{11}\mathrm{Li}) \approx 9$ fm, half of the estimated value $\xi \approx 20$ fm, it is double as large as $2 \times R_0(^{11}\mathrm{Li}) \approx 5.4$ fm. Consequently, the result displayed ($|\Psi_0(\mathbf{r}_1, \mathbf{r}_2)|^2$) in Fig. **??** (II) b) should be read with care. It is also noted that the associated mean field potential can be parametrized in terms of a standard Woods–Saxon potential (see Bohr and Mottelson (1969), Eq. (2–182) p. 239) of depth $U' \approx -36$ MeV, much weaker than the typical value of $U \approx -50$ MeV.

It will be surprising if this bootstrap–like mechanism to profit from very low, (unstable) nuclear densities to generate transient medium polarization effects which acting between Cooper pair partners separated by distances of the order of ξ to eventually stabilize a halo system, was a unique property of ^{11}Li. In fact, one can expect particular situations of s and p states at threshold eventually leading to a symbiotic halo Cooper pair with such a small value of S_{2n}, which eventually gives rise to a value of $2R \approx \xi$. A problem in the quest of such exotic, but standard Cooper pair picture in condensed matter superconductors, may be related in the nuclear case to the very short lifetime of the resulting system (within this context one is reminded of the fact that $\tau_{1/2}(^{11}\mathrm{Li})$=8.75 ms).

In the above discussion, mention has been made to a bootstrap generation of infinite, condensed–matter–like situation (also in connection with Fig. 1.7.1, in which one was referring to finite density overlap across barriers between superfluid nuclei). Let us remind us that such a methodologic approach is no new to nuclear physics. Let us bring as example the definition of a nuclear temperature and of the

[14] Bertsch, G. F. et al. (1967); Ferreira, L. et al. (1984); Matsuo, M. (2013) and refs. therein.

associated energy reservoir which can be shared statistically. How does one make a heat reservoir in the nucleus? While it is not a thermal bath in the classical sense, when the system emits a neutron or a γ–ray in the cooling process, it exchanges energy statistically the freed particle. This is in keeping with the fact that the energy distribution of the emitted nucleon or γ–ray is determined by the density of levels of the daughter states (Bortignon, P. F. et al. (1998)). Concerning the γ–decay of the compound nucleus, it proceeds through $E1$–transitions, essentially profiting of the Axel–Brink ansatz introduced in nuclear physics to deal with this types of cooling processes. Within the bootstrap ansatz of symbiotic Cooper pair binding, we introduce a straightforward generalization of the Axel–Brink hypothesis based on well established experimental results, Namely the fact that the line shape and thus also the percentage of EWSR and decay properties of the GDR will reflect the static (splitting) and dynamic (motional narrowing) deformation properties of the state on which the GDR is built upon[15]

In the case of halo nuclei this generalization is not only quantitative but also qualitative. A sensible fraction of the TRK sum rule is found almost degenerate with the ground state. From the elastic antenna–like response typical of the high energy ($\hbar\omega_{GDR} \approx 80\text{MeV}/A^{1/3}$) GDR one is now confronted with a very low energy (<1 MeV) plastic dipole response (GDPR). Regarding the consequences this has for the $L = 1$ induced interaction between nucleons one moves from dipole–dipole (static moment interactions) to dispersive (retarded) contributions, emerging essentially from quantum mechanical ZPF. In other words, and making use of an analogy with atomic physics, one moves from an interaction between polar molecules, to a "purely" quantal interaction arising from the mutual polarization of one molecule in the rapidly changing field of the other (due to the instantaneous configuration of electrons and nuclei associated with ZPF) and viceversa, only one operative in the case of non–polar molecules. It is this second one which dominates the van der Waals interaction (App. **??**) and, similarly, it is one which can lead to an almost resonant gluing of Cooper pair halos. In other words, the extension of the Axel–Brink hypothesis within the present context allegedly implies to move from a possibility to a must. If one sees a halo one expects a GDPR.

The challenges faced to learn about the physical basis of pairing in nuclei are comparable to those encountered to extract a collective vibration from a background much larger than the signal, as it was the case in the case in the discovery of the GDR in hot nuclei[16]. In trying to observe the full range of pairing effects in nuclei, one has the advantage to start with the system at zero temperature for free. On the other hand one needs to substract the very large, state dependent effects of the "external" mean field, a challenge not second to that faced by condensed matter practitioners to study low–temperature superconductivity in general, and the Josephson effect in particular.

[15]Le Tourneaux (1965); Bohr, A. and Mottelson (1975); Bortignon, P. F. et al. (1998) and refs. therein.

[16]See e.g. Bortignon, P. F. et al. (1998) Figs. 1.4 and 6.8, and refs. therein.

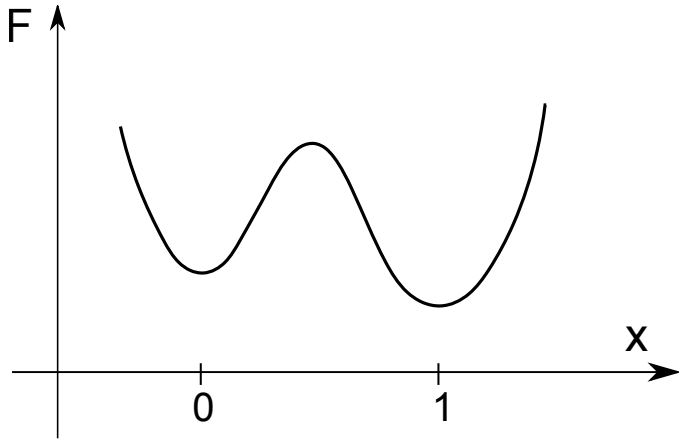

Figure 1.3.1: A schematic representation of nucleon tunneling between target and projectile. The free energy $F = U - TS$ which for the zero temperature situation under consideration (e.g. ^{120}Sn$(p,d)^{119}$Sn, ^{120}Sn$(p,d)^{118}$Sn) coincides with the potential energy as a function of the nucleon coordinate x. For $x = 0$ the nucleon is assumed to be bound to the target system. For $x = 1$ the nucleon has undergone tunneling becoming bound to the outgoing particle. In other words x_1 jumps from the value 0 to the value 1 in the tunneling process $(x_1, 0 \rightarrow 1)$, the same for the coordinate of the second nucleon.

1.3 Correlations between nucleons in Cooper pair tunneling

Let us call x_1 and x_2 the coordinates of the Cooper pair partners. Let us furthermore assume they can only take two values: 0 when they are bound to the target nucleus, 1 when they have tunneled and become part of the outgoing particle (see Fig. 1.3.1).

The correlation between the two nucleons is measured by the value[17]

$$\langle x_1 x_2\rangle - \langle x_1\rangle\langle x_2\rangle = \int d\gamma P_2 \times 1 \times 1 - \int d\gamma P_1 \times 1 \int d\gamma' P_1' \times 1 = P_2 - P_1 P_1', \tag{1.3.1}$$

$d\gamma$ being the differential volume in phase space, normalized with respect to the corresponding standard deviations, that is, with respect to

$$\sigma_{x_1}\sigma_{x_2} = \left[\left(\langle x_1^2\rangle - \langle x_1\rangle^2\right)\left(\langle x_2^2\rangle - \langle x_2\rangle^2\right)\right]^{1/2}. \tag{1.3.2}$$

Making use of the fact that

$$\langle x_1^2\rangle = \int d\gamma P_1 \times 1^2 = P_1, \tag{1.3.3}$$

[17] Basdevant and Dalibard (2005).

and

$$\langle x_1 \rangle = \int d\gamma P_1 \times 1 = P_1, \tag{1.3.4}$$

One obtains the function which measures the correlations between nucleons 1 and 2, namely,

$$C = \frac{\langle x_1 x_2 \rangle - \langle x_1 \rangle \langle x_2 \rangle}{\sqrt{\left(\langle x_1^2 \rangle - \langle x_1 \rangle^2\right)\left(\langle x_2^2 \rangle - \langle x_2 \rangle^2\right)}} = \frac{P_2 - P_1 P_1'}{\sqrt{\left(P_1 - P_1^2\right)\left(P_1' - P_1'^2\right)}}. \tag{1.3.5}$$

Because both nucleons are identical and thus interchangeable, $P_1 = P_1'$. Thus

$$C = \frac{P_2 - P_1^2}{P_1 - P_1^2}. \tag{1.3.6}$$

Making use of the empirical values

$$P_1 \approx P_2 \approx 10^{-3} \tag{1.3.7}$$

leads to,

$$C = \frac{10^{-3} - 10^{-6}}{10^{-3} - 10^{-6}} \approx 1. \tag{1.3.8}$$

In other words, within the independent pair motion regime, nucleon partners are solidly anchored to each other: if one nucleon goes over, the other does it also. This is so in spite of the very liable and fragile structure of the nuclear Cooper pairs ($\Delta/\epsilon_F \ll 1$), a clear example of which is being provided by ^{11}Li. In fact, if one picks–up a neutron from ^{11}Li (^{11}Li$(p,d)^{10}$Li), the other one breaks up essentially instantaneously, ^{10}Li being unbound. In spite of this fact, the probability associated with the reaction ^{11}Li(^{11}Li,^{9}Li(gs))^{1}H is (see Table II Potel et al. (2010) and eq. (**??**) as well as Sect. **??**) is given by,

$$P_2 = \frac{5.7 \pm 0.9\,\text{mb}}{2\pi(4.83\,\text{fm})^2} \approx 4 \times 10^{-3}, \tag{1.3.9}$$

a value which is much larger than the value of 4.81×10^{-6} associated with the breakup process mentioned above (see $l = 0$ columns 1 and 3 of Table **??**), let alone P_1^2 $(1.02{\times}10^{-3})^2 \approx 10^{-6}$ as given in Table 1.3.1. One may be surprised of this result, in keeping with the fact that most of the two–nucleon transfer reaction cross section ($\approx 80\%$) is associated with successive transfer (see Fig. **??**). The answer is in any case contained in the relation (1.2.19), applicable both for static and dynamic pair modes, in keeping with the fact that in nuclei, dynamic spontaneous breaking of gauge invariance is of similar importance as the static one[18]. It is of notice that in successive transfer processes the one– particle channels are virtual, that is with no outgoing running waves and thus with a very different coupling to the continuum

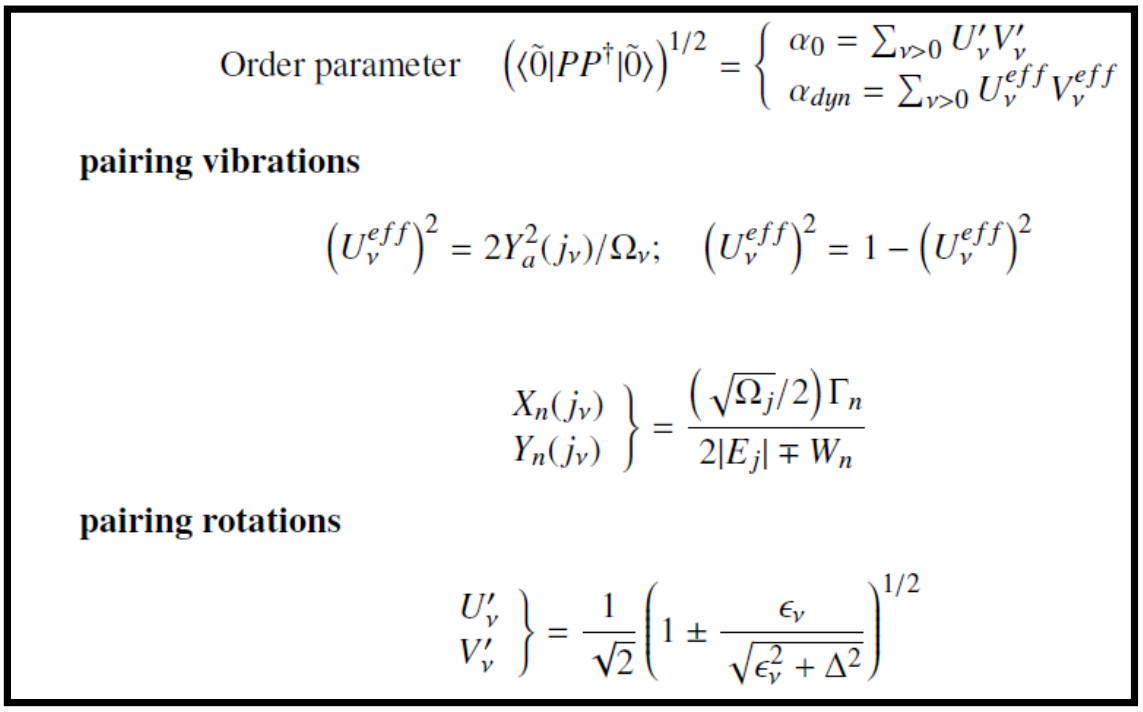

Figure 1.3.2: Order parameter associated with static and dynamic pair correlations (see Potel, G. et al. (2013b)).

1	p_l
0	1.02×10^{-3}
1	2.40×10^{-3}
2	1.26×10^{-2}
3	1.84×10^{-2}
4	6.13×10^{-3}
5	1.39×10^{-3}
6	2.89×10^{-4}
7	5.04×10^{-5}
8	6.51×10^{-6}
9	5.87×10^{-7}

Table 1.3.1: Probabilities p_l (see Eq. (1.2.14) and App. **??**) associated with the reaction ^{1}H(^{11}Li,^{10}Li(gs))^{2}H calculated with the same bombarding conditions as those associated with ^{1}H(^{11}Li,^{9}Li(gs))^{3}H cf. Table **??**. It was assumed that the amplitude with which the single particle orbital $s_{1/2}$ enters in the $|^{10}\text{Li}(1/2^+)\rangle$ (gs) is $\sqrt{0.5}$ (cf. Eqs. (**??**)–(**??**)).

states than in the case of real asymptotic waves. This coupling influences in an important way the structure aspects of the problem, less the reaction ones. But again, the simple answer is that the halo Cooper pair in its tunneling between ^{11}Li and ^{1}H does not see neither ^{10}Li nor ^{2}H, behaving as an entity. Surprisingly, the regime of independent pair motion extends also to the single pair situation. Two–particle tunneling can specifically probe such a regime.

A direct consequence of the above parlance is the fact that the Cooper pair rigidity emerges from phase coherence (in gauge space), and leads to the generalized rigidity of pairing rotational (static) and vibrational (dynamic) bands which can be instantaneously set into rotation (vibration) with just the push imparted in gauge space by the transferred pair, without this fact violating any limiting velocity, neither of medium propagating signals nor of light.

1.4 Pair transfer

The semiclassical two–nucleon transfer amplitudes fulfill, in the **independent particle limit**, the relations[19],

$$a^{(1)}_{sim} = a^{(1)}_{NO}, \tag{1.4.1}$$

and

$$a^{(2)}_{succ} = a^{(1)}_{one-part} \times a^{(1)}_{one-part}, \tag{1.4.2}$$

with

$$a + A \rightarrow f + F \rightarrow b + B, \tag{1.4.3}$$

corresponding to the product of two single nucleon transfer processes. On the other hand, in the **strong correlation limit** one can write, making use of the post–prior representation

$$\tilde{a}^{(2)}_{succ} = a^{(2)}_{succ} - a^{(1)}_{NO}. \tag{1.4.4}$$

Thus

$$\lim_{E_{corr}\rightarrow\infty} \tilde{a}^{(2)}_{succ} = 0, \tag{1.4.5}$$

and all transfer is, in this case, due to simultaneous transfer. Actual nuclei are close to the independent particle limit (E_{corr} (1–2 MeV) $\ll \epsilon_F \approx$ 37 MeV). Then successive transfer is the major contribution to pair transfer processes. But successive transfer seems to break the pair *right? Wrong. Why?* let us see below.

1.4.1 Cooper pair dimensions

Typical correlation energies of Cooper pairs are 1–2 MeV. Now, such a system (dineutron or diproton) is not bound and needs of an external field to be confined.

[18] cf. Fig. **??**, cf. also Sect. 1.8 and Fig. 4 Potel, G. et al. (2013b); cf. Fig. 1.3.2

[19] see App. **??**, also Potel, G. et al. (2013a).

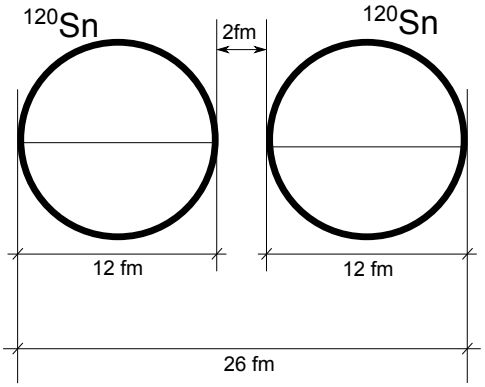

Figure 1.4.1: Schematic representation of two Sn–isotopes (radius $R_0 \approx 6$ fm) at the distance of closest approach in a heavy ion collision.

This is the role played by the single–particle field (cf. Fig. 1.1.3). Let us now calculate the dimensions of a Cooper pair (correlation length). We start with the relation

$$\delta x \delta p \geq \hbar \quad \delta\epsilon \approx 2E_{corr}, \tag{1.4.6}$$

where

$$\epsilon = \frac{p^2}{2m}; \quad \delta\epsilon = \frac{2p\delta p}{m} \approx v_F \delta p, \tag{1.4.7}$$

and thus

$$\delta\epsilon \approx 2E_{corr} \approx v_F \delta p, \tag{1.4.8}$$

leading to

$$\xi = \delta x = \frac{\hbar}{\delta p} \approx \frac{\hbar v_F}{2E_{corr}} \quad \text{(correlation length)}. \tag{1.4.9}$$

Making use of the fact that in nuclei,

$$\frac{v_F}{c} \approx 0.3, \tag{1.4.10}$$

one obtains

$$\xi \approx \frac{200 \text{ MeV fm } \times 0.3}{2 \text{ MeV}} \approx 30 \text{ fm}. \tag{1.4.11}$$

Consequently, successive and simultaneous transfer feel equally well the pairing correlations giving rise to long range order. This virtual property can become[20] real in e.g. a pair transfer between two superfluid tin isotopes (Fig. 1.4.1).

Objection

What about $v_{pairing}(= G)$ becoming zero, e.g. between the two nuclei?

[20] See von Oertzen, W. (2013)

Answer

$$\frac{d\sigma(a(=b+2)+A\rightarrow b+B(=A+2))}{d\Omega}\sim|\alpha_0|^2, \tag{1.4.12}$$

$$\alpha_0=\langle BCS(A+2)|P^\dagger|BCS(A)\rangle=\sum_{\nu>0}U_\nu(A)V_\nu(A+2). \tag{1.4.13}$$

(cf. also App. 1.8).

Objection

Relation (1.4.13) is only valid for simultaneous transfer, *right? Wrong*.

Answer

The order parameter can also be written as,

$$\begin{aligned}\alpha_0&=\sum_{\nu,\nu'>0}\langle BCS|a^\dagger_\nu|int(\nu')\rangle\langle int(\nu')|a^\dagger_{\bar\nu}|BCS\rangle\\&\approx\sum_{\nu,\nu'>0}\langle BCS(A+2)|a^\dagger_\nu\alpha^\dagger_{\nu'}|BCS(A+1)\rangle\langle BCS(A+1)|\alpha_{\nu'}a^\dagger_{\bar\nu}|BCS(A)\rangle\\&=\sum_{\nu,\nu'>0}\langle BCS(A+2)|V_\nu(A+2)\alpha_{\bar\nu}\alpha^\dagger_{\nu'}|BCS(A+1)\rangle\\&\times\langle BCS(A+1)|\alpha_{\nu'}U_\nu(A)\alpha^\dagger_{\bar\nu}|BCS(A)\rangle=\sum_{\nu>0}V_\nu(A+2)U_\nu(A),\end{aligned} \tag{1.4.14}$$

where the (inverse) quasiparticle transformation relation $a^\dagger_\nu=U_\nu\alpha^\dagger_\nu+V_\nu\alpha_{\bar\nu}$ was used. Examples of two–nucleon spectroscopic amplitudes involving superfluid targets, namely those associated with the reactions ^{112}Sn$(p,t)^{110}$Sn(gs) and ^{124}Sn$(p,t)^{122}$Sn(gs) are given in Table **??**. Making use of these amplitudes (first column) and of global optical parameters, the two–nucleon transfer absolute differential cross section of the reaction ^{112}Sn$(p,t)^{110}$Sn(gs) at center of mass bombarding energy of $E_p=26$ MeV, was calculated making use of the software cooper based on second order DWBA and taking into account successive and simultaneous transfer properly corrected for non–orthogonality (cf. Chapter **??** and App. **??**). It is compared with experimental data in Fig. 1.4.2 (a). The corresponding absolute integrated cross sections are 1310 μb and 1309±200 μb respectively. The largest contribution to the cross section arises from successive transfer, the cancellation between simultaneous and non–orthogonality amplitudes being important (Fig. 1.4.2 (b)). The above is a typical example of results of a systematic study of two–nucleon transfer reactions in terms of absolute cross sections[21].

Making use of two–nucleon spectroscopic amplitudes worked out within the framework of an extended shell model calculation (Table **??**, second column) one obtains very similar results to those displayed in Fig. 1.4.2 (a). In Fig. 1.4.3

[21] Potel, G. et al. (2013a), Potel, G. et al. (2013b) see also Ch. **??**, in particular Fig. **??**.

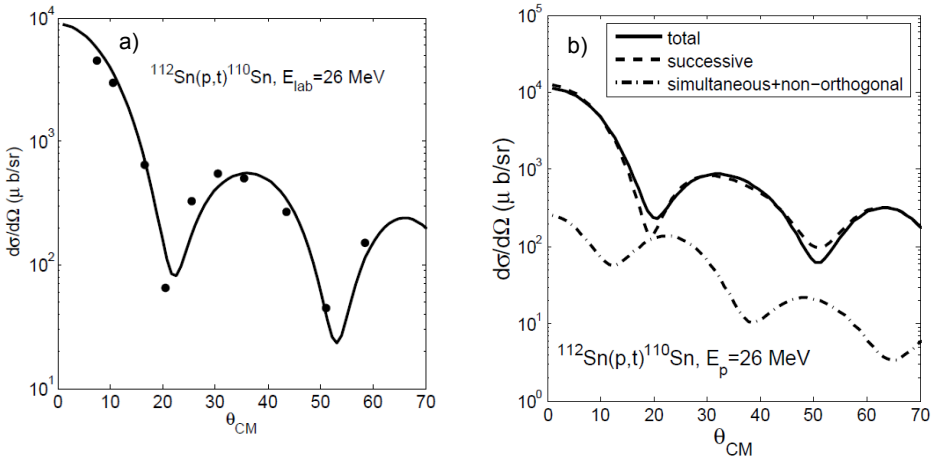

Figure 1.4.2: a) Absolute differential cross section associated with the reaction ^{112}Sn$(p,t)^{110}$Sn(gs) calculated with the software COOPER (mencionar apendice software) in comparison with the experimental data (Guazzoni, P. et al. (2006)). b) Details of the different contributions to the total absolute (p,t) differential cross section (for details see Potel, G. et al. (2013a), Potel, G. et al. (2013b)).

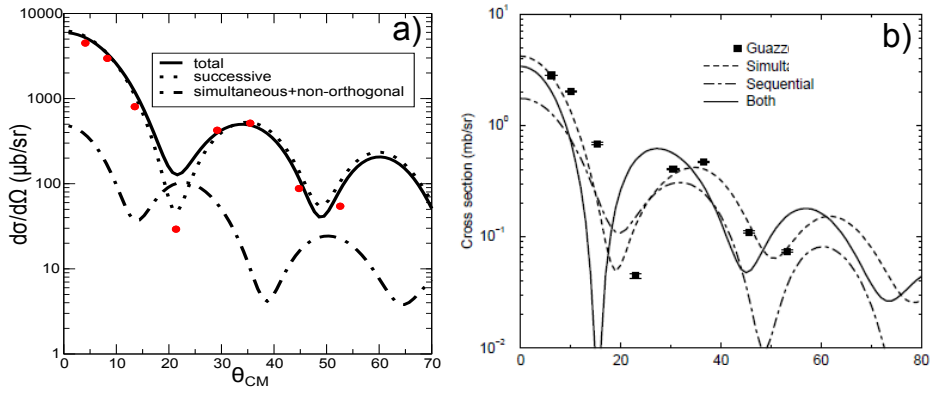

Figure 1.4.3: Absolute differential cross section associated with the reaction ^{124}Sn$(p,t)^{122}$Sn(gs) calculated making use of: a) second order DWBA taking into account non–orthogonality corrections and the two–nucleon spectroscopic amplitudes resulting from BCS (see Table **??**, third column; for details see Potel, G. et al. (2013a), Potel, G. et al. (2013b)) in comparison with experimental data (Guazzoni, P. et al. (2011)). b) As above, but making use of FRESCO (reaction) and of shell model two–nucleon overlaps (structure); cf. Table **??** fourth column (for details cf. Thompson, I.J. (2013)).

(a) we report results similar to those displayed in Fig. 1.4.2, but for the case of the reaction ^{124}Sn$(p,t)^{122}$Sn(gs) calculated within second order DWBA making use of the BCS spectroscopic amplitudes (Table **??** third column). We display in Fig. 1.4.3 (b) the absolute differential cross section calculated with NuShell spectroscopic amplitudes and the coupled channel software FRESCO[22].

Let us now provide an example of two–nucleon transfer around a closed shell nucleus displaying well defined collective pairing vibrational modes. We refer, in particular, to the pair removal mode of ^{206}Pb, that is, to the reaction, ^{206}Pb$(t,p)^{208}$Pb(gs). Making use of the spectroscopic amplitudes displayed in Tables **??** and **??** and of global optical parameters, the associated absolute differential cross sections was calculated again with the software COOPER. It is displayed in Fig. 1.4.4 in comparison with experimental findings. In the same figure, the total differential cross section is compared with that associated with the TD (Tamm–Dankoff) description of ^{206}Pb(gs), that is, setting the pairing ground state correlations to zero ($\sum_i X_r^2(i) = 1, Y_r(k) \equiv 0$, see Table **??**). In this case, theory underpredicts observation by about a factor of 2, let alone the fact that the TD solution does not conserve the two–nucleon transfer sum rule. Also given in Fig. 1.4.4 is the predicted cross section associated with the pure configuration $|p_{1/2}^{-2}(0)\rangle$. These results underscore the role pairing correlations play in the properties of ^{208}Pb pair removal mode $|r\rangle \equiv |^{206}\text{Pb(gs)}\rangle$. Not only they make the two holes correlate both in angle and, radially on the surface. It lowers the momentum by increasing the volume over which the two fermions are allowed to move (spill out) and thus correlate, as required by the calculated correlation length ξ[23].

It is of notice, that within the effective reaction mechanism described in Sect. **??** pairing correlations increase the value of $\Omega_0(\approx 0.97)$. As a consequence the $l = n = 0$ two–neutron system gives a much larger contribution to the two–nucleon transfer process than those associated with $n = 1$ and 2, that is those proportional to Ω_1 and Ω_2 whose values are 0.25 and 0.06 respectively (cf. Eq. (**??**)). All these features boost the effective absolute two–nucleon pure configuration transfer cross section to the observed experimental value. While the results displayed in Fig. 1.4.4 were calculated making use of the full formalism of second order DWBA (cf. Figs. 1.1.1 and 1.1.2) the simplified expressions given in Eqs. (**??**–**??**) are useful to gain physical insight into the two–nucleon transfer process.

1.5 Comments on the optical potential

As a rule, the depopulation of the entrance, elastic channel $\alpha(a,A)$ (see Fig. 1.5.1) is mainly due to one–particle transfer channels $\phi(f(=a-1), F(=A+1))$. Other channels, like e.g. inelastic ones $\beta(a^*,A)$, $\gamma(a,A^*)$ being operative in particular situations, for example, when deformed nuclei are involved in the reaction process.

[22] Thompson, I.J. (2013).

[23] Bertsch, G. F. et al. (1967), Ferreira, L. et al. (1984); Matsuo, M. (2013) see also Figs. **??** a) and b) i.e. left part.

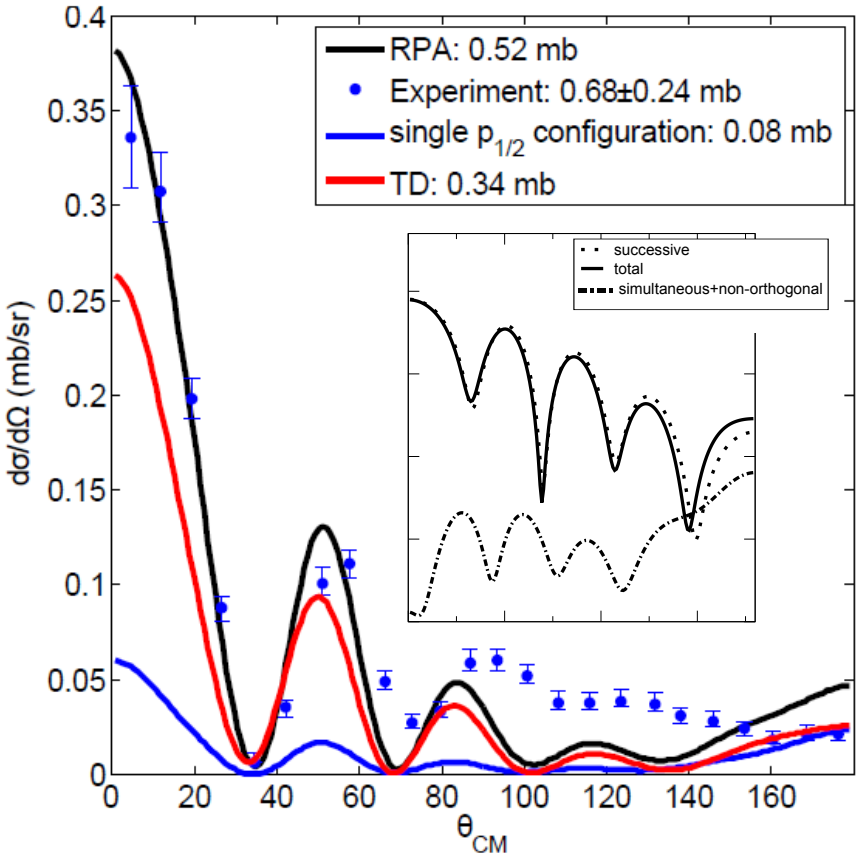

Figure 1.4.4: Absolute two–nucleon transfer differential cross section associated with the ^{206}Pb(t, p)^{208}Pb(gs) transfer reaction, that is, the annihilation of the pair removal mode of ^{208}Pb in comparison with the data (Bjerregaard, J. H. et al. (1966)). The theoretical cross sections were calculated making use of the spectroscopic amplitudes given in Tables **??** and **??** and of global optical parameters as reported in the reference above. Both RPA and TD amplitudes were used as well as a pure configuration $p^2_{1/2}(0)$.

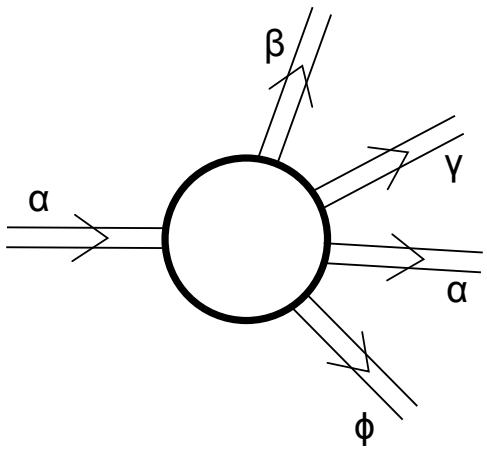

Figure 1.5.1: Schematic representation of entrance (α) and exit channels ($\beta, \gamma, \alpha, \phi$) of a nuclear reaction and of the interaction region.

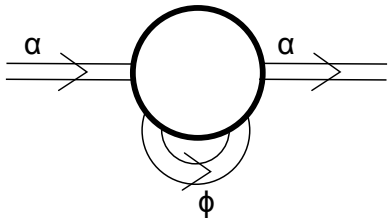

Figure 1.5.2: Schematic representation of the change in role of the one–nucleon transfer channel ϕ from being an open channel, (Fig. 1.5.1) to one which acts as a virtual channel contributing to the optical potential.

Let us assume that this is not the case. Thus, quite likely, the one–particle transfer channel ϕ is expected to be the main depopulating channel of the entrance channel α (cf. Fig. 1.5.2). This is also in keeping with the fact that the tail of the corresponding form factors, reaches further away than that of any other channel (cf. Fig. 1.5.5). In this case, the calculation of the optical potential[24], is quite reminiscent to the calculation of two–particle transfer (2nd order process), and can be carried out with essentially the same tools. In fact,

$$\begin{aligned} T^{(2)}_{succ} &\sim \langle fin|v|int\rangle\langle int|v|in\rangle \\ T^{(2)}_{NO} &\sim \langle fin|v|int\rangle\langle int|\mathbf{1}|in\rangle, \end{aligned} \tag{1.5.1}$$

where $|in\rangle = |a, A\rangle$, $|int\rangle = |f, F\rangle$ and $|fin\rangle = |b, B\rangle$ are the initial, intermediate, and final channels in a two–nucleon transfer reactions, which become

$$\begin{aligned} &\langle in|v|int\rangle\langle int|v|in\rangle \\ &\langle in|v|int\rangle\langle int|\mathbf{1}|in\rangle, \end{aligned} \tag{1.5.2}$$

as contributions to the optical potential (Fig. 1.5.2).

Let us elaborate on the above arguments within the context, for concreteness, of ^{11}Li and of the reaction $^{11}\mathrm{Li}(p,t)^{9}\mathrm{Li}$. In keeping with the fact that structure and reactions are just but two aspects of the same physics and that in the study of light halo nuclei, continuum states are to be treated on, essentially, equal footing in the calculation of the wavefunctions describing bound states (structure) as well as of the asymptotic distorted waves entering in the calculation of the absolute two-particle transfer differential cross sections (reaction; see Figs. 1.5.3 (a) and (b), the calculation of the optical potentials is essentially within reach (reaction, see Figs. 1.5.3 (c) and 1.5.4). Because the real and imaginary parts of complex functions are related by simple dispersion relations[25] it is sufficient to calculate only one of the two (real or imaginary) components of the self-energy function to obtain the full scattering, complex, nuclear dielectric function (optical potentials). Now, absorption is controlled by on-the-energy-shell contributions. Within this scenario

[24]It is of notice that the optical potential can be viewed as the complex "dielectric" function of direct nuclear reactions. In other words, the function describing the properties of the medium in which incoming and outgoing distorted waves propagate, properties which are, as a rule determined through the analysis of elastic scattering processes, under the assumption that the coupling between the relative motion(reaction) and intrinsic (structure) coordinates, occur only through a Galilean transformation (recoil effect) which smoothly matches the incoming with te outgoing waves (trajectories). Now, within the present context, namely that of the microscopic calculation of $U + iW$, non–locality and ω–dependence can be microscopically treated on equal footing through the calculation of structure properties. In particular, within the framework of NFT, taking into account the variety of correlations and couplings between single–particle and collective motion, elementary modes of nuclear excitation. Such an approach to structure and reaction provides the elements and rules for an *ab initio* calculations of the texture of the corresponding vacuum states, and thus of the bound and continuum properties of the nuclear quantal system by itself and in interaction. It is of notice that such a scenario includes also limiting situations like sub–barrier fusion processes (cf. e.g. Sargsyan, V. V. et al. (2013) and refs. therein) and also exotic decay (cf. e.g. Barranco, F. et al. (1988, 1990); Montanari et al. (2014), cf. also Brink, D. and Broglia (2005)).

[25]See, e.g., Mahaux, C. et al. (1985) and references therein.

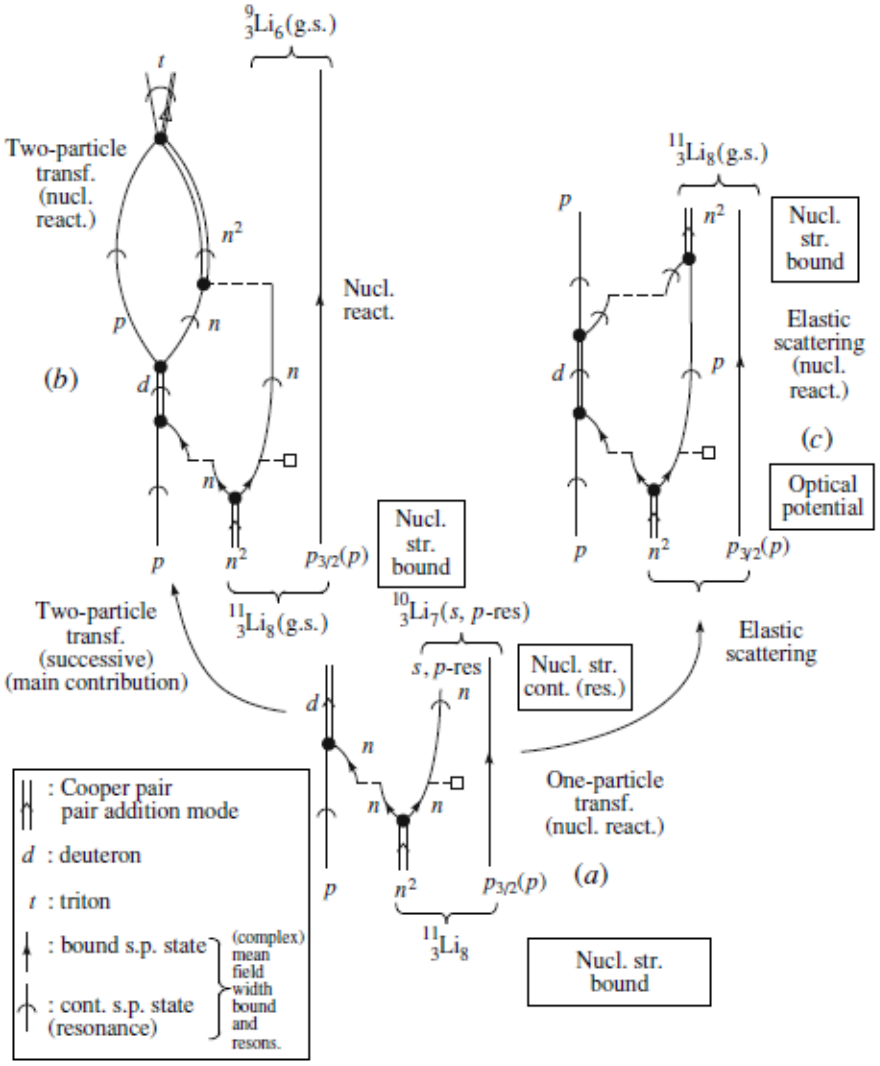

Figure 1.5.3: NFT diagrams summarizing the physics which is at the basis of the structure of ^{11}Li (Barranco, F. et al. (2001)) and of the analysis of the ^{11}Li$(p,t)^{9}$Li(g.s.) reaction (Potel et al. (2010)). In the figure emphasis is set on intermediate (like, e.g., ^{10}Li $+d$, see (a) and (b)) and elastic (see (c), see also Fig. 1.5.4) channels.

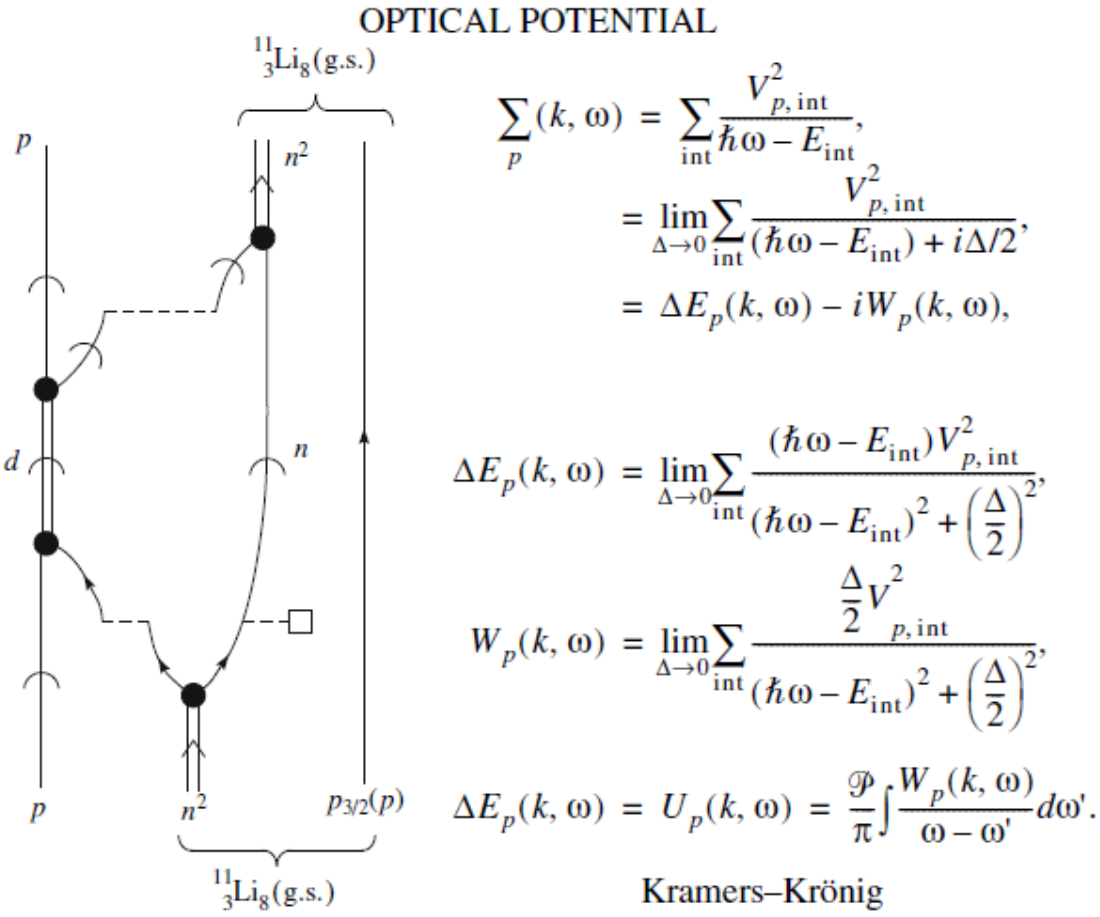

Figure 1.5.4: NFT diagrams and summary of the expression (see, e.g., Mahaux, C. et al. (1985) and references therein) entering the calculation of one of the contributions (that associated with one-particle transfer and, arguably, the dominant one) to the ^{11}Li $+p$ elastic channel optical potential. The self-energy function is denoted Σ_p, while the real and imaginary parts are denoted $\Delta E_p (= U_p)$ and W_p, respectively, the subindex p indicating the incoming proton. These quantities are, in principle, functions of frequency and momentum.

it is likely that the simplest way to proceed is that of calculating the absorptive potential and then obtain the real part by dispersion. Of notice that in heavy-ion reactions, one is dealing with leptodermous systems. Thus, the real part of the optical potential can, in principle, be obtained by convolution of the nuclear densities and of the surface tension[26]. Within the present context, one can mention the ambiguities encountered in trying to properly define a parentage coefficient relating the system of $(A + 1)$ nucleons to the system of A nucleons, and thus a spectroscopic amplitude. In other words, a prefactor which allows to express the absolute one-particle transfer differential cross section in terms of the elastic cross section. Making use of NFT diagrams like the one shown in Fig. 1.5.4 , it is possible to calculate, one at a time, the variety of contributions leading to one- and two– particle transfer processes as well as of the associated optical potential. Summing up the different contributions, taking also proper care of those arising from four-point vertex, tadpole processes, etc., a consistent description of the different channels can be worked out, in which the predicted quantities to be directly compared with observables are absolute differential cross sections, or, more generally, absolute values of strength functions for different scattering angles.

1.6 Weak link between superconductors

Two–nucleon transfer reactions involving superfluid nuclei display some similarities with Cooper pair tunneling between weakly coupled superconductors, in particular when discussing heavy ion reactions, but not only[27]. Within this context it is useful to remind the basic elements of the pair tunneling which is at the basis of the Josephson effect. In this section we essentially reproduce the description of the tunneling of Cooper pairs between two weakly coupled superconductors to be found in[28], arguably, the best physical presentation of the Josephson effect[29].

One starts with the many–body Hamiltonian of[30]

$$H = H_1 + H_2 + \sum_{kq} T_{kq}(a^{\dagger}_{k\uparrow}a_{k\uparrow} + a^{\dagger}_{-q\downarrow}a_{-q\downarrow}) + HC \tag{1.6.1}$$

where H_1 and H_2 are the separate Hamiltonian of the two superconductors on each side of the barrier, T_{kq} being the (exponentially) small tunneling matrix element from state k on one side to q on the other.

One can arrive to (1.6.1) by first finding sets of single–particle wavefunctions for each side separately, in the absence of the potential of the other system. Then one eliminates the non–orthogonality effects by perturbation theory (cf. the similarity with the arguments used in Sect. 1.2 as well as Sect. **??**; for details see

[26] Cf. e.g. Broglia and Winther (2005) and references therein.
[27] von Oertzen and Vitturi (2001); von Oertzen, W. (2013); Broglia and Winther (2004).
[28] Anderson (1964)
[29] Josephson (1962).
[30] Cohen et al. (1962)

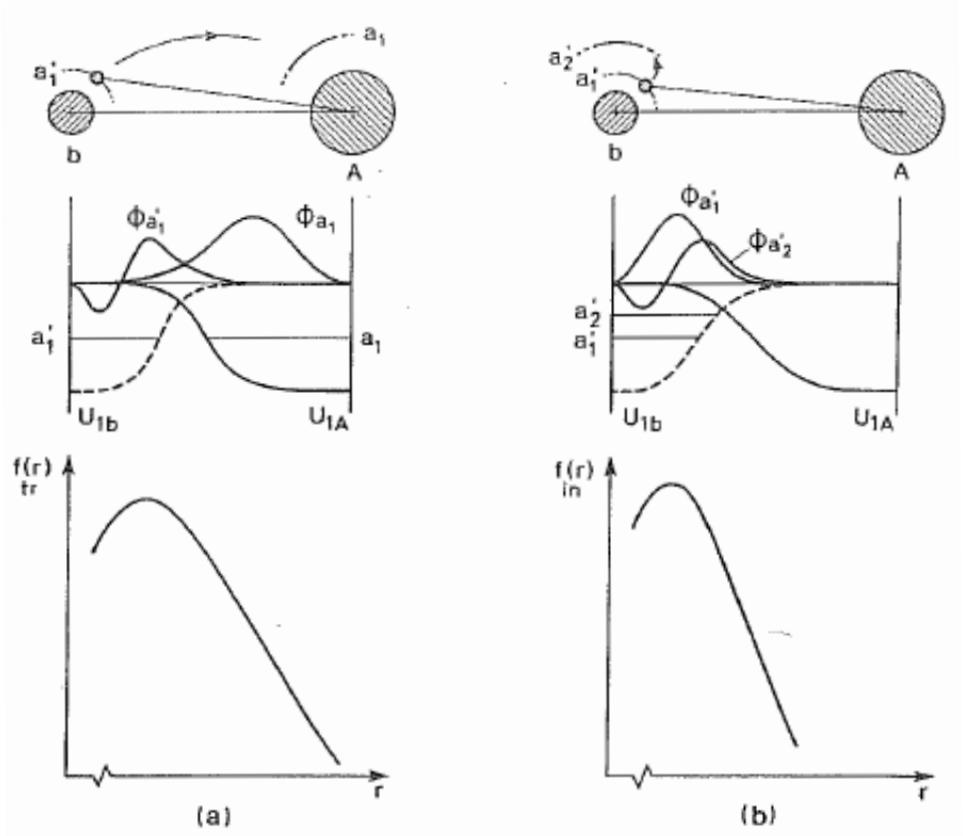

Figure 1.5.5: Schematic representation of the radial dependence of the one–particle transfer and inelastic form factors. In (a) a nucleon moving in the orbital with quantum numbers a'_1 in the projectile a is transferred under the action f the shell model potential U_{1A} to the target nucleus A into an orbital a_1. The dependence of the form factor on the distance between the two nuclei is determined by the overlap of the product of the single–particle wavefunctions $\phi_{a'_1}$ and ϕ_{a_1} with the potential U_{1A}. A schematic representation of this dependence is given at the bottom ofe target field (a). In (b) a nucleon in the projectile a is excited under the influence of the target field U_{1A} from the single–particle orbital with quantum numbers a'_1 to the orbital with quantum numbers a'_2. The dependence of the form factor on the distance between the cores is here determined by the overlap of the product of the functions $\phi_{a'_1}$ and $\phi_{a'_2}$ with the potential U_{1A}. A representation of this dependence is shown at the bottom of (b) (after Broglia and Winther (2005)).

Sect. **??**). It is of notice that a nuclear embodiment of such strategy but for the case superfluid–normal[31] tunneling is worked out in Ch. **??** and implemented in COOPER[32].

Let us now calculate the second order expression of (1.6.1) in the case in which the gaps of the two weakly linked superconductors are different. Making use of relations presented in Sect. **??** one can write, for $T = 0$,

$$\Delta E_2 = -2 \sum_{kq} |T_{kq}|^2 \frac{|V_k U_q + V_q U_k|^2}{E_k + E_q}. \tag{1.6.2}$$

With the help of

$$2U_k V_k^* = \frac{\Delta_k}{E_k}, \quad 2U_q V_q^* = \frac{\Delta_q}{E_q}, \tag{1.6.3}$$

and

$$|U_k|^2 - |V_k|^2 = \frac{\epsilon_k}{E_k}, \quad |U_q|^2 - |V_q|^2 = \frac{\epsilon_q}{E_q}, \tag{1.6.4}$$

where

$$E = \sqrt{\epsilon^2 + \Delta^2} \tag{1.6.5}$$

and

$$\Delta_k = \Delta_1 e^{i\phi_1}, \quad \Delta_q = \Delta_2 e^{i\phi_2} \tag{1.6.6}$$

one can write for the numerator of Eq. (1.6.2),

$$\begin{aligned} NUM &= \left(V_k U_q + V_q U_k\right)\left(V_k^* U_q^* + V_q^* U_k^*\right) \\ &= \left\{V_k^2 U_q^2 + V_q^2 U_k^2\right\} + \left[(U_k^* V_k)(U_q V_q^*) + (U_q^* V_q)(U_k V_k^*)\right]. \end{aligned} \tag{1.6.7}$$

It is of notice that, for simplicity, throughout this Appendix

$$V^2 \equiv |V|^2. \tag{1.6.8}$$

[31] It is of notice that pairing vibrations in nuclei are quite collective, leading to effective U and V occupation factor (cf. Fig. 1.3.2) (see also Potel, G. et al. (2013b)), the nuclear and the condensed matter expressions are very similar. Of course no supercurrent is expected between nuclei. However, the systems ^{120}Sn(gs), ^{119}Sn(j), ^{118}Sn(gs) form an ensemble of weakly coupled Fermi superfluids, with different (average) number of particles $(N, N-1, N-2)$, to which essentially all the BCS techniques, including those of the present Appendix can be applied (cf. Fig. 1.7.1). Of notice the parallel of this scenario with that associated with nuclei excited at rather high energies for which one defines a temperature. This is possible, because the excited (thermalized) nucleus is in equilibrium with the particles, namely neutrons and gamma–rays it emits, particles which act as a thermal bath, let alone the very high density of levels, of the compound nucleus (cf. Bertsch and Broglia (2005) p 171).

[32] Cf. App. **??**; cf. also Broglia and Winther (2005).

With the help of (1.6.3) the expression in the squared bracket in (1.6.7) can be written as

$$[\ ] = \frac{1}{4E_kE_q}\left(\Delta_k^*\Delta_q + (\Delta_k^*\Delta_q)^*\right) = \frac{1}{4E_kE_q}2\Re(\Delta_k^*\Delta_q). \tag{1.6.9}$$

Making use of the relations

$$\begin{aligned}\left(U_k^2 - V_k^2\right)\left(U_q^2 - V_q^2\right) &= U_k^2U_q^2 - U_k^2V_q^2 - V_k^2U_q^2 + V_k^2V_q^2 \\ &= -\left(U_k^2V_q^2 + V_k^2U_q^2\right) + \left(U_k^2U_q^2 + V_k^2V_q^2\right),\end{aligned} \tag{1.6.10}$$

and

$$\begin{aligned}1 = \left(U_k^2 + V_k^2\right)\left(U_q^2 + V_q^2\right) &= U_k^2U_q^2 + U_k^2V_q^2 + V_k^2U_q^2 + V_k^2V_q^2 \\ &= \left(U_k^2V_q^2 + V_k^2U_q^2\right) + \left(U_k^2U_q^2 + V_k^2V_q^2\right),\end{aligned} \tag{1.6.11}$$

one obtains,

$$1 - \left(U_k^2 - V_k^2\right)\left(U_q^2 - V_q^2\right) = 2\left(U_k^2V_q^2 + V_k^2U_q^2\right), \tag{1.6.12}$$

that is, twice the expression written in curly brackets in (1.6.7). Consequently

$$\{\ \} = \frac{1}{2}\left(1 - \left(U_k^2 - V_k^2\right)\left(U_q^2 - V_q^2\right)\right) = \frac{1}{2}\left(1 - \frac{\epsilon_k\epsilon_q}{E_kE_q}\right). \tag{1.6.13}$$

Thus, the sum of (1.6.9) and (1.6.13) leads to,

$$NUM = \frac{1}{2}\left(1 - \frac{\epsilon_k\epsilon_q}{E_kE_q} + \frac{\Re(\Delta_q^*\Delta_k)}{E_kE_q}\right) \tag{1.6.14}$$

and

$$\Delta E_2 = -\sum_{kq}\frac{|T_{kq}|^2}{E_k + E_q}\left(1 - \frac{\epsilon_k\epsilon_q}{E_kE_q} + \frac{\Re(\Delta_q^*\Delta_k)}{E_kE_q}\right). \tag{1.6.15}$$

With the help of (1.6.6) one can write

$$\Delta_k\Delta_q^* = \Delta_1\Delta_2e^{i(\phi_1-\phi_2)} = \Delta_1\Delta_2\left(\cos(\phi_1 - \phi_2) + i\sin(\phi_1 - \phi_2)\right). \tag{1.6.16}$$

Thus

$$\Re\Delta_k\Delta_q^* = \Delta_1\Delta_2\cos(\phi_1 - \phi_2), \tag{1.6.17}$$

where $\Re$ stands for real part. Making use of

$$\sum_k \to N_1\int d\epsilon_1, \quad \sum_q \to N_2\int d\epsilon_2 \tag{1.6.18}$$

where N_1 and N_2 are the density of levels of one spin at the Fermi energy one finally obtains

$$\begin{aligned}\Delta E_2 &\approx -N_1 N_2 \Delta_1 \Delta_2 \langle |T_{kq}|^2 \rangle \cos(\phi_1 - \phi_2) \int_{-\infty}^{\infty} \int_{-\infty}^{\infty} \frac{d\epsilon_1 d\epsilon_2}{E_1 E_2 (E_1 + E_2)} \\ &\approx -N_1 N_2 \langle |T_{kq}|^2 \rangle \cos(\phi_1 - \phi_2) 2\pi^2 \frac{\Delta_1 \Delta_2}{\Delta_1 + \Delta_2} \end{aligned} \tag{1.6.19}$$

Consequently, the maximum possible supercurrent is the same as the normal current at a voltage V_{equiv} equal to $\pi \Delta_1 \Delta_2 / (\Delta_1 + \Delta_2)$.

1.7 Phase coherence

The phase of a wavefunction and the number of nucleons (electrons in condensed matter) are conjugate variables: gauge invariance, i.e. invariance under phase changes, implies number conservation in the same way that rotational invariance implies angular momentum conservation.

Example:

$$\Psi = a_1^\dagger a_2^\dagger \cdots a_N^\dagger \Psi_{vac}.$$

Multiplying the creation operators by a phase factor,

$$a'^\dagger = e^{-i\phi} a^\dagger,$$

one can rewrite

$$\begin{aligned}\Psi =& (e^{i\phi} a_1'^\dagger)(e^{i\phi} a_2'^\dagger) \cdots (e^{i\phi} a_N'^\dagger) \Psi_{vac} \\ =& e^{iN\phi} \Psi'.\end{aligned}$$

Thus

$$-i \frac{\partial}{\partial \phi} \Phi = N e^{iN\phi} \Psi' = \Psi,$$

where

$$N = -i \frac{\partial}{\partial \phi}; \qquad \phi = i \frac{\partial}{\partial N}$$

and

$$[\phi, N] = 1; \quad \Delta\phi \Delta N = 1.$$

In this case Ψ (wavefunction referred to the laboratory system) and Ψ' (wavefunction referred to the intrinsic system) represent the same state. A phase change for a gauge invariant function is just a trivial operation. Like to rotate a rotational invariant function. Quantum mechanically nothing happens rotating a spherical system (in 3D–, gauge, etc.) space.

The situation is very different in the case of the wavefunction

$$\begin{aligned}|BCS(\phi)\rangle_{\mathcal{K}} &= \prod_{\nu>0}\left(U_\nu + V_\nu a_\nu^\dagger a_{\bar{\nu}}^\dagger\right)|0\rangle,\\ &= \prod_{\nu>0}\left(U_\nu + e^{2i\phi}V_\nu a_\nu'^\dagger a_{\bar{\nu}}'^\dagger\right)|0\rangle,\\ &= \prod_{\nu>0}\left(U_\nu' + V_\nu' a_\nu'^\dagger a_{\bar{\nu}}'^\dagger\right)|0\rangle,\\ &= |BCS(\phi=0)\rangle_{\mathcal{K}'},\end{aligned}$$

where

$$U_\nu = |U_\nu| = U_\nu'; \quad V_\nu = e^{2i\phi}V_\nu' \ (V_\nu' = |V_\nu|),$$

and

$$|BCS(\phi)\rangle_{\mathcal{K}} = \left(\prod_{\nu>0}U_\nu\right)\sum_{n=0,1,2}^{N_0/2} e^{i2n\phi}\left(\sum_{\nu>0}^{N/2}\frac{c_\nu}{\sqrt{n}}P_\nu'^\dagger\right)^n|0\rangle,$$

with

$$c_\nu = \frac{V_\nu}{U_\nu}; \quad n : \#\text{ of pairs}; \quad P_\nu'^\dagger = a_\nu'^\dagger a_{\bar{\nu}}'^\dagger,$$

is a wavepacket in particle number,

$$\begin{aligned}|BCS(\phi)\rangle_{\mathcal{K}} &= \left(\prod_{\nu>0}U_\nu\right)\sum_n e^{i2n\phi}|2n\rangle,\\ &= \left(\prod_{\nu>0}U_\nu\right)\sum_n e^{i2n\phi}|N\rangle. \qquad (1.7.1)\end{aligned}$$

Let us now apply the gauge angle operator

$$\begin{aligned}\hat{\phi}|BCS(\phi)\rangle_{\mathcal{K}} &= i\frac{\partial}{\partial N}|BCS(\phi)\rangle_{\mathcal{K}}\\ &= -\phi\left(\prod_{\nu>0}U_\nu\right)\sum_n e^{i2n\phi}|N\rangle = -\phi|BCS(\phi)\rangle_{\mathcal{K}}.\end{aligned}$$

Thus the state $|BCS(\phi=0)\rangle_{\mathcal{K}'}$ is rigidly aligned in gauge space in which it defines a privileged orientation (z').

An isolated nucleus will not remain long in this product type state. Due to the term $(G/4)\left(\sum_{\nu>0}\left(U_\nu^2+V_\nu^2\right)\left(\Gamma_\nu^\dagger-\Gamma_\nu\right)\right)^2$ in the residual quasiparticle Hamiltonian it will fluctuate, (QM, ZPF Goldstone mode) it will decay into a state

$$|N\rangle \sim \int d\phi e^{iN\phi}|BCS(\phi)\rangle_{\mathcal{K}}, \qquad (1.7.2)$$

member of a pairing rotational band around neutron mass number N: for example the ground states of the Sn–isotopes around $N_0 = 68$ (see Fig. **??**). Because $E_R = (\hbar^2/2\mathcal{I})(N - N_0)^2 = (G/4)(N - N_0)^2 = G/4(\frac{1}{\delta\phi})^2$ is the kinetic energy of rotation in (nuclear) gauge space, and $G/4 \approx 25/(4N_0) \approx 0.0092$ MeV, the wavepacket (1.7.1) will decay[33] in the state (1.7.2) in a time of the order of $\hbar/E_R \approx \hbar/(4 \times 0.0092 \text{ MeV})$ $(N = N_0 \pm 2) \approx 10^{-19}$ sec. In other words, superfluid nuclei cannot be prepared, in isolation, in states with coherent superposition of different N–values. The common assumption that N is fixed, ϕ meaningless is correct. This is also the case for real superconductors. In fact, the corresponding state (1.7.1) even if prepared in isolation would dissipate because there is actually a term in the energy of the superconductor depending on N, namely the electrostatic energy $e(N - N_0)^2/2C = e^2/2C(\partial/\partial\phi)^2$, where C is the electrostatic capacity. The system will dissipate, no matter how small $\delta\phi$ is. In fact, let us assume $\delta\phi = 1$ degree $(= \pi/180 = 0.017)$. The kinetic energy of rotation in gauge space is $\sim (e^2/2C)(1/\delta)^2(\delta N \delta\phi/2\pi \sim 1)$, and

$$\Delta E = \frac{1.44 \text{ fm MeV}}{1 \text{ cm } (1^\circ)^2} \sim 1.44 \times 10^{-13} \text{ MeV}, \tag{1.7.3}$$

which corresponds to an interval of time

$$\Delta t \approx \frac{\hbar}{1 \text{ MeV}} \frac{10^{13}}{1.44} \approx \frac{0.667 \times 10^{-21} \text{ sec}}{1.44} \times 10^{13} \approx 10^{-9} \text{ sec}. \tag{1.7.4}$$

The opposite situation is that of the case in which one considers different parts of the same superconductor. In this case one can define relative variables $n = N_1 - N_2$ and $\phi = \phi_1 - \phi_2$ and again $n = -i\partial/\partial\phi$ and $\phi = i\partial/\partial n$. Thus, locally there is a superposition of different n states: ϕ is fixed so n is uncertain. It is clear that there must be a dividing line between these two behaviors, perfect phase coherence and negligible coherence, namely the Josephson effect.

In the nuclear case, one can view the systems $|BCS(A + 2)\rangle$ and $|BCS(A)\rangle$ as parts of a fermion superfluid (superconductor) which, in presence of a proton $(p + (A + 2))$ are in weak contact to each other, the $d + |BCS(A + 1)\rangle$ system (without scattering, running waves, but as a closed, virtual, channel) acting as the dioxide layer of a Josephson junction.

Clearly, again, the total phase of the assembly is not physical. However, the relative phases can be given a meaning when one observes, as one does in e.g.

[33] Within this context note that setting in phase at $t = 0$ all the states in which a GDR breaks down through the hierarchy of doorway–states–coupling, they would dissipate like a wavepacket of free particles after 10^{-22} sec (assuming $\Gamma_{GDR} \approx 3 - 4$ MeV). It is of notice that the GDR will eventually branch into the ground state, although $\Gamma_\gamma \ll \Gamma_{GDR}$, in keeping with the fact that the $t = 0$ phase coherent states are individually stationary. What is not stationary is its phase coherence. Pushing the analogy a step further, one can say that in quantum mechanics, while the outcome of an experiment is probabilistic the associated probability evolve in a deterministic way (Born (1926)). This is the reason why a large gamma ray detector will reveal a well defined peak of the resonant dipole state long after its lifetime deadline ($\hbar/\Gamma$). Also, while one can obtain a completely (classical) picture of a face making use of single photons, provided one waits long enough.

metallic superconductors, that electrons can pass back and forth through the barrier, leading to the possibility of coherence between states in which the total number of electrons is not fixed *locally*. Under such conditions there is, for instance, a coherence between the state with $N/2$ electrons in one half of the block and $N/2$ in the other, and that with $(N/2) + 2$ on one side side and $(N/2) - 2$ on the other.

Under favorable conditions, in particular of Q–value for the different channels involved and, similarly to the so called backwards rise effect, one may, arguably, observe signals of the coherence between systems $(A + 2)$ and A in the elastic scattering process ${}^{A+2}X + p \rightarrow^{A+2} X + p$, ${}^{A+2}X$ denoting a member of a pairing rotational band (cf. Fig. 1.7.1, see also Fig **??**). It is of notice that the process ${}^{A+2}X + p \rightarrow^{A+1} X + d \rightarrow^{A+2} X + p$ is likely to be the dominant one concerning the optical potential describing the ${}^{A+2}X + p$ scattering process. Because $P_2 \approx P_1$, a likely better estimate of $U + iW$ can be obtained taking into account also the transfer back and forth of two nucleons. In keeping with the fact that the sum of the simultaneous and non–orthogonality contributions are much smaller than the successive transfer, only this last process is shown in the NFT reaction–structure diagram displayed in Fig. 1.7.1.

Whether an effect which may parallel that shown in (c) (backwards rise) can be seen or not depends on a number of factors, but very likely it is expected to be a weak effect. This was also true in the case of the Josephson effect in its varied versions (AC, DC, etc.). In fact, its observation required to take into account the effect of the earth magnetic field, let alone quantal and thermal fluctuations.

1.8 Hindsight

The formulation of superconductivity (BCS theory) described by Gor'kov[34] allows, among other things for a simple visualization of spatial dependences. In this formulation $F(\mathbf{x}, \mathbf{x}')$ is the amplitude for two Fermions (electrons) at $\mathbf{x}, \mathbf{x}'$, to belong to the Cooper pair (within the framework of nuclear physics cf. e.g. Fig. **??** $\Psi_0(\mathbf{r}_1, \mathbf{r}_2)$). The phase of F is closely related to the angular orientation of the spin variable in Anderson's quasispin formulation of BCS theory[35]. The gap function $\Delta(x)$ is given by $V(\mathbf{x})F(\mathbf{x}, \mathbf{x})$ where $V(\mathbf{x})$ is the local two–body interaction at the point $\mathbf{x}$. In the insulating barrier between the two superconductors of a Josephson junction, $V(\mathbf{x})$ is zero and thus $\Delta(x)$ is also zero.

The crucial point is that vanishing $\Delta(x)$ does not imply vanishing F, provided, of course, that one has within the insulating barrier, a non–zero particle (electron) density, resulting from the overlap of densities from right (R) and left (L) superconductors. Now, these barriers are such that they allow for one–electron–tunneling with a probability of the order of 10^{-10} and, consequently, the above requirement

[34] Gor'kov, L.P. (1959).

[35] Anderson (1958); within the framework of nuclear physics cf. e.g. Bohr and Ulfbeck (1988), Potel, G. et al. (2013b) and references therein.

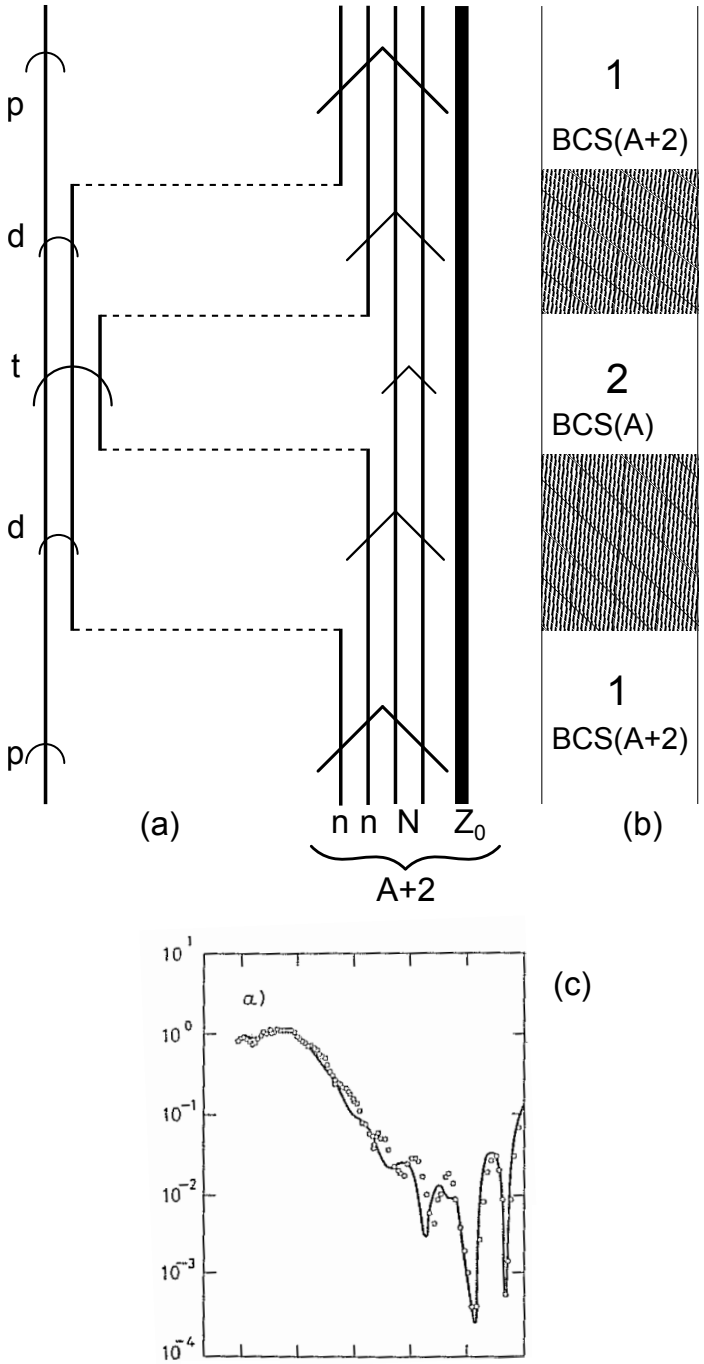

Figure 1.7.1: Gedanken experiment concerning the possibility of observing weak coupling coherence phenomena between states $|BCS(A+2)\rangle$ and $|BCS(A)\rangle$ in an elastic reaction involving superfluid nuclei (**a**), e.g. p+^{120}Sn→ p+^{120}Sn, the system ^{119}Sn+d acting as a dynamical barrier (hatched areas arguably play role of that of dioxide layers in Josephson junctions) between the two even N superfluid systems arising from the successive transfer of two nucleons (**b**) and eventually allowing for a time dependent gauge phase difference between the $(A+2)$ and A superfluid systems, thus leading, in the case in which Q–value effects are appropriate, to an oscillating enhancement of the elastic cross section at large angles as observed, for quite different reasons, in the case of the elastic angular distribution of the reaction ^{16}O+^{28}Si (**c**) (cf. Pollarolo and Broglia (1984)).

is fulfilled[36]. Nonetheless, conventional (normal) simultaneous pair transfer, with a probability of $(10^{-10})^2$ will not be observed. But because one electron at a time can tunnel profiting of the small, but finite electron density within the layer, $F(\mathbf{x}, \mathbf{x}')$ can have large amplitude for electrons, on each side of the barrier (i.e. L and R), separated by distances $|\mathbf{x} - \mathbf{x}'|$ up to the coherence length. Hence, for barriers thick to only allow for the tunneling of one electron at a time, but thin compared with the coherence length, two electrons on opposite sides of the barrier can still be correlated and the pair current can be consistent. An evaluation of its value shows that, at zero temperature, the pair current is equal to the single particle current at an equivalent voltage[37] $\pi\Delta/2e$.

The translation of the above parlance to the language of nuclear physics has to come to terms with the basic fact that nuclei are self–bound, finite many–body systems in which the surface, as well as space quantization, play a very important role both as a static element of confinement, as well as a dynamic source for renormalization effects[38,39]. Under the influence of the average potential which can be viewed as very strong external field ($|V_0| \approx 50$ MeV), Cooper pairs ($|E_{corr}| \approx 1.5$ MeV; see Fig. **??**) will become constrained within its boundaries with some amount of spill out. In the case of the single open shell superfluid nucleus ^{120}Sn, the boundary can be characterized by the radius $R_0 \approx 6$ fm ($\ll \xi \approx 30$ fm), the spill out being connected with the diffusivity $a \approx 0.65$ fm.

Let us now consider a two nucleon transfer reaction in the collision Sn+Sn assuming a distance of closest approach of $\approx$ 14 fm, in which the two nuclear surfaces are separated by ≈ 2 fm (Fig 1.4.1). In keeping with the fact that this distance is about $3\times a$, the heavy ion system will display a few percent (of saturation) density overlap in the interacting region. Ever so small this overlap of the nuclear surfaces,, and so narrow the hole between the two leptodermic systems resulting from it, in the situation in which $r \approx R_0 + 1.5a$ for each Sn ion, Cooper pairs can now extend over the two volumes, in a similar way as electron Cooper pairs could be partially found in the R and L superconductors in a Josephson junction. If this is the case, Cooper pair partners can be at distance as large as 26 fm, of the same order of magnitude of the correlation length. In other words, in the reaction Sn+Sn$\rightarrow$ Sn(gs)+Sn(gs) one expects (mainly successive) Cooper pair transfer

[36] Pippard (2012) see also McDonald (2001).

[37] In the case of Pb at low temperatures (< 7.19 K (0.62 meV)) this voltage is ≈ 1 meV/e = 1 mV (Ambegaokar and Baratoff (1963); McDonald (2001); Tinkham (1996)).

[38] Within this context it is of notice that the liquid drop model is a very successful nuclear model, able to accurately describe not only large amplitude motion (fission, exotic decay, low–lying collective density and surface vibrations, cf. e.g. Bohr and Wheeler (1939), Barranco, F. et al. (1990), Bertsch (1988), see also Brink, D. and Broglia (2005) and references therein), but also the masses of nuclides (cf. e.g. Moller and Nix), provided the superfluid inertia and shell corrections respectively, are properly considered. Thus, it is an open question whether in the quest of developing more predictive theoretical tools of the global nuclear properties one should develop ever more "accurate" zero range (Skyrme–like) forces, or deal with the long wavelength, renormalization effects and induced interaction.

[39] Broglia, R. A. (2002).

of two neutrons which are away from each other by tens of fm. An example of the fact that Cooper pairs will "expand" if the external mean field is weakened, is provided by ^{11}Li in which case, profiting of the weak binding ($\approx$ 380 keV), the extension of the constrained Cooper pair ($\approx$ 4.55 fm $\pm$0.3 fm) is similar to that expected in a nucleus of mass number $A \approx 60$, assuming a standard radial behavior, i.e. $r_0 A^{1/3}$ fm. In keeping with this scenario, it could be expected that moving from one neutron pair addition 0^+ mode of the $N = 6$ isotones to another one ($|^{11}\mathrm{Li(gs)}\rangle$, $|^{12}\mathrm{Be(gs)}\rangle$ and $|^{12}\mathrm{Be}(0^{+*}; 2.24\,\mathrm{MeV})\rangle$) one would see the system expanding, contracting and expanding again, respectively, in keeping with the fact that the external (mean) field is weak, strong, weak respectively, as testified by S_{2n} (380 keV, 3672 keV, 1432 keV). Within this context, the dipole resonance built on top of them is expected to vary in energy from very low (< 1 MeV) to high (2.71 MeV) to low (0.460 MeV), that is from a symbiotic, to an independent, and, likely, to a (quasi) symbiotic role again. Within this context, in Fig. 1.8.1 an overall view of the pairing vibrational modes associated with $N = 6$ parity inverted closed shell isotones, together with low–energy $E1$–strength modes is given. The possible candidates to the role of neutron halo pair addition modes and simbiotic state are explicitly indicated (boxed levels). In Fig. 1.8.2 the ^{11}Li(gs), ^{12}Be(gs) and Be(0^{*+}; 2.25 MeV) wavefunctions and $|\Psi_0(\mathbf{r}_1, \mathbf{r}_2)|^2$ probability distribution of one Cooper pair partner with respect to the other located at a fixed distance from the CM of the nucleus under study are shown (see also Fig. **??** (II)). While the results associated with the two ground states have been tested in connection with the experimental findings (Barranco, F. et al. (2001); Potel et al. (2010, 2014); Gori et al. (2004)), much less is known regarding the accuracy of the predictions associated with ^{12}Be(0^{*+}).

Appendix 1.A Medium polarization effects and pairing

1.A.1 Nuclei

Polarization contributions to the bare nucleon–nucleon pairing interaction through elementary modes of excitation

Elementary modes of excitation constitute a basis in which observables play an important role. As a consequence, it allows for an economic solution of the nuclear many–body problem of structure and reaction. A first step in this quest is to eliminate the non–orthogonality associated with single–particle motion in different nuclei (target and projectile (*reaction*)). Also between single–particle degrees of freedom and collective modes (vibrations and rotations (*structure*)) typical of an overcomplete , Pauli principle violating, basis. This can be done by diagonalizing, making use of the rules of nuclear field theory (NFT), the particle–vibration coupling (PVC, mainly structure) and the v_{np} (v : four point vertex, bare NN–) interaction (mainly reaction). In this way one obtains quantities (energies, transition probabilities, absolute value of reaction cross sections) which can be directly compared with the experimental findings. Such a protocol can be carried

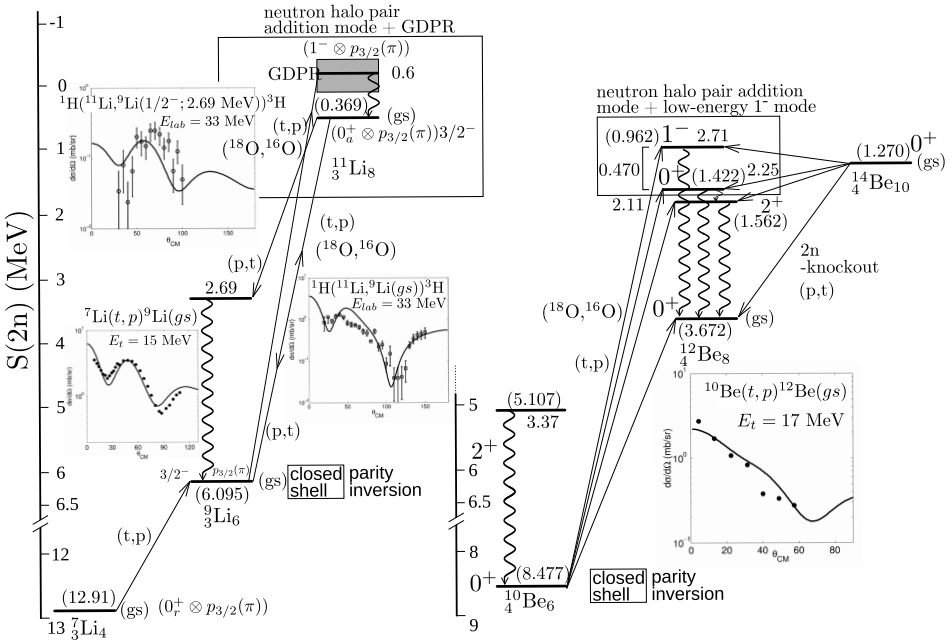

Figure 1.8.1: Monopole pairing vibrational modes associated with $N = 6$ parity inverted closed shell isotopes, together with low-energy E1-strength modes. The levels are displayed as a function of the two-neutron separation energies $S(2n)$. These quantities are shown in parenthesis on each level, the excitation energies with respect to the ground state are quoted in MeV. Absolute differential cross sections from selected (t,p) and (p,t) reactions calculated as described in the text (cf. Potel et al. (2010, 2014)), in comparison with the experimental data (Young and Stokes (1971); Fortune et al. (1994)).

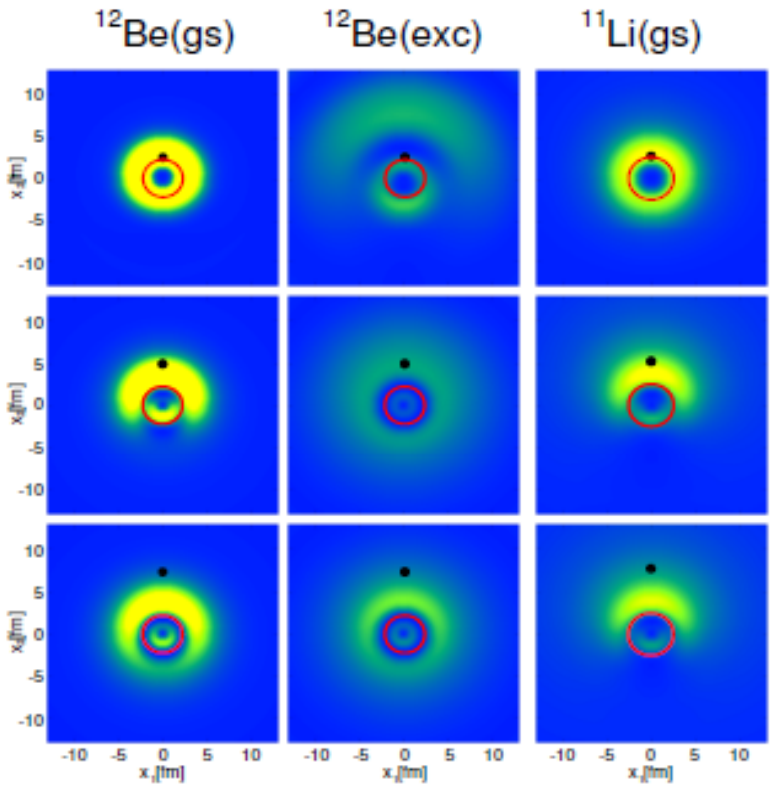

$$|0\rangle_\nu = |0\rangle + \alpha|(p,s)_{1^-} \otimes 1^-;0\rangle + \beta|(s,d)_{2^+} \otimes 2^+;0\rangle + \gamma|(p,d)_{3^-} \otimes 3^-;0\rangle$$

$$|0\rangle_\nu = a|s^2(0)\rangle + b|p^2(0)\rangle + c|d^2(0)\rangle$$

	^{11}Li(gs)	^{12}Be(gs)	^{12}Be(exc)
α	0.7	0.10	0.08
β	0.1	0.30	-0.39
γ	–	0.37	-0.1
a	0.45	0.37	0.89
b	0.55	0.50	0.17
c	0.04	0.60	0.19

Figure 1.8.2

out, in most cases, within the framework of perturbation theory. For example, second order perturbation theory, in both reaction and structure, as exemplified in Fig. **??** displaying a NFT (r+s) graphical representation of contributions to the ^{11}Li$(p,t)^{9}$Li(gs) and ^{11}Li$(p,t)^{9}$Li$(1/2^{-};2.69$ MeV) processes (see also Fig. **??**). As a result, single-particle states move in a gas of vibrational quanta and become clothed. The quanta couple, in turn, to doorway states which renormalize their properties through self energy and vertex corrections. Similar couplings renormalize the bare NN–interaction in the different channels. In particular in the $^{1}S_{0}$ (pairing) channel.

Also as a result of their interweaving, the variety of elementary modes of excitation may break in a number of states, eventually acquiring a lifetime and, within a coarse grain approximation, a damping width (imaginary component of the self energy). Moving into the continuum, as for example in the case of direct reactions, one such component is the imaginary part of the optical potential operating in the particular channel selected. It can be calculated microscopically using similar techniques and elements as e.g. those used in the calculation of the damping width of giant resonances. With the help of dispersion relations, the real part of the optical potential can be obtained from the knowledge of the energy dependence of the absorptive potential. In this way, the consistency circle structure–reaction based on elementary modes and codified by NFT could be closed. The rich variety of emergent properties found along the way eventually acquiring a conspicuous level of physical validation. In the case of halo exotic nuclei, in particular in the case of ^{11}Li (bootstrap, Van der Waals Cooper binding, halo pair addition mode (symbiosis of pairing vibration and pigmy) being few of the associated emergent properties) one is rather close to his goal. At that time it would be possible, arguably if there is one, to posit that the *ultima ratio* of structure and reactions, in any case that associated with pairing and Cooper pair transfer in nuclei, have been unveiled[40]

Effective moments

At the basis of the coupling between elementary modes of excitation, for example of single–particle motion and of collective vibrations, is the fact that, in describing the nuclear structure it is necessary to make reference to both (all) of them simultaneously and in an unified way.

Within the harmonic approximation the above statement is economically embodied in e.g. the relation existing between the collective ($\hat{\alpha}$) and the single–particle ($\hat{F}$) representation of the operator creating a $\beta = 0$ (β: transfer quantum

[40]In the above paragraph we allow ourselves to paraphrase Jacques Monod writing in connection with biology and life: L'*ultima ratio* de toutes les structures et performances téléonomiques des êtres vivants est donc enfermée dans les séquences des radicaux des fibres polypeptidiques "embryons" de ces démons de Maxwell biologiques que sont les protéines globulaires. En un sens, très réel, c'est à ce niveau d'organisation chimique qui gît, s'il y en a un, le secret de la vie. Et saurait–on non seullement décrire les séquences, mais énoncer la loi d'assemblage à laquelle obéissent, on pourrait dire que le secret est percé, l'ultima ratio découverte (J. Monod, Le hasard et la nécéssité, Editions du Seuil, Paris, 1970).

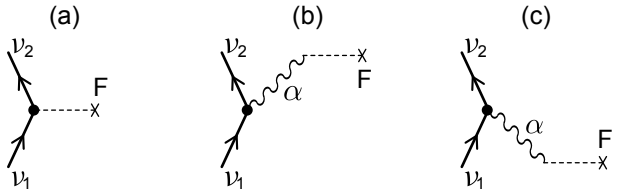

Figure 1.A.1: (a) F–moment of single–particle and (b,c) renormalization effects induced by the collective vibration α.

number) excitation. That is[41],

$$\begin{aligned} F &= \left\{ \langle k|F|\tilde{i}\rangle \Gamma^{\dagger}_{ki} + \langle \tilde{i}|F|k\rangle \Gamma_{ki} \right\} \\ &= \sum_{k,i,\alpha'} X^{\alpha'}_{ki} \Gamma^{\dagger}_{\alpha'} - Y^{\alpha'}_{ki} \Gamma_{\alpha'} \\ &= \sum_{\alpha'} \Lambda_{\alpha'} \sum_{ki} \frac{\left|\langle \tilde{i}|F|k\rangle\right|^2 2(\epsilon_i - \epsilon_k)}{(\epsilon_k - \epsilon_i)^2 - (\hbar\omega_{\alpha'})^2} \left(\Gamma^{\dagger}_{\alpha'} + \Gamma_{\alpha'}\right) \\ &= \sum_{\alpha'} \frac{\Lambda_{\alpha'}}{\kappa} \left(\Gamma^{\dagger}_{\alpha'} + \Gamma_{\alpha'}\right) = \sum_{\alpha'} \sqrt{\frac{\hbar\omega_{\alpha'}}{2C'_{\alpha}}} \left(\Gamma^{\dagger}_{\alpha'} + \Gamma_{\alpha'}\right) = \hat{\alpha} \end{aligned} \tag{1.A.1}$$

This is a consequence of the self consistent relation

$$\delta U(r) = \int d\mathbf{r}' \delta\rho(r) v(|\mathbf{r}-\mathbf{r}'|) \tag{1.A.2}$$

existing between density (collective) and potential (single–particle) distortion, typical of normal modes of many–body systems.

Relation (1.A.1) implies that at the basis of these normal modes one finds the (attractive $\kappa < 0$) separable interaction

$$H = \frac{\kappa}{2} \hat{F}\hat{F} \tag{1.A.3}$$

but where now

$$\hat{F} = \sum_{\nu_1,\nu_2} \langle \nu_1|F|\nu_2\rangle a^{\dagger}_{\nu_1} a_{\nu_2} \tag{1.A.4}$$

is a general single–particle operator, while $\hat{F}$ (see eq. (1.A.1)) is its harmonic representation acting in the particle (k)–hole (i) space, $\Gamma^{\dagger}_{ki}$ and Γ_{ki} being (quasi) bosons, i.e. respecting the commutation relation

$$\left[\Gamma_{ki}, \Gamma^{\dagger}_{k'i'}\right] = \delta(k,k')\delta(i,i'). \tag{1.A.5}$$

[41] cf. Bohr, A. and Mottelson (1975), cf. also Brink, D. and Broglia (2005) App. C.

In other words, the representation (1.A.1) which is at the basis of the RPA (as well as QRPA), does not allow for scattering vertices, processes which become operative by rewriting (1.A.3) in terms of the particle–vibration coupling Hamiltonian

$$H_c = \kappa \hat{\alpha} \hat{F} \tag{1.A.6}$$

It is of notice that κ is negative for an attractive field. Let us now calculate the effective single–particle moments (cf. Fig. 1.A.1 (b)),

$$\begin{aligned} \langle \nu_2 | \hat{F} | \nu_1 \rangle_{(b)} =& \frac{\langle \nu_2 | \hat{F} | \nu_2, n_\alpha = 1 \rangle \langle \nu_2, n_\alpha = 1 | H_c | \nu_1 \rangle}{(\epsilon_{\nu_1} - \epsilon_{\nu_2}) - \hbar\omega_\alpha}, \\ =& \frac{\langle 0 | \alpha | n_\alpha = 1 \rangle \kappa\alpha \langle \nu_2 | F | \nu_1 \rangle}{(\epsilon_{\nu_1} - \epsilon_{\nu_2}) - \hbar\omega_\alpha}, \\ =& \kappa\alpha^2 \frac{\langle \nu_2 | F | \nu_1 \rangle}{(\epsilon_{\nu_1} - \epsilon_{\nu_2}) - \hbar\omega_\alpha}, \end{aligned} \tag{1.A.7}$$

and (Fig. 1.A.1 (c))

$$\begin{aligned} \langle \nu_2 | \hat{F} | \nu_1 \rangle_{(c)} =& \frac{\langle \nu_2 | H_c | \nu_1, n_\alpha = 1 \rangle \langle \nu_1, n_\alpha = 1 | F | \nu_1 \rangle}{\epsilon_{\nu_2} - (\epsilon_{\nu_1} + \hbar\omega_\alpha)}, \\ =& \kappa\alpha^2 \left(- \frac{\langle \nu_2 | F | \nu_1 \rangle}{(\epsilon_{\nu_1} - \epsilon_{\nu_2}) + \hbar\omega_\alpha} \right), \end{aligned} \tag{1.A.8}$$

leading to

$$\begin{aligned} \langle \nu_2 | \hat{F} | \nu_1 \rangle_{(b)} + \langle \nu_2 | \hat{F} | \nu_1 \rangle_{(c)} =& \kappa\alpha^2 \frac{2\hbar\omega_\alpha \langle \nu_2 | F | \nu_1 \rangle}{(\epsilon_{\nu_1} - \epsilon_{\nu_2})^2 - (\hbar\omega_\alpha)^2}, \\ =& \frac{\kappa}{C_\alpha} \frac{(\hbar\omega_\alpha)^2 \langle \nu_2 | F | \nu_1 \rangle}{(\epsilon_{\nu_1} - \epsilon_{\nu_2})^2 - (\hbar\omega_\alpha)^2}. \end{aligned} \tag{1.A.9}$$

This is in keeping with the fact that the ZPF of the α–vibrational mode is,

$$\alpha = \sqrt{\frac{\hbar\omega_\alpha}{2C_\alpha}}, \tag{1.A.10}$$

the particle–vibration coupling strength being

$$\Lambda_\alpha = \kappa\alpha. \tag{1.A.11}$$

Together with $\langle \nu_2 | \hat{F} | \nu_1 \rangle_{(a)} = \langle \nu_2 | F | \nu_1 \rangle$ (see Fig. 1.A.1 (a)) one obtains

$$\langle \nu_2 | \hat{F} | \nu_1 \rangle = (1 + \chi(\omega)) \langle \nu_2 | F | \nu_1 \rangle, \tag{1.A.12}$$

where

$$\chi(\omega) = \frac{\kappa}{C_\alpha} \frac{\omega_\alpha^2}{\omega^2 - \omega_\alpha^2} \tag{1.A.13}$$

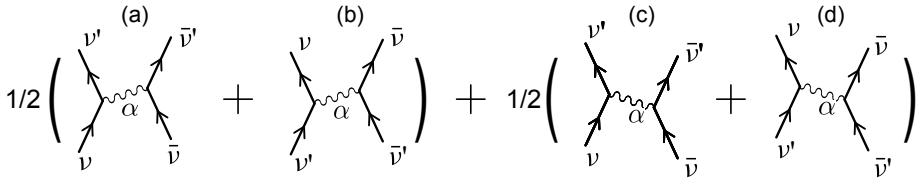

Figure 1.A.2: Diagrams associated with nuclear pairing induced interaction.

is the polarizability coefficient and

$$\omega = |\epsilon_{\nu_1} - \epsilon_{\nu_2}|/\hbar. \tag{1.A.14}$$

In the static limit, e.g. in the case in which α is a giant resonance and $\omega_\alpha \gg \omega$ one obtains

$$\chi(0) = -\frac{\kappa}{C}. \tag{1.A.15}$$

The sign of $\chi(0)$ is opposite to that of κ, since the static polarization effect produced by an attractive coupling ($\kappa < 0$) is in phase with the single–particle moment, while a repulsive coupling ($\kappa > 0$) implies opposite phases for the polarization effect and the one–particle moment[42]. Let us now calculate the two–body pairing induced interaction arising from the exchange of collective vibrations[43] (summing over the two time orderings and symmetrizing between initial and final states)[44]

$$\begin{aligned} v^{ind}_{\nu\nu'}(a) + v^{ind}_{\nu\nu'}(b) &= \kappa^2\alpha^2 \left|\langle\nu'|F|\nu\rangle\right|^2 \left(\frac{1}{\epsilon_\nu - \epsilon_{\nu'} - \hbar\omega_\alpha} + \frac{1}{\epsilon_{\nu'} - \epsilon_\nu - \hbar\omega_\alpha}\right), \\ &= \kappa^2\alpha^2 \left|\langle\nu'|F|\nu\rangle\right|^2 \left(\frac{1}{(\epsilon_\nu - \epsilon_{\nu'}) - \hbar\omega_\alpha} - \frac{1}{(\epsilon_\nu - \epsilon_{\nu'}) - \hbar\omega_\alpha}\right), \\ &= \Lambda^2_\alpha \left|\langle\nu'|F|\nu\rangle\right|^2 \left(\frac{2\hbar\omega_\alpha}{(\epsilon_\nu - \epsilon_{\nu'})^2 - (\hbar\omega_\alpha)^2}\right), \\ &= v^{ind}_{\nu\nu'}(c) + v^{ind}_{\nu\nu'}(d). \end{aligned} \tag{1.A.16}$$

Thus

$$\begin{aligned} v^{ind}_{\nu\nu'} &= \frac{1}{2}\left(v^{ind}_{\nu\nu'}(a) + v^{ind}_{\nu\nu'}(b)\right) + \frac{1}{2}\left(v^{ind}_{\nu\nu'}(c) + v^{ind}_{\nu\nu'}(d)\right) \\ &= \Lambda^2_\alpha \left|\langle\nu'|F|\nu\rangle\right|^2 \left(\frac{2\hbar\omega_\alpha}{(\epsilon_\nu - \epsilon_{\nu'})^2 - (\hbar\omega_\alpha)^2}\right). \end{aligned} \tag{1.A.17}$$

The diagonal matrix element,

$$v^{ind}_{\nu\nu'} \equiv -\frac{2\Lambda^2_\alpha \left|\langle\nu'|F|\nu\rangle\right|^2}{\hbar\omega},$$

[42] Bohr, A. and Mottelson (1975); Mottelson (1962).

[43] In the present discussion we do not consider spin modes. For details see e.g. Idini et al. (2015). See also Bortignon et al. (1983).

[44] Cf. Brink, D. and Broglia (2005) p. 217.

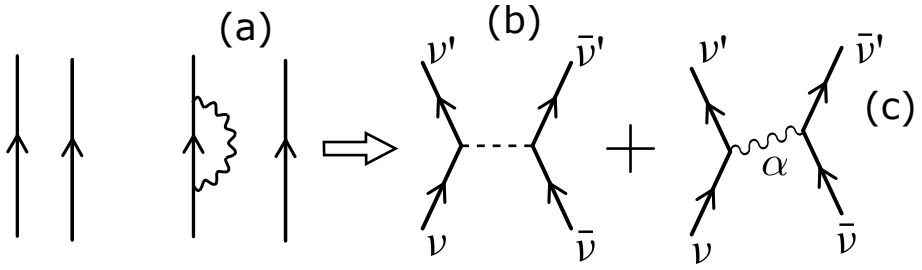

Figure 1.A.3: Starting with two bare nucleons moving around a closed shell system N_0 in Hartree–Fock orbitals (arrowed lines far left), a graphical (NFT) representation of (a) self energy processes and of (b) bare and (c) induced pairing interactions are displayed.

testifies to the fact, for values of $\omega_\alpha \gtrsim \omega$, with

$$\omega = |\epsilon_\nu - \epsilon_{\nu'}|/\hbar, \tag{1.A.18}$$

namely the frequencies of the single–particle excitation energy, the induced pairing interaction is attractive. Summing to (1.A.17) the matrix element of the bare interaction (1.A.3)

$$v^{bare}_{\nu\nu'} = \kappa \left|\langle\nu'|F|\nu\rangle\right|^2 \tag{1.A.19}$$

and making use of (1.A.13) one obtains for the total pairing matrix element[45]

$$v_{\nu\nu'} = v^{bare}_{\nu\nu'}\,(1+\chi(\omega)) = v^{bare}_{\nu\nu'}\left(1 + v^{bare}_{\nu\nu'}\Pi_{\nu\nu'}(\omega,\omega_\alpha)\right), \tag{1.A.20}$$

where

$$\Pi_{\nu,\nu'} = \begin{cases} \left(C_\alpha\,|\langle\nu'|F|\nu\rangle|^2\right)^{-1} \frac{\omega_\alpha^2}{\omega^2-\omega_\alpha^2}, \\ \left(D_\alpha\,|\langle\nu'|F|\nu\rangle|^2\right)^{-1} \frac{1}{\omega^2-\omega_\alpha^2}. \end{cases} \tag{1.A.21}$$

Concerning ω see the definition (1.A.14). It is of notice that in the second expression of $\Pi_{\nu\nu'}$ the inertia of the phonon appears in the denominator, similar to the factor (Z/AM) in (1.A.68) below.

Let us now rewrite (1.A.20) as

$$v_{\nu\nu'} = v^{bare}_{\nu\nu'}\left(1 + |\chi(0)|\frac{\omega_\alpha^2}{\omega_\alpha^2-\omega^2}\right), \tag{1.A.22}$$

[45] Within the framework of (1.A.3) and of its role in (1.A.20) one finds, in the case of superconductivity in metals, to be discussed below that the bare unscreened Coulomb interaction can be written as

$$U_c(r) = \frac{1}{2}\sum_{i,j}\frac{q_i q_j}{|\mathbf{r}_i - \mathbf{r}_j|},$$

i, j running over all particles (nuclei and electrons) and $q_i = -e$ for electrons and Ze for nuclei.

to discuss two ($i = 1, 2$) particular situations of interest:

$$1) \qquad \omega = \omega_\alpha - \delta\omega/2, \quad (\delta\omega \ll \omega_\alpha), \tag{1.A.23}$$

$$2) \qquad \omega_\alpha \gg \omega. \tag{1.A.24}$$

That is

$$\lim_{\omega\to i} \frac{\omega_\alpha^2}{\omega^2 - \omega_\alpha^2} = \begin{cases} \frac{\omega_\alpha}{\delta\omega} \gg 1 & (i = 1) \text{ plastic–}\alpha \text{ modes} \\ 1 & (i = 2) \text{ elastic–}\alpha \text{ modes} \end{cases} \tag{1.A.25}$$

The first situation is typical of low–lying collective surface vibrations. The second of high lying giant resonances. While in this last case one can parametrize the effect in terms of constant effective moments[46], the explicit treatment of the state–(ω–dependence) of the first one is unavoidable.

Let us conclude this section by making a simple estimate of the contribution of the induced pairing interaction to the (empirical) nuclear pairing gap. For this purpose we introduce the quantity

$$\lambda = N(0) v^{ind}_{\nu\nu'} \tag{1.A.26}$$

where $N(0)$ is the density of levels of a single spin orientation at the Fermi energy. The above quantity is known as the nuclear mass enhancement factor. This is because of the role it plays in the nucleon ω–mass

$$m_\omega = (1 + \lambda)m. \tag{1.A.27}$$

Systematic studies of this quantity, and of the related discontinuity occurring by the single–particle occupation number at the Fermi energy, namely $Z_\omega = (m/m_\omega)$ testifies to the fact that $\lambda \approx 0.4$.

The BCS expressions of the pairing gap in terms of λ are

$$\Delta = \begin{cases} 2\hbar\omega_D e^{-1/\lambda}, & (\text{weak coupling } \lambda \ll 1) \\ \hbar\omega_D \lambda, & (\text{strong coupling } \lambda \geq 1) \end{cases} \tag{1.A.28}$$

where ω_D is the limiting frequency of the low–lying collective modes of nuclear excitation, typically of quadrupole and octupole vibrations. While for weak coupling one can use $\hbar\omega_D \approx 10$ MeV, for the strong coupling situation seem more proper $\hbar\omega_D \approx 2$ MeV.

Making use of $\lambda = 0.4$, intermediate between weak and strong coupling situation one obtains

$$\Delta \approx 1.6\,\text{MeV} \tag{1.A.29}$$

and

$$\Delta \approx 0.8\,\text{MeV}, \tag{1.A.30}$$

[46] See e.g. Bohr, A. and Mottelson (1975) pp. 421 and 432.

to be compared with the empirical value

$$\Delta \approx 1.4\,\mathrm{MeV} \tag{1.A.31}$$

of superfluid medium heavy mass nuclei like ^{120}Sn.

While the relations (1.A.28) can hardly be relied to provide a quantitative number, they testify to the fact that induced pairing is expected to play an important role in nuclei. These expectations have been confirmed by detailed confrontation of theory and experiment[47].

Hindsight

Static polarization effects can be important in clothing single–particle states. For example, effective charges and induced interactions associated with moments induced by giant resonances[48]. However, retarded ω–dependent self–energy effects and induced interactions are essential in describing structure and reactions of many–body systems. Examples are provided by the bootstrap binding of the halo neutrons (pair addition mode) to ^{9}Li, leading to the fragile $|^{11}\mathrm{Li}(gs)\rangle$, displaying a $S_{2n} \approx 0.380$ MeV as compared to typical values of $S_{2n} \approx 18$ MeV as far as structure goes, and by the $^{1}\mathrm{H}(^{11}\mathrm{Li},^{9}\,\mathrm{Li}(1/2^{-}; 2.69\,\mathrm{MeV}))^{3}\mathrm{H}$ population of the lowest member of the $(2^{+} \times p_{3/2}(\pi))_{J^{-}}$ multiplet of ^{9}Li, as far as reaction goes. If there was need for support coming from other fields of research, one can mention just two: van der Waals force and superconductivity.

It was recognized early in the study of dipole–dipole interaction in atomic systems that, of the variety of contributions to the van der Waals interaction, the retarded, fully quantal contribution, arising from (dipole) zero point fluctuations (ZPF) of the two interacting atoms or molecules, and only active also in the case of non–polar molecules[49], play an overwhelming role, static–induced interactions being less important. A consequence of this result is the fact that the limiting size of globular proteins (≈ 50 Å) is controlled by the strong damping undergone by the retarded contribution to the amino acid interaction, when the frequency associated with the back and forth propagation of the force matches the molecules electronic frequencies[50].

[47] See e.g. Idini et al. (2015).

[48] See e.g. Bohr, A. and Mottelson (1975), Eqs. (6-217) and (6-228).

[49] Within this context van der Waals and gravitation are two forces which are universally operative, acting among all bodies.

[50] It is of notice that similar arguments (cf. Sect. **??**) are at the basis of the estimate (**??**) concerning the size of the halo nucleus ^{11}Li, a quantity which is influenced to a large extent by the maximum distance (correlation length) over which partners of a Cooper pair are virtually (it materializes only if particle, normal, density allows for) but solidly anchored to each other (localized), and have to be seen as an (extended) bosonic entity and not as two fermions. The fact that Cooper pair transfer proceeds mainly in terms of successive transfer controlled by the single–particle mean field, reinforces the above physical picture of nuclear pairing. Even under the effect of extremely large, as compared to the pair correlation energy, external single–particle field, namely that of target and projectile, the Cooper pair field extends over the two nuclei, permeating the whole summed nuclear volume also through a tiny density overlap.

Concerning superconductivity, the overscreening effect which binds weakly Cooper pairs stems from a delicate ω–dependent phenomenon leading, eventually, to one of the first macroscopic manifestations of quantum mechanics, as e.g. "permanent" magnetic fields associated with supercurrents.

The statement "*Life at the edge of chaos*"coined in connection with the study of emergent properties in biological molecules (e.g. protein evolution, folding and stability) reflects the idea, as expressed by de Gennes[51], that truly important new properties and results can emerge in systems lying at the border between rigid order and randomness, as testified by the marginal stability and conspicuous fluctuations characterizing, for example, nuclear Cooper pairs at the dripline and in metals, and that of proteins of e.g. viral particles like the HIV–1– and HCV–proteases[52].

Let us conclude this short comment, quoting again de Gennes but doing so with the hindsight of twenty years of nuclear research which have elapsed since "Les objets fragiles" was first published. The chapter entitled "Savoir s'arreter, savoir changer" starting at p. 180 opens with the statement "En ce moment, la physique nucléaire (la science des noyaux atomiques) est une science qui, à mon avis, se trouve en fin de parcours...C'est une physique qui demande des moyens coûteux, et qui s'est constituée par ailleurs en un puissant lobby. Mais elle me semble naturellement exténuée...je suis tenté de dire: "Arretons"...mais ce serait aussi absurde que de vouloir arreter un train a grande vitesse. Le mieux serait d'aiguiller ce train sur une autre voie, plus nouvelle et plus utile à la collectivité."

In a way, and even without knowing de Gennes remark, part of the nuclear physics community have followed it, capitalizing on the novel embodiment that concepts like elementary modes of excitation, spontaneous symmetry breaking and phase transitions have had in this paradigm of finite many–body system the nucleus is, where fluctuations, as a rule, dominate over potential energy effects. The use of these concepts tainted by FMB system effects as applied to proteins, in particular to the understanding of protein folding may, arguably shed light on the possibility of designing leads to drugs which are less prone to create resistance[53].

1.A.2 Metals

Plasmons and phonons (jellium model)

The expression of the electron plasmon frequency of the antenna–like oscillations of the free, conduction electrons against the positive charged background (jellium model) is

$$\omega_{ep}^2 = \frac{4\pi n_e e^2}{m_e} = \frac{3e^2}{m_e r_s^2}, \tag{1.A.32}$$

where

$$n_e = \frac{3}{4\pi}\frac{1}{r_s^3}, \tag{1.A.33}$$

[51] de Gennes (1994).

[52] See e.g. Broglia, R. A. (2013).

[53] See e.g. Broglia, R. A. (2013) and refs. therein.

are the number of electrons per unit volume, r_s being the radius of a sphere whose volume is equal to the volume per conduction electron,

$$r_s = \left(\frac{3}{4\pi n_e}\right)^{1/2}, \tag{1.A.34}$$

that is, the radius of the Wigner–Seitz cell.

For metallic Li[54]

$$n_e = 4.70\frac{10^{22}}{\mathrm{cm}^3} = \frac{4\times 10^{-2}}{\mathring{\mathrm{A}}^3} \tag{1.A.35}$$

while

$$r_s = \left(\frac{3\mathring{\mathrm{A}}^3}{4\pi\times 4.7\times 10^{-2}}\right)^{1/3} = 1.72\mathring{\mathrm{A}} \tag{1.A.36}$$

implying a value $(r/a_0) = 3.25$ in units of the Bohr radius ($a_0 = 0.529\mathring{\mathrm{A}}$).

Making use of

$$\alpha = 7.2973 = \frac{e^2}{\hbar c} \tag{1.A.37}$$

and

$$e^2 = 14.4\,\mathrm{eV}\ \mathring{\mathrm{A}}, \tag{1.A.38}$$

one obtains

$$\hbar c = \frac{14.4\,\mathrm{eV}\ \mathring{\mathrm{A}}}{7.2973} = 1973.3\,\mathrm{eV}\ \mathring{\mathrm{A}}. \tag{1.A.39}$$

Making use of the above values and of

$$m_e c^2 = 0.511\,\mathrm{MeV}, \tag{1.A.40}$$

one can write

$$\hbar^2\omega_{ep}^2 = \frac{(\hbar c)^2}{m_e c^2}\frac{3e^2}{r_s^3} = \frac{(1973.3\,\mathrm{eV}\ \mathring{\mathrm{A}})}{0.511\times 10^6\,\mathrm{eV}}\frac{3\times 14.4\,\mathrm{eV}\ \mathring{\mathrm{A}}}{(1.72\,\mathring{\mathrm{A}})^3} = 64.69\,\mathrm{eV}^2 \tag{1.A.41}$$

leading to[55]

$$\hbar\omega_{ep} = 8.04\,\mathrm{eV} \approx 1.94\times 10^9\,\mathrm{MHz} \tag{1.A.42}$$

For the case of metal clusters of Li, the Mie resonance frequency is

$$\hbar\omega_M = \frac{\hbar\omega_{ep}}{\sqrt{3}} = 4.6\,\mathrm{eV}. \tag{1.A.43}$$

[54] cf. page 5, table 1.1 of Ashcroft and Mermin (1987).

[55] Kittel (1996) Table 2, p. 278.

1.A.3 Elementary theory of phonon dispersion relation

Again, within the framework of the jellium model, one can estimate the long wavelength ionic plasma frequency introducing, in (1.A.32) the substitution $e \to Ze$, $m_e \to AM$ ($A = n + Z$, mass number, M nucleon mass), $n_e \to n_i = n_e/Z$,

$$\omega_{ip}^2 = \frac{4\pi n_i (Ze)^2}{AM} = \frac{Zm_e}{AM}\omega_{ep}^2. \tag{1.A.44}$$

For metallic Li, one obtains

$$\begin{aligned}\hbar\omega_{ip} = \left(\frac{Zm_e}{AM}\right)^{1/2}\hbar\omega_{ep} &= \left(\frac{3\times 0.5}{9\times 10^3}\right)^{1/2} \times 1.94\times 10^{15}\,\mathrm{sec}^{-1} \\ &\approx 2.5\times 10^{-2}\times 10^{15}\,\mathrm{sec}^{-1} \approx 10^{13}\,\mathrm{sec}^{-1} \approx 1.04\times 10^2\,\mathrm{meV}.\end{aligned} \tag{1.A.45}$$

Now, both the relations (1.A.32) and (1.A.44), although being quite useful, are wrong from a many–body point of view: ω_{ep} because electrons appear as bare electrons not dressed by the phonons, neither by the plasmons; ω_{ip} because the static negative background does not allow for an exchange of electron plasmons between ions, exchange eventually leading to a screened, short–range ionic Coulomb repulsive field. Namely ions interact, in the approximation used above, in terms of the "bare" ion–ion Coulomb interaction. Being it infinite range it does not allow for a dispersion relation linear in k at long wavelengths (sound waves) but forces a finite "mass" also to the lattice phonons. Allowing for electron screening of the "bare" ion–ion Coulomb interaction, as embodied in the electron gas dielectric function $\epsilon(0,q) = q^2/(k_s^2 + q^2)$, one obtains the dressed phonon frequency

$$\omega_q^2 = \frac{\omega_{ip}^2}{\epsilon(q)} = \frac{Zm_e}{AM}\frac{\omega_{ep}^2}{q^2 + k_s^2}q^2. \tag{1.A.46}$$

The quantity k_s is the Thomas–Fermi screening wave vector, a quantity which is of the order of the Fermi momentum, the associated screening length being then of the order of the Wigner–Seitz radius. Thus,

$$\lim_{q\to 0}\omega(q) = c_s q \tag{1.A.47}$$

where

$$c_s^2 = \frac{Zm_e}{AM}\frac{\omega_{ep}^2}{k_s^2}, \tag{1.A.48}$$

is the sound velocity. Making use of[56]

$$k_s = \left(\frac{6\pi^2 n_e e^2}{\epsilon_F}\right)^{1/2} = \left(\frac{6\pi^2 Z n_i e^2}{\epsilon_F}\right) \approx 1.6\,\text{Å}^{-1} \tag{1.A.49}$$

[56]cf. Ashcroft and Mermin (1987) p. 342.

and of (1.A.32), one can write

$$c_s^2 = \frac{Zm_e}{AM}\frac{4\pi n_e e^2}{m_e}\frac{\epsilon_F}{6\pi^2 n_e e^2} = \frac{2Z}{3\pi AM}\epsilon_F = \frac{Zm_e}{3\pi AM}v_F^2, \tag{1.A.50}$$

where use has been made of

$$n_e = \frac{3}{4\pi}\frac{1}{r_s^3} = 4.7\times 10^{-2}\,\text{Å}^{-3}\ (r_s = 1.72\,\text{Å}, \text{Li}), \tag{1.A.51}$$

and

$$\epsilon_F = \frac{50.1}{(r_s/a_0)} \approx 15.42\,\text{eV}\ (r_s/a_0 = 3.25\,, \text{Li}), \tag{1.A.52}$$

With the help of

$$k_F = \frac{1.92}{r_s}, \tag{1.A.53}$$

and of the velocity of light,

$$c = 3\times 10^{10}\,\text{cm/sec}, \tag{1.A.54}$$

one obtains,

$$\begin{aligned} v_F = \left(\frac{\hbar}{m_e}\right)k_F &= \left(\frac{\hbar c}{m_e c^2}\right)\times 3\times 10^{10}\frac{\text{cm}}{\text{sec}}\frac{1.92}{r_s} \\ &= \left(\frac{2\times 10^3\,\text{ÅeV}}{0.5\times 10^6\,\text{eV}}\right)\times 3\times 10^{10}\frac{\text{cm}}{\text{sec}}\frac{1.92}{r_s} \approx 10^8\frac{\text{cm}}{\text{sec}} \end{aligned} \tag{1.A.55}$$

Thus, for Li (^{9}Li)

$$c_s^2 = \frac{1}{3}\frac{3m_e}{9M}v_F^2 \approx 4.2\times 10^{-3}v_F^2, \tag{1.A.56}$$

and

$$c_s \approx 0.4210^{-2}v_F \approx 0.5410^6\frac{\text{cm}}{\text{sec}}. \tag{1.A.57}$$

That is, about a hundreth of the Fermi velocity, oro of the order of 10^6 cm/sec, in overall agreement with order of magnitude experimental findings[57]. Let us now discuss the effective electron–electron interaction. Within the jellium model used above one can write it as

$$V(\mathbf{q},\omega) = \frac{U_c(q)}{\epsilon(\mathbf{q},\omega)}, \tag{1.A.58}$$

where the dielectric function

$$\epsilon(\mathbf{q},\omega) = \frac{\omega^2(q^2+k_s^2)-\omega_{ip}^2 q^2}{\omega^2 q^2} = \frac{(q^2+k_s^2)(\omega^2-\omega_q^2)}{\omega^2 q^2} \tag{1.A.59}$$

[57] Ashcroft and Mermin (1987), p. 51.

contains the effects due to both the ions and the background electrons, while

$$U_c(q) = \frac{4\pi n_e e^2}{q^2} \tag{1.A.60}$$

is the Fourier transform of the bare Coulomb interaction

$$U_c(r) = \frac{e^2}{r}. \tag{1.A.61}$$

For $\omega \gg \omega_{ip}$ one obtains the so called screened Coulomb field,

$$U_c^{scr}(q) = \frac{4\pi e^2 n_e}{q^2 + k_s^2}, \tag{1.A.62}$$

its **r** space Fourier transform being

$$U_c^{scr}(r) = \frac{e^2}{r} e^{-k_s r}. \tag{1.A.63}$$

A quantity that for large values of r falls off exponentially. Thus, in the high frequency limit, the electron–electron interaction, although strongly renormalized by the exchange of plasmons, as testified by the fact that (e.g. for Li),

$$U_c^{scr}(r = 5\,\text{Å}) \approx U_c(r = 5\,\text{Å}) e^{-1.6\times 5} \approx 1\text{meV}, \tag{1.A.64}$$

as compared to $U_c(r = 5\,\text{Å} \approx 2.9\text{ eV})$, is still repulsive.

Let us now consider frequencies $\omega \ll \omega_{ip}$ but for values of q of the order of a^{-1}, where a is the lattice constant ($a \approx 3 - 5$Å, $a^{-1} \approx 0.25\text{Å}^{-1}$) to be compared to $k_s \approx 1.6\text{Å}^{-1}$ and $k_F \approx 1.12\text{Å}^{-1}$ (metallic Li). In the case in which $\omega_{ip}^2/\omega^2 > (q^2+k_s^2)/q^2$, V is attractive (see Eqs. (1.A.58) and (1.A.59)). This behavior explicitly involves the ions through ω_{ip} (electron–phonon coupling).

The dispersion relation of the associated frequency collective modes follows from

$$\epsilon(\mathbf{q}, \omega) = 0. \tag{1.A.65}$$

Making use of Eq. (1.A.59) one obtains the relation (1.A.46), as expected. One can now rewrite the reciprocal of the dielectric functions in terms of ω_q, that is,

$$\frac{1}{\epsilon(\mathbf{q}, \omega)} = \frac{\omega^2 q^2}{(q^2 + k_s^2)(\omega^2 - \omega_q^2)} = \frac{q^2}{q^2 + k_s^2}\left[1 + \frac{\omega_q^2}{\omega^2 - \omega_q^2}\right]. \tag{1.A.66}$$

For $\omega \gg \omega_q$ one recovers the Thomas–Fermi dielectric function. For ω near, but smaller than ω_q the interaction is attractive[58]. The effective electron–electron interaction can be then written as

$$\begin{aligned} V(q, \omega) &= \frac{4\pi n_e e^2}{q^2 + k_s^2} + \frac{4\pi n_e e^2}{q^2 + k_s^2} \frac{\omega_q^2}{\omega^2 - \omega_q^2} \\ &= U_c^{scr}(q) + U_c^{scr}(q) \frac{\omega_q^2}{\omega^2 - \omega_q^2} = U^{scr}(q)\left(1 + U^{scr}(q)\Pi(q, \omega)\right) \end{aligned} \tag{1.A.67}$$

[58] Schrieffer (1964), Fig. 6–11, p. 152.

The quantity

$$\Pi(q,\omega) = \left(\frac{Z}{AM}\right)\frac{q^2}{\omega^2 - \omega_q^2} \tag{1.A.68}$$

is intimately connected with Lindhard's function[59]. See also the close relation with the expression (1.A.20) of the nuclear renormalized pairing interaction. The first term of $V(q,\omega)$ contains the screened Coulomb field arising from the exchange of plasmons between electrons (cf. Fig. **??**). The second term with the exchange of collective low frequency phonons calculated making use of the same screened interaction as emerges from (1.A.67).

Let us now introduce the dimensionless quantity

$$\lambda = \langle F|V|I\rangle = N(0)U_c^{scr}\left(1 + U_c^{scr}\Pi\right). \tag{1.A.69}$$

In the weak coupling limit ($\lambda^2 \ll \lambda$)

$$\Delta = 2\omega_D e^{-1/\lambda}, \tag{1.A.70}$$

where ω_D is the Debye energy. Now, provided that we are in a situation in which ω is consistently different from ω_q,

$$\frac{1}{\lambda} = \frac{1}{N(0)U_c^{scr}\left(1 + U_c^{scr}\Pi\right)} \approx \frac{1}{N(0)U_c^{scr}}\left(1 - U_c^{scr}\Pi\right), \tag{1.A.71}$$

Thus

$$\frac{1}{\lambda} = \frac{1}{N(0)U_c^{scr}} - \frac{\Pi}{N(0)}, \tag{1.A.72}$$

and

$$\Delta = \left(2\omega_D e^{\frac{\Pi}{N(0)}}\right) e^{-\frac{1}{N(0)U_c^{scr}}}. \tag{1.A.73}$$

Consequently, the renormalization effects of the pairing gap associated with phonon exchange are independent of the approximation used to calculate U_c^{scr} (Thomas–Fermi in the above discussion), provided one has used the same "bare" (screened) Coulomb interaction to calculate ω_q^2. Otherwise, the error introduced through a resonant renormalization process entering the expression of e.g. the pairing gap may be quite large.

1.A.4 Pairing condensation (correlation) energy beyond level density

The condensation energy, namely the energy difference $W_N - W_S$ between the normal N– and superfluid S–state is defined as (Eq. (2-35) of ref[60])

$$W_{cond} = W_N - W_S = \frac{1}{2}N(0)\Delta_0^2, \tag{1.A.74}$$

[59] Lindhard (1953).
[60] Schrieffer (1964)

where $N(0)$ is the density of single–electron states of one–spin orientation evaluated at the Fermi surface (p. 31 of ref.[61])

$$E_{corr} = -\frac{1}{2d}\Delta^2 \tag{1.A.75}$$

to represent $W_S - W_N$ in the nuclear case, was calculated making use of a (single particle) spectrum of two–fold degenerate (Kramer degeneracy) equally spaced (spacing d) single–particle levels. Consequently, $2/d$ corresponds to the total level density, and $1/d = N(0)$. In keeping with the fact that a nucleus in the ground state (or in any single quantal state), is at zero temperature, (1.A.74) coincides with (1.A.75), taking into account the difference in sign in the definitions.

Nuclei

The empirical value of the level density parameter for both states $(\nu, \bar{\nu})$ (Kramers degeneracy, spin orientation in condensed matter) is $a = A/8$ MeV^{-1}, $A = N + Z$ being the mass number. Thus, for neutrons one can write $a_N = N/8$ and $N_N(0) = N/16$ MeV^{-1}. Thus, for $^{120}_{50}\mathrm{Sn}_{70}$, $N_N(0) \approx 4$ MeV^{-1}. Because $\Delta = 1.46$ MeV, (Table **??**)

$$W_{con} = \frac{1}{2} \times 4 \text{ MeV}^{-1} \times (1.46)^2 \text{ MeV}^2 \approx 4.3 \text{ MeV}. \tag{1.A.76}$$

The binding energy per nucleon is $BE/A = 8.504$ MeV. Thus $BE = 120{\times}8.504$ MeV $= 1.02 \times 10^3$ MeV, and

$$\frac{W_{cond}}{BE} \approx 4.2 \times 10^{-3}. \tag{1.A.77}$$

Superconducting lead

Making use of the value[62]

$$N(0) = \frac{0.276 \text{ eV}^{-1}}{\text{atom}}, \tag{1.A.78}$$

and of $\Delta_0 = 1.4$ meV, one obtains

$$W_{cond} = 0.27 \times 10^{-6} \text{ eV/atom}. \tag{1.A.79}$$

In keeping with the fact that the cohesive energy of lead, namely the energy required to break all the bonds associated with one of its atoms is

$$E_c = 2.03 \frac{\text{eV}}{atom}, \tag{1.A.80}$$

one obtains

$$\frac{W_{con}}{E_c} \approx 1.3 \times 10^{-7}. \tag{1.A.81}$$

The different quantities are summarized in Table (**??**).

[61] Bohr, A. and Mottelson (1975)

[62] **?**

Appendix 1.B Cooper pair: radial dependence

The fact that one is still trying to understand (BCS–like) pairing (abnormall density phenomena) in nuclei is, to a non negligible extent, due to the fact that, as a rule, pairing in these systems is constrained to manifest itself subject to a very strong "external" (mean, normal density) field[63]. Also, to same extent, due to the fact that the analysis of two–nucleon transfer data was made in terms of relative cross sections and not absolute cross sections as done now[64]. Within this context, Cooper pair transfer was viewed as simultaneous transfer, successive implying a breakup or, at least an anti–pairing disturbance of the pair. There exist a number of evidences which testify to the fact that the picture in which nucleon Cooper pairs are viewed as independent correlated entities over distances of the order of tens of fm (fig. 1.2.1), contains a number of correct elements (see e.g. Fig. 1.B.1). In this Appendix an attempt at summarizing these evidences, already mentioned or partially discussed before is attempted.

[65] The problem that Cooper solved was that of a pair of electrons which interact above a quiescent Fermi sphere with an interaction of the kind that might be expected due to the phonon and screened Coulomb field[66]. What he showed approximating this retarded interaction by a non–local one, active on a thin energy shell near (above) the Fermi surface[67], was that the resulting spectrum has an eigenvalue $E = 2\epsilon_F - 2\Delta$, regardless how weak the interaction is (and as a consequence the binding energy 2Δ of the pair), so long as the interaction is attractive. This result is a consequence of the Fermi statistic and of the existence of a Fermi sea background –the two electrons interact with each other but not with those in the sea, except via the Pauli principle– since it is well known that binding does not ordinarily occur in the two–body problem in three dimensions, until the strength of the attraction exceeds a finite threshold value.

The wavefunction of the two electrons can be written as

$$\Psi(\mathbf{r}_1, \mathbf{r}_2) = \phi_q(\mathbf{r}) e^{i\mathbf{q}\cdot\mathbf{R}} \chi(\sigma_1, \sigma_2) \tag{1.B.1}$$

where $\mathbf{R} = (\mathbf{r}_1 + \mathbf{2}_2)/2$, $\mathbf{r} = \mathbf{r}_1 - \mathbf{r}_2$, and σ_1 and σ_2 denote the spins[68].

Let us consider the state with zero center of mass ($q = 0$) and relative momenta momentum, so that the two electrons carry equal and opposite momenta, aside of

[63] c.f. e.g. Matsuo, M. (2013).

[64] See Potel, G. et al. (2013a) and references therein.

[65] Of course such manifestation will be latent, expressing itself indirectly. In other words, abnormal density can only be present when normal density, at ever so low values already is. The pairing field does not have within this context an existence by itself uncoupled from the normal density. On the other hand this, in most cases latent (more than virtual), and in only few cases factual existence, has important consequences on nuclear properties.

[66] Cooper (1956).

[67] States below the Fermi surface are frozen because of Pauli principle.

[68] In the limit $q \to 0$ the relative coordinate problem is spherically symmetric so that $\phi_0(\mathbf{r})$ (Schrieffer (1964)).

being in the singlet spin state state, with

$$\chi = \frac{1}{\sqrt{2}}\left[\begin{pmatrix} 1 \\ 0 \end{pmatrix}\begin{pmatrix} 0 \\ 1 \end{pmatrix} - \begin{pmatrix} 0 \\ 1 \end{pmatrix}\begin{pmatrix} 1 \\ 0 \end{pmatrix}\right] \tag{1.B.2}$$

We have thus a pair of electrons moving in time reversal states and can write[69],

$$\phi_0(\mathbf{r}) = \sum_{k>k_F} g(\mathbf{k}) e^{i\mathbf{k}\cdot\mathbf{r}}. \tag{1.B.3}$$

In the above wavefunction Pauli principle ($k > k_F$) and translational invariance (dependence on the relative coordinate $\mathbf{r}$) are apparent. The pair wavefunction is likely a superposition of one–electron levels with energies of the order pf 2Δ close to ϵ_F, since tunneling experiments indicate that for higher energies the one–electron density is little altered from the form it has in normal metals. The spread in momenta of the single–electron levels entering (1.B.3) is thus fixed by the condition

$$2\Delta \approx \delta E \approx \delta\left(\frac{p^2}{2m}\right)_{\epsilon_F} \approx v_F \delta p. \tag{1.B.4}$$

Consequently

$$\frac{\delta p}{p_F} = \frac{2\Delta}{m v_F^2} = \frac{\Delta}{\epsilon_F} \ll 1. \tag{1.B.5}$$

Thus, $\phi_0(\mathbf{r})$ consists mainly of waves of wavenumber k_F. Now, because the wavefunction of a Cooper pair represents a bound s–state, the motion it describes is a periodic back and forth movement of the two electrons in directions which are uniformly distributed, concerning a relative distance ($\delta x \delta p = \hbar$)

$$\xi = \delta x = \frac{\hbar}{\delta p} = \frac{\hbar v_F}{2\Delta} \tag{1.B.6}$$

as schematically shown in Fig. 1.B.1 (**i**). It is analogous to the motion of the two nucleon in a deuteron or the main ($L = 0$) component of the two neutrons in the triton. The hydrogen atom in s–state is also an example; in that case it is the electron that does most of the back and forth moving, whereas the proton only recoils slightly.

In keeping with the above arguments and with (1.B.5), $\phi_0(\mathbf{r})$ will look like $e^{i\mathbf{k}_F\cdot\mathbf{r}}$ for $r \ll \xi$, while for $r \gg \xi$ the waves $e^{i\mathbf{k}\cdot\mathbf{r}}$ weighted by $g(k)$ will destroy themselves by interference (1.B.2). From the above physical arguments, $\phi_0(\mathbf{r})$ will look like $e^{i\mathbf{k}_F\cdot\mathbf{r}}$ for $r \ll \xi$ while for $r \gtrsim \xi$ one can approximate the weighing function as,

$$g(k) \sim \delta(\mathbf{k}, \mathbf{k}_F + i\hat{\mathbf{k}}_F/\xi), \tag{1.B.7}$$

[69] In other words, one expands the $l = 0$ wavefunction ϕ_0 in terms of s–states of relative momentum k and total momentum zero.

resulting in

$$\phi_0(\mathbf{r}) \sim e^{-r/\xi} e^{ik_F r}. \tag{1.B.8}$$

Because we are dealing with a singlet state, and the total wavefunction has to be antisymmetric,

$$\phi_0(\mathbf{r}) \sim e^{-r/\xi} \cos k_F r, \tag{1.B.9}$$

A more proper solution of the Cooper pair problem leads to[70]

$$\phi_0(\mathbf{r}) \sim K_0(r/\pi\xi) \cos k_F r, \tag{1.B.10}$$

where K_0 id the zeroth–order modified Bessel function. For $x \gg 0$, $K_0(x) \sim (\pi/2x)^{1/2} \exp(-x)$, where $x = r/\pi\xi$.

A wavefunction which extends over distances much larger than the binding potential is a well–known phenomenon when the binding energy is small. For example, in the case of the deuteron. In any case, it is of notice that here we are discussing a rather subtle phenomenon, pairing or better Cooper pairing, which has to express itself in the presence of a very strong "external" field. Unless one does not relate the *NN* interaction binding the deuteron to proton–neutron pairing.

[70] Kadin (2007).

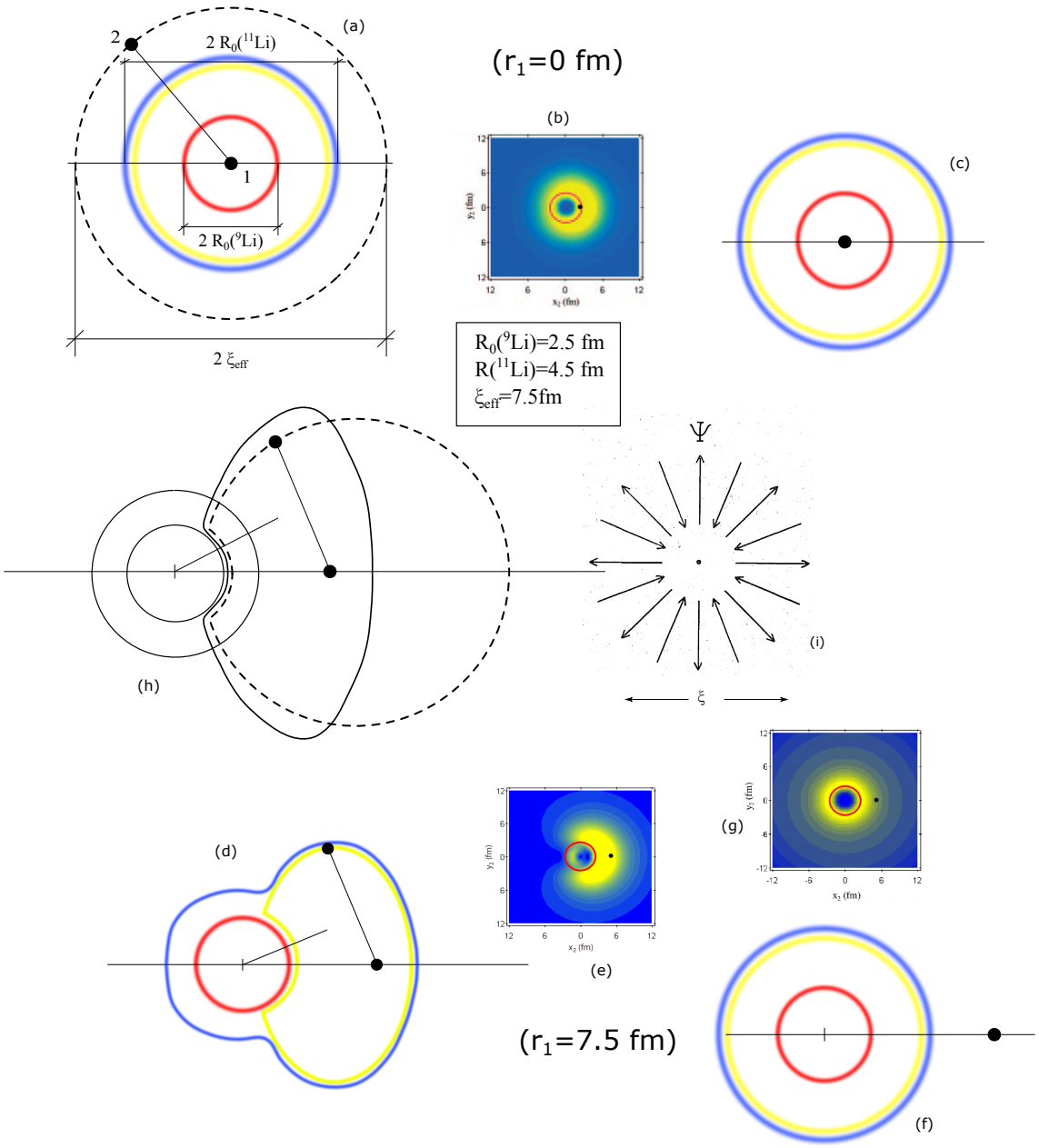
(a)
2
2 R0(11Li)
1
2 R0(9Li)
2 ξeff
(r1=0 fm)
(b)
(c)
R0(9Li)=2.5 fm
R(11Li)=4.5 fm
ξeff=7.5fm
Ψ
(i)
ξ
(h)
(d)
(e)
(g)
(r1=7.5 fm)
(f)

Figure 1.B.1

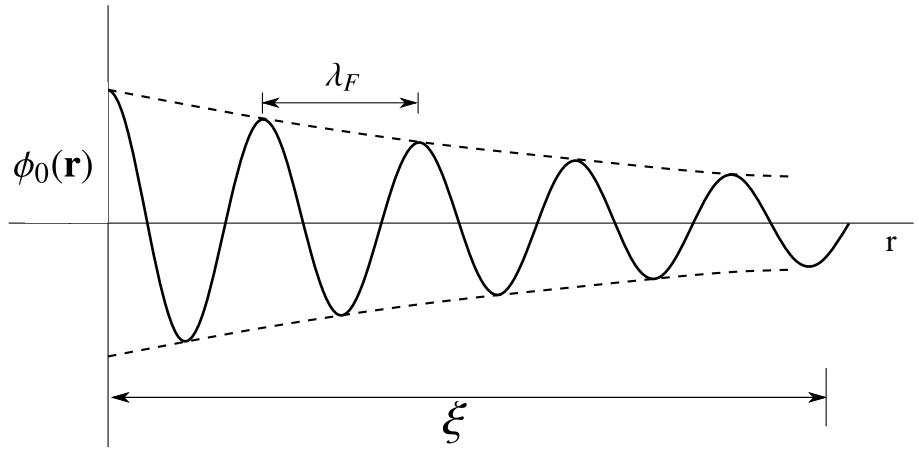

Figure 1.B.2: Schematic representation of the Cooper pair wavefunction. Indicated are the coherence length and the Fermi wavelength $\lambda_F = h/p_F = 2\pi/k_F$. In the nuclear case $\lambda_F \approx 4.6$ fm and $\xi \approx \hbar v_F/2\Delta \approx 30$ fm ($v_F/c \approx 0.3, \Delta \approx 1$ MeV). Thus $\xi/\lambda_F \approx 7$ (after **?**).

Caption Fig 1.B.1

Synthesis of the spatial structure of ^{11}Li neutron halo Cooper pair calculated in NFT (Barranco, F. et al. (2001)). To make more direct the comparison between the simple estimates and the results of the above reference, it is assumed that $\xi = 7.5$ fm (dashed circle) instead of 10–11 fm as obtained from $\xi = \hbar v_F/\pi|E_{corr}|$ ($v_F/c \approx 0.08, E_{corr} \approx 0.4$ MeV). **(a)** The continues line circles correspond to the relative distance r at the radius of the ^{9}Li core and of ^{11}Li. The Cooper pair "intrinsic coordinate" r_{12} is also shown. Particle 1 of the Cooper pair is assumed to occupy the center of the nucleus ($r = 0$). **(b)** result of NFT for a situation similar to the above. **(c)** Schematic representation of an uncorrelated pair in a potential weakly binding the pure configuration $p^2_{1/2}(0)$. **(d)** same as (a) but for $r = 7.5$ fm. **(e)** result of the NFT calculation for this configuration. **(f)** Schematic configuration of a pure configuration $p^2_{1/2}(0)$, **(g)** the result of the microscopic calculation for a weakly bound $p^2_{1/2}(0)$ configuration. **(h)** The variety of situations in (a) and (d) in comparison to each other in a single representation. (**i**) Schematic picture of the dynamics in the quantum state of the Cooper pair. It is a linear combination of motions away and towards ona another. The electrons stay within a distance of the order ξ, root mean square radius of the Cooper pair (After **?**, see also Kadin (2007) and **?**). Be as it may, the large size of the Cooper pair wavefunction also explains why the electrostatic repulsion between electron pair does not appreciably influence the binding. The repulsion acts only over distances of the order of the Debye length, in keeping with the fact that one has to do with a screened Coulomb field.

Within the nuclear scenario, to interact at profit through long wavelength medium

Vibrations

(ph) | (pp), (hh)

correlated excitations (E_{corr})
with transfer quantum number

α=0 | $\alpha = \pm 2$

waves on

the nuclear | the Fermi

surface

correlation length
infinite medium ($|E_{corr}| = \frac{\hbar^2 k^2}{2m}$)

$$\lambda\!\!\!^{-} = \frac{1}{k} \approx \frac{\langle k \rangle_F}{2m} \frac{1}{|E_{corr}|} = \frac{\hbar v_F}{\pi |E_{corr}|}$$

typical values (finite nuclei), E_{corr}=-2.0 MeV (-0.4 MeV, 11Li), $v_F/c \approx 0.3$ (0.1,^{11} Li)

$$\xi \approx 10$$

genralized quantality parameter

$$q_\xi = \frac{\hbar^2}{2m(\xi)^2} \frac{1}{|E_{corr}|} \approx 0.1 \quad (0.08,^{11}\text{ Li})$$

strongly correlated (cluster like $q_\xi \ll 1$), weakly bound ($|E_{corr}|/\epsilon_F \lesssim 0.06$)
very extended ($\xi/d \approx 5$, $d = \left(\frac{4\pi R^3}{3A}\right)^{1/3}$) objects

subject to a strong external field

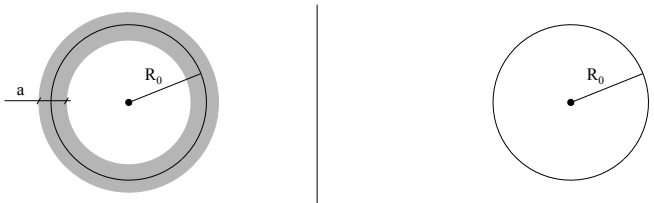

example

$^{223}\text{Ra} \rightarrow {}^{14}\text{C} + {}^{209}\text{Pb}$ ($\lambda = PfT$)

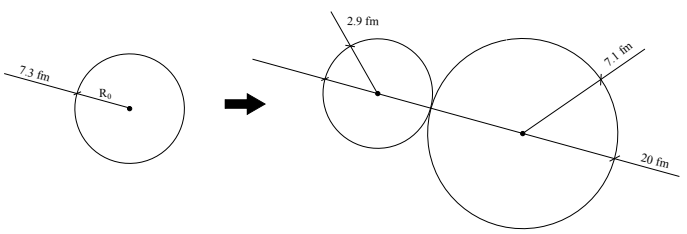

$$P = \begin{cases} 10^{-76} & (\Delta = 0) \\ 10^{-10} & \Delta_{exp} \end{cases}$$

$$\langle r^2 \rangle^{1/2}_{Cooper} = \xi = \frac{\hbar v_F}{\pi \Delta} \quad (\approx 24\,\text{fm}; \Delta = 0.8\,\text{MeV})$$

Figure 1.B.3

Metals | Nuclei

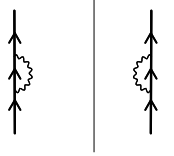

dressed

electrons (m=0.5 MeV) | nucleons (m=10^3 MeV)

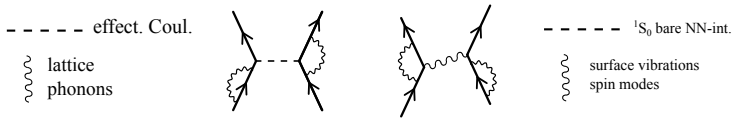

spontaneous breaking of gauge symmetry

$\left(U_\nu + V_\nu a^\dagger a_{\bar{\nu}^\dagger}\right)|0\rangle \quad U'_\nu + e^{-2i\phi} V'_\nu a^\dagger_\nu a^\dagger_{\bar{\nu}}$

independent pair motion

$\xi\,(\xi/d)$

10^4 Å(10^4) | 20 fm (5)

$\Delta(\Delta/\epsilon_F)$

$\approx$ 1 meV (10^{-4}) | $\approx$ 1 MeV (10^{-2})

generalized quantality parameter

$$q_\xi = \frac{\hbar^2}{2m\xi^2}\frac{1}{\Delta}$$

10^{-5} | 10^{-2}

probing of gauge deformation

observation of currents between two weakly coupled superconductors (barrier) allows essentially for single tunneling, with 2e carriers (Josephson effect)

Single Cooper pair tunneling mainly as successive transfer between member of a piring rotational band fulfilling

$$\frac{\sigma(gs(N) \to gs(N+2))}{\sum_{exc}\sigma(gs(N) \to 0^+_{exc}(N+2))} \gg 1$$

$$N = N_0, N_0+2, N_0+4 \ldots N_0+14 \ldots (N_0 = 10)$$

P_2=P_1

Figure 1.B.4

polarization pairing, pairs of nucleons have to have low momentum. To do so they have to reduce the effect of the strong external (mean) field by moving away from it, possible mechanisms being among other: halo (1.B.1), transfer processes (see e.g. 1.4.1), exotic decay[71] (see Fig. 1.B.3.

[71] In Fig. 1.B.3, a parallel is made between correlation lengths between pairing particle–particle modes and particle–hole vibrations, modes which also display a consistent spatial correlation (see e.g. Broglia et al. (1971)).

Caption Fig 1.B.3

Vibrations can be classified by the transfer quantum number α. Collective modes with $\alpha = 0$ correspond to correlated particle–hole (ph) excitation. For example low–lying quadrupole or octupole (surface and/or density) vibrations. Modes with $\alpha = \pm 2$ are known as correlated (pp) or (hh) modes, that is, pair addition and pair substraction modes. Thinking that these modes propagate in uniform nuclear matter, the reduced wavelength $\lambda\!\!\!^{-} = \lambda/2\pi = 1/k$ is estimated in terms of the correlation energy E_{corr}. The (generalized) quantality parameter, been the ratio of the quantal kinetic energy of localization and the correlation energy, and gives a measure of the tendency to independent particle ($q_\xi \approx 1$) or pair ($q_\xi \ll 1$) motion, in keeping with the fact that potential energy is best profited by special arrangements between nucleonos and thus lower symmetry than the original Hamiltonian, while fluctuations favor symmetry. In going from the infinite to the finite nuclear system, e.g. example density becoming surface modes, they are strongly distorted by the mean field which acts as a strong external field (see also Fig. 1.B.1). A concrete example which testifies to the fact that (ph) excitations (large amplitude surface distortion) and independent (pp) motion (superfluidity) are correlated over dimensions larger than the nuclear size is provided by e.g. fission and exotic decay, in particular ^{223}Ra$\rightarrow{}^{14}$C+^{209}Pb exotic decay. In keeping with the uncertainties affecting the above simple estimates (factor 2 or π in the denominator of $\xi, \langle r^2\rangle^{1/2}_{Cooper}$ or $\sqrt{\frac{3}{5}}\langle r^2\rangle^{1/2}_{Cooper}$, etc.), it seems fair to conclude that $10 \lesssim \xi \lesssim 20$. Thus, one is likely faced with an intermediate situation in which $1.3 \lesssim \xi/R \lesssim 2.6$. The parallel which can be traced between Cooper pairs and correlated particle–hole excitations is further testified by the fact that two–nucleon transfer reaction do excite quite strongly also these modes (see Tables A and B).

In the nuclear case, the number of Cooper pairs participating in the condensate is

$$\alpha_0 = \langle BCS|P^\dagger|BCS\rangle = \sum_j \frac{2j+1}{2} U'_j V'_j. \tag{1.B.11}$$

A simple estimate of this number can be made with the help of the single j–shell model, in which case $V_j = (N/2\Omega)^{1/2}$ and $U_j = (1 - N/2\Omega)^{1/2}$, where $\Omega = (2j+1)/2$. For a half–filled shell ($N = \Omega$) one obtains[72] $\alpha'_0 = \Omega/2$. In the case of $^{120}Sn, \alpha'_0 = 6 - 8$. In keeping with the fact that $\xi > R_0$, in the nuclear case one has a complete overlap between all Cooper pairs participating in the condensate. This, together with the fact that the nuclear Cooper pairs press against the nuclear surface in an attempt to expand and are forced to bounce elastically off from it, receive strong circumstantial evidence from the following experimental results: **1**) while the moment of inertia of rotational bands is $\mathcal{J}_r/2$ it is $5\mathcal{J}_{irrot}$. In other words, while pairing in nuclei is important its role is only partially exhausted, and certainly strongly distorted (Bohr, A. and Mottelson (1975)). **2**) One and two–nucleon transfer reactions in pairing correlated nuclei have the same order of magnitude. For example $\sigma(^{120}\mathrm{Sn}(p,d)^{119}\mathrm{Sn}(5/2^+; 1.09\ \mathrm{MeV})) = 5.35\mathrm{mb}$ ($2^\circ < \theta_{cm} < 55^\circ$), while $\sigma(^{120}\mathrm{Sn}(p,t)^{118}\mathrm{Sn}(gs)) = 2.25\mathrm{mb}$ ($7.6^\circ < \theta_{cm} < 59.7^\circ$). In this last reaction Cooper pair partners can be as far as 12–13 fm. In the case of a heavy ion reaction this distance becomes almost double (Fig. 1.4.1). 3) The decay constant of the exotic decay $^{223}_{88}\mathrm{Ra}_{135} \rightarrow ^{14}_{6}\mathrm{C}_8 + ^{209}_{82}\mathrm{Pb}_{127}$ has been measured to be $\lambda_{exp} = 4.3 \times 10^{-16}\mathrm{sec}^{-1}$. For theoretical purposes it can be written as $\lambda = PfT$, product of the formation probability P of ^{14}C in ^{223}Ra (saddle configuration, see Fig. 1.B.3), the knocking rate f and the tunneling probability T. These two last quantities hardly depend on pairing. On the other hand P changes from $\approx 2\times10^{-76}$ to 2.3×10^{-10}, and consequently the associated lifetimes from 10^{75}y to the observed value of 10^8y by allowing Cooper pairs to be correlated over distances which can be as large as 20 fm.

Within the above context, exotic halo nuclei open new possibilities to understand the physics at the basis of pairing in nuclei.

1.B.1 tunneling probabilities

In general, the coefficients U_ν, V_ν entering the BCS wavefunction $\prod_{\nu>0}(U_\nu + V_\nu a^\dagger_\nu a^\dagger_{\bar\nu})|0\rangle$ are complex. Let us employ the standard phasing $U_\nu = U'_\nu e^{i\phi}$, $V_\nu = V'_\nu e^{-i\phi}$, where U'_ν and V'_ν are real, and define the state,

$$\begin{aligned}|BCS(\phi)\rangle_{\mathcal{K}} =& \mathcal{G}(\phi)\prod_{\nu>0}(U_\nu + V_\nu a^\dagger_\nu a^\dagger_{\bar\nu})|0\rangle = e^{\frac{iN}{2}\phi}\prod_{\nu>0}(U'_\nu + V'_\nu e^{-2i\phi} a^\dagger_\nu a^\dagger_{\bar\nu})|0\rangle \\ &= e^{\frac{iN}{2}\phi}\prod_{\nu>0}(U'_\nu + V'_\nu a'^\dagger_\nu a'^\dagger_{\bar\nu})|0\rangle = |BCS(\phi)\rangle_{\mathcal{K}'}\end{aligned} \tag{1.B.12}$$

[72] Making use of the harmonic oscillator, one can write $\Omega = \frac{1}{2}(N+1)(N+2) \sim A^{2/3}$, where the proportionality constant has a value between 1/2 and 2/3.

where use has been made of the gauge transformation $a_\nu'^\dagger = \mathcal{G}(\phi)\, a_\nu^\dagger\, \mathcal{G}^{-1}(\phi), \mathcal{G}(\phi) = e^{-iN\phi}$ inducing a rotation in gauge space. The labels $\mathcal{K}$ and $\mathcal{K}'$ indicate the laboratory and body–fixed reference frames respectively.

The state (1.B.12) displays off–diagonal–long–range–order (ODLRO) because each pair is in a state $(U_\nu' + V_\nu' e^{-2i\phi} a_\nu^\dagger a_{\bar\nu}^\dagger)|0\rangle$ with the same phase as all the others. In fact, the wavefunction (1.B.12) leads to a two–particle density matrix with the property $\lim_{\mathbf{r}_1,\mathbf{r}_2;\mathbf{r}_3,\mathbf{r}_4\to\infty} \phi(\mathbf{r}_1,\mathbf{r}_2;\mathbf{r}_3,\mathbf{r}_4) \neq 0$ under the assumption that $r_{12}, r_{34} < \xi, (\mathbf{r}_1,\mathbf{r}_2)$ and $(\mathbf{r}_3,\mathbf{r}_4)$ being the coordinates of a Cooper pair, r_{ij} the relative modulus of it and ξ the coherence length[73].

1.B.2 Number of overlapping pairs

The coherence length for low–temperature superconductors is of the order of 10^4Å. In fact, in the case of e.g. Pb, for which[74] $\Delta = 0.62$ meV and $v_F = 1.83 \times 10^8$ cm/s one obtains $\xi \approx 10^4$ cm, where use of $c = 3 \times 10^{10}$ cm/s and $\hbar c \approx 2 \times 10^3$ÅeV has been made.

Since electrons in metals typically occupy a volume of the order of $(2\text{Å})^3$ (Wigner–Seitz cell), there would be of the order of[75] $\xi^3/(2\text{Å})^3 \approx 10^{11}$ other electrons within a "coherence volume". Eliminating the electrons deep within the Fermi sea as they behave essentially as the metal was in the normal phase, one gets[76] 10^6. In other words, about a million of other Cooper pairs have their center of mass falling inside the coherence volume of a pair. Thus, the isolated pair picture is not correct. Let us bring this structure result into reaction. The fact that the wavefunction of the nucleons in the pair are phase–coherent ($(U_\nu' + V_\nu' e^{-2i\phi} a_\nu^\dagger a_{\bar\nu}^\dagger)|0\rangle$) implies that to calculate the probability of two–nucleon transfer, one has to add the amplitudes of one–nucleon transfer before taking modulus squared, that is,

$$\begin{aligned} P_2 &= \lim_{\epsilon\to 0} \left| \frac{1}{\sqrt{2}} \left(e^{i\phi'} \sqrt{P_1} + e^{i\phi} \sqrt{P_1} \right) \right|^2 \quad (\epsilon = \phi - \phi') \\ &= P_1 \lim_{\epsilon\to 0} (1 + \cos\epsilon) = P_1. \end{aligned} \tag{1.B.13}$$

In keeping with the parallel made with superconductors (see Fig. **??**) one can mention that Josephson showed that at very low temperatures, the pair current is equal to the single–particle current at an equivalent voltage[77] $\pi\Delta/2e$. How conclusive this result is concerning the mechanism at the basis of Cooper pair transfer is connected with the fact that the probability of one–electron–tunneling across a typical dioxide layer giving rise to a weak $S-S$ coupling is 10^{-10}, Consequently,

[73] See e.g. Ambegaokar (1969) and refs. therein.

[74] The standard quoted value is $\Delta_0 = 7.19$ K. Making use of the conversion factor 1k→ 8.6217×10^{-5} eV one obtains 0.62 meV.

[75] **?** p. 198.

[76] Schrieffer (1964) p. 43.

[77] In the case of Pb this voltage is $(\pi \times 0.62/2)$eV/e≈ 1V (see e.g. McDonald (2001)).

simultaneous pair transfer between two superconductors (S), with a probability $(10^{-10})^2$ cannot be observed[78].

One could argue that in the reaction $^{120}\mathrm{Sn}(p,t)^{118}\mathrm{Sn}(\mathrm{gs})$ one can hardly consider the triton as a condensate. While this is correct one can hardly claim either that 6 Cooper pairs make a *bona fide* one. In any case, when one experimentally observes such unexpected behaviour ($\sigma_{2n} \approx \sigma_{1n}$) one is likely somewhat authorized at using similar concepts[79].

1.B.3 Correlation energy

The BCS mean field can be written as[80]

$$H_{MF} = U + H_{11} \tag{1.B.14}$$

where

$$U = 2\sum_{\nu>0}(\epsilon_\nu - \epsilon_F)V_\nu^2 - G\alpha_0^2 \tag{1.B.15}$$

while

$$H_{11} = \sum_{\nu>0} E_\nu(\alpha_\nu^\dagger\alpha_\nu + \alpha_{\bar{\nu}}^\dagger\alpha_{\bar{\nu}}), \tag{1.B.16}$$

E_ν being the quasiparticle energy, and $\alpha_\nu^\dagger$ the quasiparticle creation operator. The pair–correlation energy is the difference between the energy with and without pairing. the energy including pair correlations is

$$E_p = 2\sum_{\nu>0}|V_\nu|^2\epsilon_\nu - G\,|\alpha_0|^2 \tag{1.B.17}$$

while the energy without correlation is

$$E_0 = \sum_{\nu>0}|V_\nu^0|^2\epsilon_\nu. \tag{1.B.18}$$

The occupation probabilities $|V_\nu^0|$ are unity below the Fermi energy level and zero above. In both Eqs. (1.B.17) and (1.B.18) the Fermi energy has to be chosen to give the correct number of particles. The pairing correlation energy is

$$E_{corr} = E_S - G\,|\alpha_0|^2, \tag{1.B.19}$$

where

$$E_S = \sum_{\nu>0} 2(|V_\nu|^2 - |V_\nu^0|^2)\,\epsilon_\nu. \tag{1.B.20}$$

[78] See e.g. McDonald (2001).

[79] Anderson (1972).

[80] Brink, D. and Broglia (2005), Appendix G.

The total pairing energy $-G|\alpha_0|^2$ is partially canceled by the first term describing the fact that, in the BCS ground state, particles moving in levels close to the Fermi energy are partially excited across the Fermi surface, in keeping with the fact that V_ν^2 changes smoothly from 1 to 0 around ϵ_F, being 1/2 at the Fermi energy.

In other words, the energy gain resulting from the potential energy term, where G is the pairing coupling constant while $|\alpha_0|$ measures the number of Cooper pairs is partially compensated by a quantal, zero point fluctuation like term. It can, in principle, be related to the Cooper pair kinetic energy of confinement $T_\xi = \frac{\hbar^2}{2m}\frac{1}{\xi^2}$ already discussed in connection with the generalized quantality parameter according to $2|\alpha_0|T_\xi$ (for one type of nucleons), in keeping with the fact that (1.B.20) is expressed in term of single nucleon energies. Let us make a simple estimate which can help at providing a qualitative exmple of the above argument, and consider for the purpose the nucleus ^{223}Ra and $G \approx (22/A)$ MeV, $|\alpha_0| \approx 6$ and $\xi \approx 10$ fm: $T_\xi \approx 0.2$ MeV, $2 \times (2 \times |\alpha_0| \times T_\xi) = 4.8$ MeV, $2 \times (-G|\alpha_0|^2) = -7.2$ MeV[81] (factors of 2,both protons and neutrons). The resulting pairing correlation energy thus being $E_{corr} = -2.6$ MeV. This number can be compared with a "realistic" estimate provided by the relation[82]

$$E_{corr} = -\frac{g\Delta^2}{4}, \tag{1.B.21}$$

where $g_n = N/16$ MeV^{-1} and $g_p = Z/16$ MeV^{-1}. Taking into account both type of particles $g = g_n + g_p = A/16$ MeV^{-1} and making use of $\Delta = 12/\sqrt{A}$ MeV, one obtains $E_{corr} = -\frac{144}{64}$ MeV =-2.25 MeV. With the help of E_{corr} and T_ξ, one can estimate the generalized quantality parameter, $q_\xi = T_\xi/|E_{corr}| = 0.2/2 \approx 0.08$, as well as make a consistency check on the value of ξ used, namely $\hbar v_F/(2|E_{corr}|) \approx 11.5$ fm.

1.B.4 Coherence length and quantality parameter for (ph) vibrations

Vibrations: correlated (ph) $(\alpha = 0)(pp)(\alpha = +2)$ and $(hh)(\alpha = -2)$ modes, with energy $E_{corr}(< 0)$ and fulfilling the dispersion relation in nuclear matter,

$$\begin{aligned} |E_{corr}| &= \frac{\hbar^2 k^2}{2m}. \\ \lambda\!\!\!^{-} = \frac{1}{k} &\approx \frac{\hbar^2 k_F}{2m}\frac{1}{|E_{corr}|} = \frac{\hbar p_F}{|E_{corr}|} \\ &= \frac{\hbar v_F}{2|E_{corr}|} \end{aligned} \tag{1.B.22}$$

[81] This quantity, but divided by 2, i.e. -3.6 MeV can be compared with the effective pairing matrix element $v = \left(\frac{\Delta_\pi^2+\Delta_\nu^2}{4} \approx -2.9\right)$ MeV, operative at level crossing in the calculation of the inertia of the exotic decay ^{223}Ra$\rightarrow{}^{14}$Ca+^{209}Pb, cf. Brink (1955).

[82] Brink, D. and Broglia (2005).

To be compared with

$$\xi = \frac{\hbar v_F}{2\Delta} \tag{1.B.23}$$

for superfluid nuclei. Thus one can assume both $\lambda\!\!\!^{-}$ and ξ describe the same physical phenomenon: correlation length of two fermions in normal $((pp), (ph), (hh)$ or in superfluid $((pp))$ nuclei.

Typical order of magnitude: $E_{corr} \approx -1.2$ MeV and $\Delta \approx 1.2$ MeV for medium heavy nuclei lying along the stability valley. Thus

$$\xi = \frac{\hbar v_F}{2|E_{corr}|} \approx \frac{\hbar c(V_F/c)}{2.4 \text{ MeV}} \approx \frac{200 \text{ MeV fm} \times 0.3}{2.4} \approx 25 \text{ fm} \tag{1.B.24}$$

In the case of ^{11}Li, $E_{corr} \approx -400$ keV and $v_F/c \approx 0.1$. Thus

$$\xi = \frac{200 \text{ MeV fm} \times 0.1}{0.8} \approx 25 \text{ fm}. \tag{1.B.25}$$

Generalized quantality parameter

$$q_\xi = \frac{\hbar^2}{2m\xi^2}\frac{1}{|E_{corr}|} = \begin{cases} \frac{20 \text{ MeV fm}}{25^2 1.2 \text{ MeV}} \approx 0.03 & \\ \frac{20 \text{ MeV fm}}{25^2 0.4 \text{ MeV}} \approx 0.08 & ^{11}\text{Li} \end{cases} \tag{1.B.26}$$

1.B.5 Possible (dream?) experiment[83]

The nuclear Cooper pair not only is forced to exist in a very strong external field, the HF mean field, of very reduced dimensions as compared to the correlation length. Because of spatial quantization, it is also forced to exist on selected orbitals of varied angular momentum and parity.

Correlations, in particular pairing correlations within such constrains will have opposite and apparently contradictory effects. As an example let's consider two neutrons moving around ^{9}Li in the $s^2_{1/2}(0)$ or in the $p^2_{1/2}(0)$ (pure) uncorrelated configurations. In such a situation, fixing one of the neutrons of the pair at a radius r_1, the other one will display equal possibility to be close or in the opposite side of the nucleus ($\theta_{12} = 0^\circ$ or $\theta_{12} = 180^\circ$), the average distance between neutrons being of the order of $d = \left(\frac{\frac{4\pi}{3}R^3}{A}\right)^{1/3} \approx 2$ fm (3.3 fm using $R(^{11}\text{Li})$=4.6 fm instead of $R = 1.2A^{1/3}$ fm).

By exchanging the GDPR between the two outer neutrons, the halo Cooper pair becomes stabilized, becoming weakly bound ($S_{2n} = 380$ keV). Assuming that

[83] The breaking of a prejudice: pairing plus long range force, i.e. pairing short range, many (high) relative angular momenta contributing (Kisslinger,Leonard S. and Sørensen,Raymond A. (1963); Soloviev (1965); Mottelson (1962, 1998).

the odd neutron $p_{3/2}(\pi)$ plays only a spectator role, the ground state of ^{11}Li can be written as $|^{11}\mathrm{Li}(gs)\rangle = |\tilde{0}\rangle \otimes |p_{3/2}(\pi)\rangle$, the neutron halo Cooper pair state being

$$|\tilde{0}\rangle \approx 0.45|s^2_{1/2}(0)\rangle + 0.55|p^2_{1/2}(0)\rangle + 0.04|d^2_{5/2}(0)\rangle \quad (1.B.27)$$

$$+ 0.71|(p_{1/2}, s_{1/2})_{1^-} \otimes 1^-; 0\rangle + 0.1|(s_{1/2}, d_{5/2})_{2^+} \otimes 2^+; 0\rangle. \quad (1.B.28)$$

Studying this state microscopically one observes two contrasting effects taking place:

1. The two neutrons will switch from a regime of independent pair motion and adopt the configuration proper to a Cooper pair (radial motion against each other, Weisskopf) and expand radially consistent with the fact that its mean surface radius ($\xi = \langle r^2 \rangle \approx \frac{\hbar v_F}{\pi E_{corr}} \approx \hbar c(v_F/c)/\pi E_{corr} \approx \frac{200 \text{ MeV fm} \times 0.15}{\pi 0.4 \text{ MeV}} = 24$ fm, $\epsilon_F(^{11}\mathrm{Li}) \approx 24$ MeV $\rightarrow v_F/c \approx 0.15$). This can be appreciated by the fact that the radius of ^{11}Li is much larger than that expected from systematic ($R(^{11}\mathrm{Li}) = 4.6$ fm, corresponding to an effective mass number $A_{eff} \approx 60$). Such long range correlations are likely at the basis of the large cross section observed in the reaction $^1\mathrm{H}(^{11}\mathrm{Li},^9\mathrm{Li})^3\mathrm{H}$, in keeping with the fact that a large interval of relative motion coordinate will contribute to the transfer amplitude, in keeping with the fact that the process is dominated by successive transfer. In other words, large two–nucleon transfer cross sections are not a consequence of the fact that the two halo neutrons are close to each other like in the triton, as simultaneous transfer (a process resulting from the single action of the mean field, the second nucleon coming along because of correlation) contributes little to the transfer amplitude, which is dominated by successive transfer. The associated (p, d) and subsequent (d, t) processes are both mediated by the mean field over a range of relative distances between target and projectile determined by the tail of the Cooper pair partners wave function, each decaying with a $\kappa \approx \left(\frac{2mS_n}{\hbar}\right)^{1/2}$ ($S_n \approx 380$ keV). They extend over distances not incompatible with a consistent fraction of the correlation length (i.e. $r \approx 1/\kappa \approx 7$ fm). Within this scenario, one can expect, that the cross section associated with the reaction $^{10}\mathrm{Be}(^{11}\mathrm{Li},^9\mathrm{Li})^{12}\mathrm{Be}(0^{+*}$; 2.24 MeV) can be larger than that populating the ground state (eventually correcting for Q–value effects), in keeping with the expected halo character of the excited 0^{+*} state. the eventual population , in the same reaction, can provide important information concerning the alleged symbiotic character of neutron halo par addition modes.

2. Intterference between positive ($(-1)^l = +1$) and negative ($(-1)^l = -1$) single–particle based $|(l, j)^2_0\rangle$ configurations, constructive at $\theta = 0°$ and destructive at $\theta = 180°$, $\theta = r_1\hat{r}_2$ been the relative angle between the coordinates $\mathbf{r}_1$ and $\mathbf{r}_2$ of the Cooper pair partners. In other words the two nucleons will tend to be close to each other, in particular on the nuclear surface. As can be seen from (1), this effect is extreme in the case of the ground state

of ^{11}Li. Now, such an effect has not much to do with pairing, BCS pairing at it and thus superconductivity[84] , but with the properties of the nuclear mean field, result of spatial quantization which not only distorts the Cooper pair through isotropic confinement, but through admixtures of odd and even parity states controlled also by the very strong spin orbit term.

Summing up, the difficulties of understanding pairing in nuclei as compared with condensed matter is (at least threefold): **a**) the bare interaction is attractive, a fact which lead to the prejudice that pairing force is short range and delayed the discovery of the other half of pairing, namely the retarded, medium polarization interaction, for a long time; **b**) particle number is small, thus pairing vibrations are important, and renormalize in a conspicuous way the variety of nuclear phenomena, in particular single–particle motion. The fact that such effects are still not being really considered is testified by the fact that a serious treatment of multipole pairing vibrations is still missing; **c**) spatial quantization leading to phenomena which by themselves can be very interesting[85], but which again has conditioned nuclear structure research, let alone reaction mechanism studies and the physics emerging from their interweaving.

Appendix 1.C Absolute Cooper pair tunneling cross section: quantitative novel physics at the edge between stability and chaos

In the study of many–body systems, in particular of finite many–body systems (FMBS) like the atomic nucleus, much can be learned from symmetries (group theory) as well as from the general phenomena of of spontaneous symmetry breaking. However, it is the texture of the associated emergent properties, concrete embodiment of symmetry breaking (potential energy) and of its restoration (fluctuations, collective modes), which provides insight into the eventual new physics. in fact, when one understands the many–body under study, in terms of the detailed motion of single–particles (nucleons) and collective motion, taking properly into account their couplings and associated zero point fluctuations, is that one can hope to have reached a solid, quantitative, understanding of the problem and of its solutions. Even more, that these solutions are likely transferable, at profit, to the study of

[84]Within this context it is of notice that in condensed matter literature Cooper pairs are viewed as fragile, extended di–electron entities, overlapping with a conspicuous number of other pairs, and displaying a delicate "rigid" quantal correlation between partners (generalized quantality parameter) and among Cooper pairs (off diagonal long range order). In fact, Weisskof's representaion of the radial (opposite) motion of electrons provides a useful picture of Cooper pir internal dynamics, In other words, approaching to or recessing from each other does not favour a particular anisotropic configuration , the two electrons being at the mean square radius of the Cooper pair, i.e. the coherence length ξ.

[85]Bertsch, G. F. et al. (1967); Ferreira, L. et al. (1984); **?**); **?**); Matsuo, M. (2013)

other FMBS like e.g. metal clusters, fullerenes[86], quantum dots[87], and eventually proteins, let alone the fact that one can make predictions. Predictions which, in connection with the study of halo nuclei, in particular of pairing[88] in such exotic, highly extended systems lying at the nucleon drip line, involve true novel physics[89]. Within this context one can quote from Leon Cooper's contribution to the volume[90] BCS: 50 years: "It has become fashionable... to assert... that once gauge symmetry is broken the properties of superconductors follow... with no need to inquire into the mechanism by which the symmetry is broken[91]. This is not ... true, since broken gauge symmetry might led to molecule–like and a Bose–Einstein rather than BCS condensation... in 1957... the major problem was to show... how... an order parameter or condensation in momentum space could come about... to show how... gauge–invariant symmetry of the Lagrangian could be spontaneously broken due to interactions which were themselves gauge invariant".

Nuclear physics has brought this quest a step further. This time in connection with the "extension" of the study of BCS condensation to its origin, a single Cooper pair in the rarified atmosphere resulting from the strong radial (isotropic) deformation observed in light halo, exotic nuclei in general, and in ^{11}Li in particular. During the last few years, the probing of this system in terms of absolute two–nucleon transfer (pick–up) reactions, has made this field a quantitative one, errors below the %10 limit being the rule. This achievement which has its basis on the remarkable experiments of Tanihata, I. et al. (2008), is also the result of the combined effort made in treating the structure and reaction aspects of the subject, two sides of the same physics, on equal footing. In particular regarding the description of the continuum and of the fluctuations leading to both single–particle and collective modes clothing, as well as present as ZPF of the ground state. New physics has been seen to emerge from situations in which these fluctuations diverge (like was also known to occur in the case of e.g. pairing rotational bands) or are on (quasi) resonance, as in the case of the halo pair addition mode of ^{9}Li (i.e. ^{11}Li(gs))

[86] cf. e.g. Broglia et al. (2004).

[87] Lipparini (2003).

[88] Cf. e.g. Broglia, R. A. and Zelevinsky, V. (2013).

[89] Cf. e.g. Barranco, F. et al. (2001); Tanihata, I. et al. (2008); Potel et al. (2010) and references therein.

[90] Cooper (2011).

[91] Detailed quoting (Weinberg (2011)): "... In consequence of this spontaneous symmetry breaking, products of any even number of electron fields have non–vanishing expectation values in a superconductor, though a single electron field does not. All of the dramatic exact properties of superconductors –zero electric resistance, the expelling of the magnetic fields from superconductors known as the Meissner effect, the quantization of magnetic flux through a thick superconducting ring, and the Josephson formula for the frequency of the ac current at a junction between two superconductors with different voltages– follow from the assumption that electromagnetic gauge invariance is broken in this way, with no need to inquire into the mechanism by which the symmetry is broken." The above quotation is similar to saying that once the idea of a double DNA helix was thought, all about inheritance was solved and known, and that one could forget the X–ray plates of Rosalind Franklin, Maurice Wilkins and collaborators, let alone how DNA and protein interact with each other (cf. e.g. **?** and references therein).

and likely of ^{10}Be (i.e. Be(0^{+*}; 2.24 MeV)).

Saturation density, spill out and halo

In the incipit to the Chapter on bulk properties of nuclei of Bohr and Mottelson (1969) one reads: "The almost constant density of nuclear matter is associated with the finite range of nuclear forces; the range of the forces is r_0 (where r_0 enters the nuclear radius in the expression $R = r_0 A^{1/3}$) thus small compared to nuclear size. This "saturation" of nuclear matter is also reflected in the fact that the total binding energy of the nucleus is roughly proportional to A. In a minor way, thee features are modified by surface effects and long–range Coulomb forces acting between the protons".

Electron scattering experiments (see the figure 2-1 and the corresponding caption containing the references in p. 159 of the above reference) yield

$$\rho(0) = 0.17\,\mathrm{fm}^{-3}. \tag{1.C.1}$$

Thus, one can posit that

$$\frac{4\pi}{3} R_0^3 \rho(0) = A, \tag{1.C.2}$$

leading to

$$r_0 = \left(\frac{3}{4\pi}\frac{1}{\rho(0)}\right)^{1/3} \approx 1.12\,\mathrm{fm}. \tag{1.C.3}$$

Because the above relations imply a step function distribution, we have to add to (1.C.3) the nucleon spill out[92] $(a_0/R_0)\ln 2 \approx 0.07\,(\approx (a_0/R_0)\ln 2 \approx (0.5/6) \times 0.69\,(A = 120))$ associated with the fact that a more realistic distribution is provided by a Fermi function of diffusivity $a_0 \approx 0.5$ fm. Thus $r_0 = (1.12 + 0.07)$ fm ≈ 1.2 fm. In the case of the nucleus ^{11}Li, observations indicate a mean square radius $\langle r^2\rangle^{1/2} = 3.55 \pm 0.1$ fm[93]. Thus

$$R(^{11}\mathrm{Li}) = \sqrt{\frac{5}{3}}\langle r^2\rangle^{1/2} \approx 4.58 \pm 1.3\,\mathrm{fm}. \tag{1.C.4}$$

Making use of the relation $R_0 = 1.2A^{1/3}$ fm, the quantity (1.C.4) leads to $(4.58/1.2)^3 \approx 56$, an effective mass number larger five times the actual value $A = 11$. To be noted that the actuel mass number predicts a "systematic" value of the nuclear radius $R_0(^{11}\mathrm{Li}) \approx 2.7$ fm.

The above results testifies to a very large "**radial deformation**", or halo region (skin), in keeping with the fact that[94] $R(^{11}\mathrm{Li})$-$R_0(^{11}\mathrm{Li})$=$R_0(^{9}\mathrm{Li})(\frac{R(^{11}\mathrm{Li})}{R_0(^{9}\mathrm{Li})} - 1)$ =

[92] Bertsch and Broglia (2005).

[93] Kobayashi, T. et al. (1989).

[94] Ona can parametrize the radius of ^{11}Li as (see Bohr, A. and Mottelson (1975)), $R = R_0(1 + \alpha_{00}Y_{00}) = R_0(1 + \beta_0\frac{1}{\sqrt{4\pi}})$. Thus $\beta_0 = \sqrt{4\pi}(\frac{R}{R_0} - 1) \approx 2.5$ which testifies to the extreme "exoticity" of the phenomenon.

$0.83R_0(^9\mathrm{Li})$. In other words, ^{11}Li can be viewed as a normal ^{9}Li core and of a skin made out of two neutrons and extending over a radius of the order of that of the core. But even more that the above mentioned "deformation" affects matter which is little complient to undergo either compressions or, for that sake, "depressions", without resulting in nuclear instability. In one case, through a mini supernova. In the second, by obliterating the effect of the short range strong force acting in the $^1S_0$ channel (pairing interaction).

In fact, in the case of the halo Cooper pair of ^{11}Li, that is of the last two weakly bound neutrons, one is dealing with a rarefied nuclear atmosphere of density

$$\rho \approx \frac{2}{\frac{4\pi}{3}(R^3(^{11}\mathrm{Li}) - R_0^3(^9\mathrm{Li}))} \approx 0.6 \times 10^{-2}\,\mathrm{fm}^{-3} \tag{1.C.5}$$

where the value $R_0(^9\mathrm{Li}) \approx 2.5$ fm was used. That is, we are dealing with pairing in a nuclear system at a density which is only 4% of saturation density.

The quest for the long range pairing mechanism which is at the basis of the binding of the halo Cooper pair of ^{11}Li to the ^{9}Li core ($S_{2n} \approx 0.380$ keV, to be compared to typical systematic values of $S_{2n} \approx 16$ MeV), has lead to the discovery of a novel nuclear mode of elementary excitation. The symbiotic halo pair addition mode, which has to carry its own source of binding (glue) like the hermit crab who carries a gastropod shell to protect his body. A novel embodiment of the Axel–Brink scenario in which not only the line shape, but the main structure of the resonance depends on the state on which it is built, and to which it is deeply interweaved as to guarantee its stability[95]. It also provides a novel realization of the Bardeen–Frölich–Pines microscopic mechanism to break gauge invariance: through the exchange of quite large ZPF which ensures Galilean invariance to a nucleus displaying essentially a permanent dipole moment, as a consequence of the almost degeneracy of the giant dipole pigmy resonance (centroid $\lesssim 1$ MeV) with the ground state. To our knowledge, this is the first example of a van der Waals Cooper pair, atomic or nuclear.

The NFT diagram shown in Fig. 1.A.1 describing this binding seems quite involved and high order. Thus unlikely to be at the basis of a new elementary mode of nuclear excitation, if nothing else because of the apparent lack of "elementarity'. This is not the case and, in fact, the physics at the basis of the process depicted by the oyster–like and eagle–like networks displayed in (a) and (b) is quite simple and present throughout nuclear structure and reactions, let alone many–body theories and QED. In fact, it encompasses (see Fig. 1.A.1): (I,II) the changes in energy of single–particle levels as a function of quadrupole deformations (Nilsson model) (III) the interaction between particles through the exchange of (bosons) vibrations, (IV,V) Pauli principle, (VI,VII) the softening of collective modes due to ground state correlations ((ZPF)–components, QRPA) and eventually the permanent distortion of the system (phase transition), (VIII) the interaction between two

[95] Axel (1962); Brink (1955).

non–polar systems through ZPF generated dipoles. Referring to general many–degree of freedom systems, (I,II) and (III) are at the basis of the fact that, in QED, the coupling between one and two photons is zero (Furry's theorem). It is also at the basis, through cancellation, of the small width displayed by giant resonances as compared with single–particle widths at similar energies as well as quadrupole inhomogeneous damping in NMR of molecules and in GDR of atomic nuclei. Concerning (VIII), one can mention resonant interactions between fluctuating systems like e.g. two coupled harmonic oscillators. It is like to find a new particle. Either one is at the right energy (on resonance) or one would not see it.

In the case of halo Cooper pair binding by GDPR in ^{11}Li, the system is essentially on resonance, in keeping with the fact $\epsilon_{p_{1/2}} - \epsilon_{s_{1/2}} \approx 0.3$ MeV, and that independent particle motion emerges from the same properties of the force from which collective modes emerge. In other words the ^{10}Li inverted parity system is poised to acquire a permanent dipole moment or, almost equivalent, to display a large amplitude, dipole mode at very low energy as well as a collective $B(E1)$ to the halo ground state, of the order of a single–particle unit B_{sp}. This is the GDPR (see Fig. **??**) with centroid about 0.6–0.8 MeV, 8% of the EWSR and so screened from the GDR through the poor overlap between core and single–particle wavefunctions so as to be able to retain essentially all of its B_{sp}, $E1$–strength which can rightly be considered a new mode of excitation (see discussion after eq. (**??**)). In other words we are faced, already at the level of single–particle spectrum, with the possibility of a plastic dipole mode, as it materializes in ^{11}Li. In this case, and making use of the relation

$$\frac{dn}{d\beta_L} = \frac{1}{4}\sqrt{\frac{2L+1}{3\pi}}A \tag{1.C.6}$$

defining the number of crossings n in terms of deformation (cf. Bertsch and Broglia (2005)), one obtains for $L = 0$ and $\beta_0 = 2.5$, $n \approx 2$.

It is of notice that all of these processes takes place inside the halo neutron pair addition vibrational mode of the closed shell system $^{9}_{3}$Li$_6$(gs), and thus in terms of virtual states. On the other hand intervening the processes depicted in Fig. 1.A.1 with external fields, e.g. those associated with one–and two–particle transfer processes, provides much of the physics which is at the basis of the exotic properties of ^{10}Li and ^{11}Li (see e.g. Fig. **??** (I), **??** and **??**. See also **??**).

But let us now proceed one step at a time. A very attractive, simple and economic picture of the giant dipole pygmy resonance was proposed in[96]. To explain parity inversion use is made of the fact that, for large prolate quadrupole deformations ($\beta_2 \approx 0.6 - 0.7$), the $m = 1/2$ member of the $1d_{5/2}$ and $1p_{1/2}$ orbitals, i.e. [220 1/2] and [101 1/2] in the Nilsson labeling of levels ($[Nn_3\Lambda\Omega]$), cross. This is in keeping with the fact that quadrupole distortion changes the energy of single–particle states; those having orbits lying in a plane containing the poles become, in the case of prolate deformations, lower their energy, while those lying

[96] Hamamoto and Shimoura (2007).

preferentially in a plane perpendicular to the symmetry axis, increase their energy. Now, this parity inversion is already observed between the resonant $1/2^-$ ($\approx$ 0.5 MeV) and the virtual $1/2^+$ ($\approx$ 0.2 MeV) states of ^{10}Li ($p_{1/2}$ and $2_{1/2}$ states). Thus, the energy difference of 0.3 MeV is not very different from the value of 0.6-0.7 MeV of the GDPR centroid. In any case, adjusting β_2 to the appropriate value this centroid energy is within reach. On the other hand, because the radius is affected by deformation, one can posit that the above model predicts $R = R_0(1 + \frac{\beta_2}{\sqrt{5}}\sqrt{\frac{5}{4\pi}}) = 2.7\,\text{fm} \times 1.2\,\text{fm} \approx 3.2$ fm ($\beta_2 \approx 0.7$), in disagreement with the experimental finding.

Nonetheless, the fact furthermore that the observed $\approx 8\%$ of the EWSR below ≈ 5 MeV for the GDPR corresponds to about $1B_{sp}(E1)$ for a single particle transition, provides another confirmation of the attractiveness of the model. Now, static models (including also the group theoretical models like that provided by SU_3) imply that single–particle states are either occupied or empty. Experimentally, this does not seem the case in the reaction $^9\text{Li}(d,p)^{10}\text{Li}$, although one can argue that the situation is different in the case of the single–particle states in ^{11}Li.

Second, the $1/2^+ \longleftrightarrow 1/2^-$ single–particle transitions are also part of the GDR transition, resonance which will essentially absorb most of the $E1$ strength into the high energy mode. In fact, typical $E1$–low energy single particle transition display $\approx 10^{-4}B_{sp}(E1)$. Now, inhomogeneous damping brings the dipole oscillations along the symmetry axis to an energy of

$$(\hbar\omega_D) \approx \frac{100\,\text{MeV}}{3.2} \approx 30\,\text{MeV} \tag{1.C.7}$$

far away from the less than 1 MeV energy corresponding to the GDPR centroid.

Now, in order to calculate the giant dipole pygmy resonance based on the ground state of ^{11}Li one needs to know the occupation factors of the $s_{1/2}$ and $p_{1/2}$ states. This has been done microscopically making use of the diagonalization of the NFT diagrams taking into account self–energy and induced interaction (vertex renormalization processes) leading to

$$|\tilde{0}\rangle = |0\rangle + 0.71|(p_{1/2}, s_{1/2})_{1^-} \otimes 1^-; 0\rangle + 0.1|(s_{1/2}, d_{5/2})_{2^+} \otimes 2^+; 0\rangle, \tag{1.C.8}$$

and

$$|0\rangle = 0.45|s^2_{1/2}\rangle + 0.55|p^2_{1/2}\rangle + 0.04|d^2_{5/2}\rangle. \tag{1.C.9}$$

In Eq. (1.C.8), the state $|1^-\rangle$ and $|2^+\rangle$ stand for the giant dipole pygmy resonance, and for the low–lying collective quadrupole vibration of ^{9}Li, respectively. As it emerges from (1.C.8) and (1.C.9), to calculate the microscopic structure of the state $|1^-\rangle$ (both wavefunction and transition density and consequently the particle–vibration coupling vertex) one needs to calculate $|0\rangle$. But to do so one needs to know the same $|1^-\rangle$ state, the vibrational mode which exchanged between the two neutrons of the halo provides most of its glue to the ^{9}Li core. From here, the symbiotic character of the 0^+ and 1^- (GDPR) entering the $|^{11}\text{Li}(0^+_\nu \otimes p_{3/2}(\pi))_{3/2^-}; gs\rangle$ and $|^{11}\text{Li}(1^-_\nu \otimes p_{3/2}(\pi))_{1/2,3/2,5/2^+}; \approx 0.8\,\text{MeV}\rangle$ states.

Similar calculations have been carried out for ^{12}Be(gs) and ^{12}Be(0^{+*}; 2.24 MeV). In the first case no pygmy is found, while in the second case a well developed GDPR is predicted displaying a number of peaks below 2 MeV and carrying a summed EWSR in the interval 0-5 of $\approx 6\%$. This result testifies to the fact that the symbiotic halo pair addition mode is a *bona fide* elementary mode of excitation. Its symbiotic GDPR allows to probe the state on which it is based, making the Axel–Brink mechanism a tool to probe the structure of halo states. Within this context see Fig. 1.8.1

Bibliography

Kisslinger,Leonard S. and Sørensen,Raymond A. Spherical nuclei with simple residual forces. *Review of Modern Physics*, 35:853, 1963.

V. Ambegaokar. *The Green's function method in superconductivity, Vol I*, page 259. Marcel Dekker, New York, 1969.

V. Ambegaokar and A. Baratoff. Tunneling between superconductors. *Phys. Rev. Lett.*, 10:486, 1963.

P. W. Anderson. New method in the theory of superconductivity. *Phys. Rev.*, 110: 985, 1958.

P. W. Anderson. Special effects in suprconductivity. In E. R. Caianello, editor, *The Many–Body Problem, Vol.2*, page 113. Academic Press, New York, 1964.

P. W. Anderson. More is different. *Science*, 177:393, 1972.

N. W. Ashcroft and N. D. Mermin. *Solid state physics*. Holt, Reinhardt and Winston, Hong Kong, 1987.

P. Axel. Electric Dipole Ground-State Transition Width Strength Function and 7–Mev Photon Interactions. *Phys. Rev.*, 126:671, 1962.

J. Bardeen. Tunnelling from a many-particle point of view. *Phys. Rev. Lett.*, 6:57, 1961.

J. Bardeen. Tunneling into superconductors. *Physical Review Letters*, 9:147, 1962.

Barranco, F., R. A. Broglia, and G. F. Bertsch. Exotic radioactivity as a superfluid tunneling phenomenon. *Phys. Rev. Lett.*, 60:507, 1988.

Barranco, F., G. Bertsch, R. Broglia, and E. Vigezzi. Large-amplitude motion in superfluid fermi droplets. *Nuclear Physics A*, 512:253, 1990.

Barranco, F., P. F. Bortignon, R. A. Broglia, G. Colò, and E. Vigezzi. The halo of the exotic nucleus ^{11}Li: a single Cooper pair. *Europ. Phys. J. A*, 11:385, 2001.

J. L. Basdevant and J. Dalibard. *Quantum Mechanics*. Springer, Berlin, 2005.

Bayman, B. F. and C. F. Clement. Sum rules for two–nucleon transfer reactions. *Phys. Rev. Lett.*, 29:1020, 1972.

G. Bertsch. In R. Broglia and J. R. Schrieffer, editors, *International School of Physics "Enrico Fermi" Collective motion in Fermi droplets*, page 41, Amsterdam, 1988. North Holland.

G. Bertsch and R. Broglia. *Oscillations in Finite Quantum Systems*. Cambridge University Press, Cambridge, 2005.

Bertsch, G. F., R. A. Broglia, and C. Riedel. Qualitative description of nuclear collectivity. *Nucl. Phys. A*, 91:123, 1967.

Bjerregaard, J. H., O. Hansen, Nathan, and S. Hinds. States of ^{208}Pb from double triton stripping. *Nucl. Phys.*, 89:337, 1966.

A. Bohr and B. R. Mottelson. *Nuclear Structure, Vol.I*. Benjamin, New York, 1969.

A. Bohr and O. Ulfbeck. Quantal structure of superconductivity gauge angle. In *First Topsøe summer School on Superconductivity and Workshop on Superconductors*, Roskilde, Denmark Riso/M/2756, 1988.

N. Bohr and J. A. Wheeler. The mechanism of nuclear fission. *Phys. Rev.*, 56:426, 1939.

Bohr, A. and B. R. Mottelson. *Nuclear Structure, Vol.II*. Benjamin, New York, 1975.

M. Born. Zur Quantenmechanik der Stoßvorgänge. *Zeitschr. f. Phys.*, 37:863, 1926.

P. F. Bortignon, R. A. Broglia, and C. H. Dasso. Quenching of the mass operator associated with collective states in many–body systems. *Nuclear Physics A*, 398: 221, 1983.

Bortignon, P. F., A. Bracco, and R. A. Broglia. *Giant Resonances*. Harwood Academic Publishers, Amsterdam, 1998.

D. M. Brink. *PhD Thesis*. Oxford University, 1955.

Brink, D. and R. A. Broglia. *Nuclear Superfluidity*. Cambridge University Press, Cambridge, 2005.

R. Broglia and A. Winther. *Heavy Ion Reactions, 2nd ed.* Westview Press, Perseus Books, Boulder, 2005.

R. Broglia, G. Coló, G. Onida, and H. Roman. *Solid State Physics of Finite Systems: metal clusters, fullerenes, atomic wires*. Springer Verlag, Berlin, Heidelberg, 2004.

R. A. Broglia and A. Winther. On the pairing field in nuclei. *Physics Letters B*, 124:11, 1983.

R. A. Broglia and A. Winther. *Heavy Ion Reactions*. Westview Press, Boulder, CO., 2004.

R. A. Broglia, C. Riedel, and T. Udagawa. Coherence properties of two-neutron transfer reactions and their relation to inelastic scattering. *Nuclear Physics A*, 169:225, 1971.

Broglia, R. A. The surfaces of compact systems: from nuclei to stars. *Surface Science*, 500:759, 2002.

Broglia, R. A. More is different: 50 Years of Nuclear BCS. In R. A. Broglia and V. Zelevinsky, editors, *50 Years of Nuclear BCS*, page 642. World Scientific, Singapore, 2013.

Broglia, R. A., C. Riedel, and T. Udagawa. Sum rules and two-particle units in the analysis of two-neutron transfer reactions. *Nuclear Physics A*, 184:23, 1972.

Broglia, R. A. and Zelevinsky, V. . In R. A. Broglia and V. Zelevinsky, editors, *50 Years of Nuclear BCS*. World Scientific, Singapore, 2013.

Broglia, R.A., O. Hansen, and C. Riedel. Two–neutron transfer reactions and the pairing model. *Advances in Nuclear Physics*, 6:287, 1973. URL `www.mi.infn.it/?vigezzi/BHR/ BrogliaHansenRiedel.pdf`.

M. H. Cohen, L. M. Falicov, and J. C. Phillips. Superconductive tunneling. *Phys. Rev. Lett.*, 8:316, 1962.

L. Cooper. In L. Cooper and D. Feldman, editors, *BCS: 50 years*. World Scientific, Singapore, 2011.

L. N. Cooper. Bound electron pairs in a degenerate fermi gas. *Phys. Rev.*, 104: 1189, 1956.

P. G. de Gennes. *Les objets fragiles*. Plon, Paris, 1994.

Ferreira, L., R. Liotta, C. Dasso, R. A. Broglia, and A. Winther. Spatial correlations of pairing collective states. *Nuclear Physics A*, 426:276, 1984.

H. T. Fortune, G.-B. Liu, and D. E. Alburger. $(\ sd\ )^2$ states in ^{12}Be. *Phys. Rev. C*, 50:1355, 1994.

G. Gori, F. Barranco, E. Vigezzi, and R. A. Broglia. Parity inversion and breakdown of shell closure in Be isotopes. *Phys. Rev. C*, 69:041302, 2004.

Gor'kov, L.P. Microscopic derivation of the Ginzburg–Landau eqautions in the theory of superconductivity. *Soviet Phys. JETP*, 9:1364, 1959.

Guazzoni, P., L. Zetta, A. Covello, A. Gargano, B. F. Bayman, G. Graw, R. Hertenberger, H.-F. Wirth, and M. Jaskola. Spectroscopy of ^{110}Sn via the high-resolution ^{112}Sn(p,t) ^{110}Sn reaction. *Phys. Rev. C*, 74:054605, 2006.

Guazzoni, P., L. Zetta, A. Covello, A. Gargano, B. F. Bayman, T. Faestermann, G. Graw, R. Hertenberger, H.-F. Wirth, and M. Jaskola. High-resolution measurement of the ^{118,124}Sn(p,t) ^{116,122} reactions: Shell-model and microscopic distorted-wave Born approximation calculations. *Phys. Rev. C*, 83:044614, 2011.

I. Hamamoto and S. Shimoura. Properties of ^{12}Be and ^{11}Be in terms of single-particle motion in deformed potential. *Journal of Physics G: Nuclear and Particle Physics*, 34:2715, 2007.

A. Idini, G. Potel, F. Barranco, E. Vigezzi, and R. A. Broglia. Interweaving of elementary modes of excitation in superfluid nuclei through particle-vibration coupling: Quantitative account of the variety of nuclear structure observables. *Phys. Rev. C*, 92:031304, 2015.

J. G. Johansen, V. Bildstein, M. J. G. Borge, M. Cubero, J. Diriken, J. Elseviers, L. M. Fraile, H. O. U. Fynbo, L. P. Gaffney, R. Gernhäuser, B. Jonson, G. T. Koldste, J. Konki, T. Kröll, R. Krücken, D. Mücher, T. Nilsson, K. Nowak, J. Pakarinen, V. Pesudo, R. Raabe, K. Riisager, M. Seidlitz, O. Tengblad, H. Törnqvist, D. Voulot, N. Warr, F. Wenander, K. Wimmer, and H. De Witte. Experimental study of bound states in ^{12}Be through low-energy ^{11}Be(d, p)-transfer reactions. *Phys. Rev. C*, 88:044619, 2013.

B. D. Josephson. Possible new effects in superconductive tunnelling. *Phys. Lett.*, 1:251, 1962.

A. M. Kadin. Spatial structure of the cooper pair. *Journal of Superconductivity and Novel Magnetism*, 20:285, 2007.

C. Kittel. *Introduction to solid state physics*. Wiley, NJ, 1996.

Kobayashi, T., S. Shimoura, I. Tanihata, K. Katori, K. Matsuta, T. Minamisono, K. Sugimoto, W. Mller, D. L. Olson, T. J. M. Symons, and H. Wieman. Electromagnetic dissociation and soft giant dipole resonance of the neutron-dripline nucleus ^{11}Li. *Physics Letters B*, 232:51, 1989.

Le Tourneaux. *Mat. Fys. Medd. Dan. Vid. Selsk.*, 34, 1965.

A. Leggett. *Quantum Liquids*. Oxford University Press, Oxford, 2006.

J. Lindhard. *Kgl. Danske Videnshab. Selskab, Mat. Fys. Medd.*, 28, 1953.

E. Lipparini. *Modern Many–Particle Physics: Atomic gases, Quantum Dots and Quantum Fluids,*. World Scientific, Singapore, 2003.

Mahaux, C., P. F. Bortignon, R. A. Broglia, and C. H. Dasso. Dynamics of the shell model. *Physics Reports*, 120:1–274, 1985.

Matsuo, M. Spatial Structure of Cooper Pairs in Nuclei. In R. A. Broglia and V. Zelevinsky, editors, *50 Years of Nuclear BCS*, page 66. World Scientific, Singapore, 2013.

D. G. McDonald. The nobel laureate versus the graduate student. *Physics Today*, page 46, July 2001.

D. Montanari, L. Corradi, S. Szilner, G. Pollarolo, E. Fioretto, G. Montagnoli, F. Scarlassara, A. M. Stefanini, S. Courtin, A. Goasduff, F. Haas, D. Jelavi ć Malenica, C. Michelagnoli, T. Mijatović, N. Soić, C. A. Ur, and M. Varga Pajtler. Neutron Pair Transfer in ^{60}Ni +^{116} Sn Far below the Coulomb Barrier. *Phys. Rev. Lett.*, 113:052501, 2014.

B. Mottelson. Elementary features of nuclear structure. In Niefnecker, Blaizot, Bertsch, Weise, and David, editors, *Trends in Nuclear Physics, 100 years later, Les Houches, Session LXVI*, page 25, Amsterdam, 1998. Elsevier.

B. R. Mottelson. Selected topics in the theory of collective phenomena in nuclei. In G. Racah, editor, *International School of Physics "Enrico Fermi" Course XV , Nuclear Spectroscopy*, page 44, New York, 1962. Academic Press.

A. B. Pippard. The historical context of Josephson discovery. In H. Rogalla and P. H. Kes, editors, *100 years of superconductivity*, page 30. CRC Press, Taylor and Francis, FL, 2012.

G. Pollarolo and R. A. Broglia. Microscopic Description of the Backward Rise of the Elastic Angular Distribution ^{16}O+^{28}Si. *Nuovo Cimento*, 81:278, 1984.

G. Potel, F. Barranco, E. Vigezzi, and R. A. Broglia. Evidence for phonon mediated pairing interaction in the halo of the nucleus ^{11}Li. *Phys. Rev. Lett.*, 105:172502, 2010.

G. Potel, A. Idini, F. Barranco, E. Vigezzi, and R. A. Broglia. Nuclear Field Theory predictions for ^{11}Li and ^{12}Be: shedding light on the origin of pairing in nuclei. *Phys. At. Nucl.*, 7:941, 2014.

Potel, G., A. Idini, F. Barranco, E. Vigezzi, and R. A. Broglia. Cooper pair transfer in nuclei. *Rep. Prog. Phys.*, 76:106301, 2013a.

Potel, G., A. Idini, F. Barranco, E. Vigezzi, and R. A. Broglia. Quantitative study of coherent pairing modes with two–neutron transfer: Sn isotopes. *Phys. Rev. C*, 87:054321, 2013b.

H. Rogalla and P. H. Kes. . In H. Rogalla and P. H. Kes, editors, *100 years of superconductivity*. CRC Press, Taylor and Francis, FL, 2012.

J. J. Sakurai. *Modern Quantum Mechanics*. Addison-Wesley, Cambridge, MA, 1994.

Sargsyan, V. V., G. Scamps, G. G. Adamian, N. V. Antonenko, and D. Lacroix. Neutron pair transfer in sub–barrier capture processes. *arXiv:1311.4353v1*, 2013.

G. Satchler. *Introduction to Nuclear Reactions*. Mc Millan, New York, 1980.

J. Schrieffer. *Superconductivity*. Benjamin, New York, 1964.

V. G. Soloviev. Quasi–particle and collective structure of the states of even, strongly-deformed nuclei. *Nuclear Physics*, 69(1):1, 1965.

Tanihata, I., M. Alcorta, D. Bandyopadhyay, R. Bieri, L. Buchmann, B. Davids, N. Galinski, D. Howell, W. Mills, S. Mythili, R. Openshaw, E. Padilla-Rodal, G. Ruprecht, G. Sheffer, A. C. Shotter, M. Trinczek, P. Walden, H. Savajols, T. Roger, M. Caamano, W. Mittig, P. Roussel-Chomaz, R. Kanungo, A. Gallant, M. Notani, G. Savard, and I. J. Thompson. Measurement of the two-halo neutron transfer reaction ^{1}H(^{11}Li,^{9}Li)^{3}H at 3A MeV. *Phys. Rev. Lett.*, 100:192502, 2008.

Thompson, I.J. Reaction mechanism of pair transfer. In R. A. Broglia and V. Zelevinsky, editors, *50 Years of Nuclear BCS*, page 455. World Scientific, Singapore, 2013.

M. Tinkham. *Introduction to Superconductivity*. Mc Graw-Hill, New York, 1996.

W. von Oertzen and A. Vitturi. Pairing correlations of nucleons and multi–nucleon transfer between heavy nuclei. *Reports on Progress in Physics*, 64:1247, 2001.

von Oertzen, W. Enhanced two–nucleon transfer due to pairing correlations. In R. A. Broglia and V. Zelevinsky, editors, *50 Years of Nuclear BCS*, page 405. World Scientific, Singapore, 2013.

L. Weinberg. Bcs: 50 years. In L. Cooper and D. Feldman, editors, *BCS: 50 years*. World Scientific, Singapore, 2011.

P. G. Young and R. H. Stokes. New States in ^{9}Li from the Reaction ^{7}Li$(t, p)^{9}$Li. *Phys. Rev. C*, 4:1597, 1971.

Bibliography

Kisslinger,L. S. and Sørensen,R. A. Spherical nuclei with simple residual forces. *Review of Modern Physics*, 35:853, 1963.

V. Ambegaokar. *The Green's function method in superconductivity, Vol I*, page 259. Marcel Dekker, New York, 1969.

V. Ambegaokar and A. Baratoff. Tunneling between superconductors. *Phys. Rev. Lett.*, 10:486, 1963.

P. W. Anderson. New method in the theory of superconductivity. *Phys. Rev.*, 110: 985, 1958.

P. W. Anderson. Special effects in suprconductivity. In E. R. Caianello, editor, *The Many–Body Problem, Vol.2*, page 113. Academic Press, New York, 1964.

P. W. Anderson. More is different. *Science*, 177:393, 1972.

N. W. Ashcroft and N. D. Mermin. *Solid state physics*. Holt, Reinhardt and Winston, Hong Kong, 1987.

P. Axel. Electric Dipole Ground-State Transition Width Strength Function and 7–Mev Photon Interactions. *Phys. Rev.*, 126:671, 1962.

J. Bardeen. Tunnelling from a many-particle point of view. *Phys. Rev. Lett.*, 6:57, 1961.

J. Bardeen. Tunneling into superconductors. *Physical Review Letters*, 9:147, 1962.

Barranco, F., R. A. Broglia, and G. F. Bertsch. Exotic radioactivity as a superfluid tunneling phenomenon. *Phys. Rev. Lett.*, 60:507, 1988.

Barranco, F., G. Bertsch, R. Broglia, and E. Vigezzi. Large-amplitude motion in superfluid fermi droplets. *Nuclear Physics A*, 512:253, 1990.

Barranco, F., P. F. Bortignon, R. A. Broglia, G. Colò, and E. Vigezzi. The halo of the exotic nucleus ^{11}Li: a single Cooper pair. *Europ. Phys. J. A*, 11:385, 2001.

J. L. Basdevant and J. Dalibard. *Quantum Mechanics*. Springer, Berlin, 2005.

Bayman, B. F. and C. F. Clement. Sum rules for two–nucleon transfer reactions. *Phys. Rev. Lett.*, 29:1020, 1972.

G. Bertsch. In R. Broglia and J. R. Schrieffer, editors, *International School of Physics "Enrico Fermi" Collective motion in Fermi droplets*, page 41, Amsterdam, 1988. North Holland.

G. Bertsch and R. Broglia. *Oscillations in Finite Quantum Systems*. Cambridge University Press, Cambridge, 2005.

Bertsch, G. F., R. A. Broglia, and C. Riedel. Qualitative description of nuclear collectivity. *Nucl. Phys. A*, 91:123, 1967.

Bjerregaard, J. H., O. Hansen, Nathan, and S. Hinds. States of ^{208}Pb from double triton stripping. *Nucl. Phys.*, 89:337, 1966.

A. Bohr and B. R. Mottelson. *Nuclear Structure, Vol.I*. Benjamin, New York, 1969.

A. Bohr and O. Ulfbeck. Quantal structure of superconductivity gauge angle. In *First Topsøe summer School on Superconductivity and Workshop on Superconductors*, Roskilde, Denmark Riso/M/2756, 1988.

N. Bohr and J. A. Wheeler. The mechanism of nuclear fission. *Phys. Rev.*, 56:426, 1939.

Bohr, A. and B. R. Mottelson. *Nuclear Structure, Vol.II*. Benjamin, New York, 1975.

M. Born. Zur Quantenmechanik der Stoßvorgänge. *Zeitschr. f. Phys.*, 37:863, 1926.

P. F. Bortignon, R. A. Broglia, and C. H. Dasso. Quenching of the mass operator associated with collective states in many–body systems. *Nuclear Physics A*, 398: 221, 1983.

Bortignon, P. F., A. Bracco, and R. A. Broglia. *Giant Resonances*. Harwood Academic Publishers, Amsterdam, 1998.

D. M. Brink. *PhD Thesis*. Oxford University, 1955.

Brink, D. and R. A. Broglia. *Nuclear Superfluidity*. Cambridge University Press, Cambridge, 2005.

R. Broglia and A. Winther. *Heavy Ion Reactions, 2nd ed.* Westview Press, Perseus Books, Boulder, 2005.

R. Broglia, G. Coló, G. Onida, and H. Roman. *Solid State Physics of Finite Systems: metal clusters, fullerenes, atomic wires*. Springer Verlag, Berlin, Heidelberg, 2004.

R. A. Broglia and A. Winther. On the pairing field in nuclei. *Physics Letters B*, 124:11, 1983.

R. A. Broglia and A. Winther. *Heavy Ion Reactions*. Westview Press, Boulder, CO., 2004.

R. A. Broglia, C. Riedel, and T. Udagawa. Coherence properties of two-neutron transfer reactions and their relation to inelastic scattering. *Nuclear Physics A*, 169:225, 1971.

Broglia, R. A. The surfaces of compact systems: from nuclei to stars. *Surface Science*, 500:759, 2002.

Broglia, R. A. More is different: 50 Years of Nuclear BCS. In R. A. Broglia and V. Zelevinsky, editors, *50 Years of Nuclear BCS*, page 642. World Scientific, Singapore, 2013.

Broglia, R. A., C. Riedel, and T. Udagawa. Sum rules and two-particle units in the analysis of two-neutron transfer reactions. *Nuclear Physics A*, 184:23, 1972.

Broglia, R. A. and Zelevinsky, V. . In R. A. Broglia and V. Zelevinsky, editors, *50 Years of Nuclear BCS*. World Scientific, Singapore, 2013.

Broglia, R.A., O. Hansen, and C. Riedel. Two–neutron transfer reactions and the pairing model. *Advances in Nuclear Physics*, 6:287, 1973. URL `www.mi.infn.it/?vigezzi/BHR/ BrogliaHansenRiedel.pdf`.

M. H. Cohen, L. M. Falicov, and J. C. Phillips. Superconductive tunneling. *Phys. Rev. Lett.*, 8:316, 1962.

L. Cooper. In L. Cooper and D. Feldman, editors, *BCS: 50 years*. World Scientific, Singapore, 2011.

L. N. Cooper. Bound electron pairs in a degenerate fermi gas. *Phys. Rev.*, 104: 1189, 1956.

P. G. de Gennes. *Les objets fragiles*. Plon, Paris, 1994.

Ferreira, L., R. Liotta, C. Dasso, R. A. Broglia, and A. Winther. Spatial correlations of pairing collective states. *Nuclear Physics A*, 426:276, 1984.

H. T. Fortune, G.-B. Liu, and D. E. Alburger. $(\ sd\ )^2$ states in ^{12}Be. *Phys. Rev. C*, 50:1355, 1994.

G. Gori, F. Barranco, E. Vigezzi, and R. A. Broglia. Parity inversion and breakdown of shell closure in Be isotopes. *Phys. Rev. C*, 69:041302, 2004.

Gor'kov, L.P. Microscopic derivation of the Ginzburg–Landau eqautions in the theory of superconductivity. *Soviet Phys. JETP*, 9:1364, 1959.

Guazzoni, P., L. Zetta, A. Covello, A. Gargano, B. F. Bayman, G. Graw, R. Hertenberger, H.-F. Wirth, and M. Jaskola. Spectroscopy of ^{110}Sn via the high-resolution ^{112}Sn(p,t) ^{110}Sn reaction. *Phys. Rev. C*, 74:054605, 2006.

Guazzoni, P., L. Zetta, A. Covello, A. Gargano, B. F. Bayman, T. Faestermann, G. Graw, R. Hertenberger, H.-F. Wirth, and M. Jaskola. High-resolution measurement of the ^{118,124}Sn(p,t) ^{116,122} reactions: Shell-model and microscopic distorted-wave Born approximation calculations. *Phys. Rev. C*, 83:044614, 2011.

I. Hamamoto and S. Shimoura. Properties of ^{12}Be and ^{11}Be in terms of single-particle motion in deformed potential. *Journal of Physics G: Nuclear and Particle Physics*, 34:2715, 2007.

A. Idini, G. Potel, F. Barranco, E. Vigezzi, and R. A. Broglia. Interweaving of elementary modes of excitation in superfluid nuclei through particle-vibration coupling: Quantitative account of the variety of nuclear structure observables. *Phys. Rev. C*, 92:031304, 2015.

J. G. Johansen, V. Bildstein, M. J. G. Borge, M. Cubero, J. Diriken, J. Elseviers, L. M. Fraile, H. O. U. Fynbo, L. P. Gaffney, R. Gernhäuser, B. Jonson, G. T. Koldste, J. Konki, T. Kröll, R. Krücken, D. Mücher, T. Nilsson, K. Nowak, J. Pakarinen, V. Pesudo, R. Raabe, K. Riisager, M. Seidlitz, O. Tengblad, H. Törnqvist, D. Voulot, N. Warr, F. Wenander, K. Wimmer, and H. De Witte. Experimental study of bound states in ^{12}Be through low-energy ^{11}Be(d,p)-transfer reactions. *Phys. Rev. C*, 88:044619, 2013.

B. D. Josephson. Possible new effects in superconductive tunnelling. *Phys. Lett.*, 1:251, 1962.

A. M. Kadin. Spatial structure of the cooper pair. *Journal of Superconductivity and Novel Magnetism*, 20:285, 2007.

C. Kittel. *Introduction to solid state physics*. Wiley, NJ, 1996.

Kobayashi, T., S. Shimoura, I. Tanihata, K. Katori, K. Matsuta, T. Minamisono, K. Sugimoto, W. Mller, D. L. Olson, T. J. M. Symons, and H. Wieman. Electromagnetic dissociation and soft giant dipole resonance of the neutron-dripline nucleus ^{11}Li. *Physics Letters B*, 232:51, 1989.

Le Tourneaux. *Mat. Fys. Medd. Dan. Vid. Selsk.*, 34, 1965.

A. Leggett. *Quantum Liquids*. Oxford University Press, Oxford, 2006.

J. Lindhard. *Kgl. Danske Videnshab. Selskab, Mat. Fys. Medd.*, 28, 1953.

E. Lipparini. *Modern Many–Particle Physics: Atomic gases, Quantum Dots and Quantum Fluids,*. World Scientific, Singapore, 2003.

P. Lotti, F. Cazzola, P. F. Bortignon, R. A. Broglia, and A. Vitturi. Spatial correlation of pairing modes in nuclei at finite temperature. *Phys. Rev. C*, 40:1791, 1989.

Mahaux, C., P. F. Bortignon, R. A. Broglia, and C. H. Dasso. Dynamics of the shell model. *Physics Reports*, 120:1–274, 1985.

Matsuo, M. Spatial Structure of Cooper Pairs in Nuclei. In R. A. Broglia and V. Zelevinsky, editors, *50 Years of Nuclear BCS*, page 66. World Scientific, Singapore, 2013.

D. G. McDonald. The nobel laureate versus the graduate student. *Physics Today*, page 46, July 2001.

D. Montanari, L. Corradi, S. Szilner, G. Pollarolo, E. Fioretto, G. Montagnoli, F. Scarlassara, A. M. Stefanini, S. Courtin, A. Goasduff, F. Haas, D. Jelavi ć Malenica, C. Michelagnoli, T. Mijatović, N. Soić, C. A. Ur, and M. Varga Pajtler. Neutron Pair Transfer in ^{60}Ni +^{116} Sn Far below the Coulomb Barrier. *Phys. Rev. Lett.*, 113:052501, 2014.

B. Mottelson. Elementary features of nuclear structure. In Niefnecker, Blaizot, Bertsch, Weise, and David, editors, *Trends in Nuclear Physics, 100 years later, Les Houches, Session LXVI*, page 25, Amsterdam, 1998. Elsevier.

B. R. Mottelson. Selected topics in the theory of collective phenomena in nuclei. In G. Racah, editor, *International School of Physics "Enrico Fermi" Course XV , Nuclear Spectroscopy*, page 44, New York, 1962. Academic Press.

A. B. Pippard. The historical context of Josephson discovery. In H. Rogalla and P. H. Kes, editors, *100 years of superconductivity*, page 30. CRC Press, Taylor and Francis, FL, 2012.

G. Pollarolo and R. A. Broglia. Microscopic Description of the Backward Rise of the Elastic Angular Distribution ^{16}O+^{28}Si. *Nuovo Cimento*, 81:278, 1984.

G. Potel, F. Barranco, E. Vigezzi, and R. A. Broglia. Evidence for phonon mediated pairing interaction in the halo of the nucleus ^{11}Li. *Phys. Rev. Lett.*, 105:172502, 2010.

G. Potel, A. Idini, F. Barranco, E. Vigezzi, and R. A. Broglia. Nuclear Field Theory predictions for ^{11}Li and ^{12}Be: shedding light on the origin of pairing in nuclei. *Phys. At. Nucl.*, 7:941, 2014.

Potel, G., A. Idini, F. Barranco, E. Vigezzi, and R. A. Broglia. Cooper pair transfer in nuclei. *Rep. Prog. Phys.*, 76:106301, 2013a.

Potel, G., A. Idini, F. Barranco, E. Vigezzi, and R. A. Broglia. Quantitative study of coherent pairing modes with two–neutron transfer: Sn isotopes. *Phys. Rev. C*, 87:054321, 2013b.

H. Rogalla and P. H. Kes. . In H. Rogalla and P. H. Kes, editors, *100 years of superconductivity*. CRC Press, Taylor and Francis, FL, 2012.

J. J. Sakurai. *Modern Quantum Mechanics*. Addison-Wesley, Cambridge, MA, 1994.

Sargsyan, V. V., G. Scamps, G. G. Adamian, N. V. Antonenko, and D. Lacroix. Neutron pair transfer in sub–barrier capture processes. *arXiv:1311.4353v1*, 2013.

G. Satchler. *Introduction to Nuclear Reactions*. Mc Millan, New York, 1980.

J. Schrieffer. *Superconductivity*. Benjamin, New York, 1964.

V. G. Soloviev. Quasi–particle and collective structure of the states of even, strongly-deformed nuclei. *Nuclear Physics*, 69(1):1, 1965.

Tanihata, I., M. Alcorta, D. Bandyopadhyay, R. Bieri, L. Buchmann, B. Davids, N. Galinski, D. Howell, W. Mills, S. Mythili, R. Openshaw, E. Padilla-Rodal, G. Ruprecht, G. Sheffer, A. C. Shotter, M. Trinczek, P. Walden, H. Savajols, T. Roger, M. Caamano, W. Mittig, P. Roussel-Chomaz, R. Kanungo, A. Gallant, M. Notani, G. Savard, and I. J. Thompson. Measurement of the two-halo neutron transfer reaction ^{1}H(^{11}Li,^{9}Li)^{3}H at 3A MeV. *Phys. Rev. Lett.*, 100:192502, 2008.

Thompson, I.J. Reaction mechanism of pair transfer. In R. A. Broglia and V. Zelevinsky, editors, *50 Years of Nuclear BCS*, page 455. World Scientific, Singapore, 2013.

M. Tinkham. *Introduction to Superconductivity*. Mc Graw-Hill, New York, 1996.

W. von Oertzen and A. Vitturi. Pairing correlations of nucleons and multi–nucleon transfer between heavy nuclei. *Reports on Progress in Physics*, 64:1247, 2001.

von Oertzen, W. Enhanced two–nucleon transfer due to pairing correlations. In R. A. Broglia and V. Zelevinsky, editors, *50 Years of Nuclear BCS*, page 405. World Scientific, Singapore, 2013.

L. Weinberg. Bcs: 50 years. In L. Cooper and D. Feldman, editors, *BCS: 50 years*. World Scientific, Singapore, 2011.

P. G. Young and R. H. Stokes. New States in ^{9}Li from the Reaction ^{7}Li(t, p)^{9}Li. *Phys. Rev. C*, 4:1597, 1971.